AFSC PROCESSED REPORT 2020-07

Alaska Fisheries Science Center
Resource Assessment and Conservation Engineering Division
Midwater Assessment and Conservation Engineering Program

Results of the Acoustic-Trawl Survey of Walleye Pollock (*Gadus chalcogrammus*) on the U.S. Bering Sea Shelf in June -August 2018 (DY1807)

SEPTEMBER 2020

This report does not constitute a publication
and is for information only.
All data herein are to be considered provisional.

U.S. Department of Commerce | National Oceanic and Atmospheric Administration | National Marine Fisheries Service

AFSC Processed Report

This document should be cited as follows:

McCarthy, A., T. Honkalehto, N. Lauffenburger, and A. De Robertis. 2020. Results of the acoustic-trawl survey of walleye pollock (*Gadus chalcogrammus*) on the U.S. Bering Sea Shelf in June - August 2018 (DY1807). AFSC Processed Rep. 2020-07, 83 p. Alaska Fish. Sci. Cent., NOAA, Natl. Mar. Fish. Serv., 7600 Sand Point Way NE, Seattle WA 98115.

.

This document is available online at: https://repository.library.noaa.gov/

Reference in this document to trade names does not imply endorsement
by the National Marine Fisheries Service, NOAA.

Results of the Acoustic-Trawl Survey of Walleye Pollock (*Gadus chalcogrammus*) on the U.S. Bering Sea Shelf in June - August 2018 (DY1807)

A. McCarthy, T. Honkalehto, N. Lauffenburger, and A. De Robertis

Resource Assessment and Conservation Engineering Division
Alaska Fisheries Science Center
National Marine Fisheries Service
National Oceanic and Atmospheric Administration
7600 Sand Point Way, NE
Seattle, WA 98115

September 2020

ABSTRACT

Eastern Bering Sea shelf walleye pollock (*Gadus chalcogrammus*) midwater abundance and distribution were assessed from Bristol Bay to the U.S.-Russia Convention Line from 6 June to 26 August 2018 using acoustic-trawl (AT) survey methods aboard the NOAA ship *Oscar Dyson*. In addition to surveying the traditional (core) survey area, we also surveyed a region northeast of St. Matthew (the northern extension). Water column temperatures were cooler in 2018 (mean sea surface temperature (SST) 8.5 °C, bottom temperature 3.7 °C) compared with temperatures during the previous AT survey in 2016 (mean SST 11.4°C, bottom temperature 3.9 °C), but still much warmer than in prior cold years (2006-2014; SST means between 4.9° and 6.8 °C). Walleye pollock biomass was concentrated in the regions north of Pribilof and Zhemchug canyons, and east of Pervenets Canyon, primarily between the 100- and 200-m isobaths. The estimated amount of pollock in midwater (between 16 m from the sea surface and 0.5 m off the sea floor) in the U.S. EEZ core survey area was 5.57 billion fish with a biomass of 2.50 million metric tons (t), less than half of the 2016 estimate of 12.2 billion fish with a biomass of 4.83 million metric tons. This estimate includes the lower water column (3 m to 0.5 m), estimated by combining acoustic and bottom trawl data and previously reported separately. Pollock east of 170° W numbered 1.28 billion fish and weighed 0.74 million t (27% of the total shelf-wide biomass, including the northern extension which represented 9% of shelf-wide biomass). Five- and 6-year-old pollock (43 and 45 cm mean fork lengths (FL), respectively) together composed 77.6% of the biomass east of 170° W. Pollock abundance west of 170° W was 4.29 billion fish weighing 1.75 million t (64% of total shelf-wide biomass). These estimates include an 'unsampled' portion of the core area (the three westernmost transects, comprising 6.1% of the core area) which was not surveyed due to ship motor failure. Most pollock west of 170° W were aged 5 and 6 years (42 and 44 cm mean FLs, respectively). The mean biomass-weighted depth of adult pollock (≥ 30 cm FL, age-3+) was 79 m in the region east of 170° W and 97 m west of 170° W. The mean weighted depth of juveniles (< 30 cm FL, ages 1 and 2) west of 170° W (relatively few juveniles were observed east of 170° W) was 106 m, 9 m deeper than adults (97 m). The mean euphausiid abundance estimate for 2018 was similar to that in 2004, a relatively low year in the index.

CONTENTS

ABSTRACT iii

INTRODUCTION 1

METHODS 2

ACOUSTIC EQUIPMENT, CALIBRATION, AND DATA COLLECTION 2
TRAWL GEAR AND OCEANOGRAPHIC EQUIPMENT 3
SURVEY DESIGN 5
DATA ANALYSIS 9

RESULTS AND DISCUSSION 11

CALIBRATION 11
WATER TEMPERATURE 17
TRAWL SAMPLING 18
ACOUSTIC BACKSCATTER AND ABUNDANCE ESTIMATES 13
POLLOCK LENGTH AND AGE COMPOSITION 15
LENGTH AND WEIGHT AT AGE 13
POLLOCK VERTICAL DISTRIBUTION 16
HISTORICAL POPULATION TRENDS 17
AN ACOUSTIC INDEX OF EUPHAUSIID BIOMASS IN THE EBS 25

ACKNOWLEDGMENTS 27

CITATIONS 29

TABLES AND FIGURES 35

APPENDIX I. -- ITINERARY 75

APPENDIX II. -- SCIENTIFIC PERSONNEL 77

INTRODUCTION

Scientists from the Midwater Assessment and Conservation Engineering (MACE) Program of the Alaska Fisheries Science Center (AFSC) have conducted summer acoustic-trawl (AT) surveys to estimate the abundance and distribution of walleye pollock (*Gadus chalcogrammus*) on the eastern Bering Sea (EBS) shelf since 1979. Surveys were conducted triennially through 1994 and have been conducted either annually or biennially since 1994. The surveys generally extend from seafloor depths of 50 m to 1,000 m, encompassing the middle (50 to 100 m isobaths) and outer (100 to 200 m isobaths) domains of the Bering Sea shelf. The 2018 AT survey was carried out between 6 June and 26 August aboard the NOAA ship *Oscar Dyson*. The primary objective was to estimate walleye pollock midwater abundance and distribution within the U.S. portion of the Bering Sea shelf using AT survey methods. Due to vessel propulsion problems, the survey was cut short, and the last three transects were not completed. This unsampled area (the filled polygon in Fig. 2) constituted 6.1% of the traditional (core) survey area. Abundance in this unsampled area was estimated by using acoustic observations from the bottom trawl surveys in combination with AT survey trawls on two transects adjacent to the unsampled area.

An area to the north of the core survey area (northern extension) was added in 2018 in response to reports of observations of pollock extending north of the core survey area in 2016 (Honkalehto et al. 2018), Saildrone observations (Mordy et al. 2017, De Robertis et al. 2019), and analysis of trawl and fish backscatter data collected in this northern region from the NOAA summer EBS bottom trawl survey in 2017 (Stevenson and Lauth, 2018, Levine and De Robertis, 2019). The adjoining Russian portion of the EBS shelf was not surveyed as permission to survey that region was not granted in 2018. Additional sampling included conductivity-temperature-depth (CTD) probes to characterize shelf oceanographic conditions.

Here we report estimates of walleye pollock abundance and biomass by size and age from near the sea surface to 0.5 m off the seafloor (Honkalehto et al. 2018, and see Lauffenburger et al. 2017). Other survey results presented include 1) acoustic system calibration, 2) physical

oceanographic (temperature) spatial patterns, 3) pollock biomass spatial patterns, 4) spatial patterns of non-pollock backscatter, 5) pollock biomass-weighted vertical distributions, 6) AT survey time series of pollock abundance estimates, and 7) a preliminary estimate of an AT euphausiid biomass index.

METHODS

MACE scientists conducted the AT survey (cruise DY2018-07) aboard the NOAA ship *Oscar Dyson*, a 64-m stern trawler equipped for fisheries and oceanographic research. The vessel itinerary and scientific personnel list are presented in Appendices I and II.

Acoustic Equipment, Calibration, and Data Collection

Acoustic measurements were collected with a Simrad EK60 scientific echo sounding system (Simrad 2008, Bodholt and Solli 1992). Five split-beam transducers operating at 18, 38, 70, 120, and 200 kHz were mounted on the bottom of the vessel's retractable centerboard, which was extended 9.15 m below the water surface.

Standard sphere acoustic system calibrations were conducted at the start and end of the cruise to measure acoustic system performance. The vessel dynamic positioning system was used to maintain the vessel in a stationary position during calibrations. A tungsten carbide sphere (38.1 mm diameter) suspended below the centerboard-mounted transducers was used to calibrate the 38-, 70-, 120-, and 200-kHz systems. A 64-mm diameter copper sphere was used to calibrate the 18-kHz system. On-axis sensitivity (i.e., transducer gain and s_A correction) was estimated from measurements with the sphere placed in the center of the beam following the on-axis method described in Demer et al. (2015). Transducer beam characteristics (i.e., beam angles and angle offsets) were estimated by moving the sphere in a horizontal plane through the beam and fitting these data to a second order polynomial model of the beam pattern using the EK60's calibration utility (Simrad 2008, Jech et al. 2005). The equivalent beam angle (which is used to characterize the volume sampled by the beam) cannot be estimated from the calibration approach used (knowledge is required of the absolute position of the sphere, see Demer et al. 2015). Thus,

the transducer-specific equivalent beam angle measured by the echosounder manufacturer, and corrected for the local sound speed (see Bodholt 2002), was used in data processing.

Acoustic (raw) data were collected at the five frequencies with Simrad ER60 (v. 2.4.3) software. Acoustic telegram data were also logged with Echoview EchoLog 500 (v. 8.0.1) software as a backup. Echosounder ping rate was variable depending on range to the seafloor but was typically about 1.0 s^{-1} at depths < 200 m. Results derived from volume backscatter presented in this report, including calibration, are based on 38 kHz raw echo integration data with a post-processing S_v threshold of –70 dB re 1 m^{-1}. Acoustic measurements were analyzed from 16 m below the surface to within 0.5 m of the sounder-detected bottom using Echoview post-processing software (v. 8.0.104). The sounder-detected bottom was calculated using the mean of sounder-detected bottom lines for all five frequencies (Jones et al. 2011), and then manually quality-checked.

Trawl Gear and Oceanographic Equipment

Midwater and near-bottom acoustic backscatter was sampled using an Aleutian wing 30/26 trawl (AWT). This trawl was constructed with full-mesh nylon wings and polyethylene mesh in the codend and aft section of the body. The headrope and footrope each measured 81.7 m (268 ft). Mesh sizes tapered from 325.1 cm (128 in) in the forward section of the net to 8.9 cm (3.5 in) in the codend, where it was fitted with a single 12 mm (0.5 in stretched-mesh) codend liner. An 83-112 Eastern bottom trawl without roller gear and fitted with a 12 mm codend liner was used in three locations to supplement bottom-trawl data used to compute near-bottom biomass for the northern extension area of the survey. The AWT and bottom trawl were fished with 5 m^2 Fishbuster trawl doors each weighing 1,089 kg. The AWT was fished with ~113 kg (250 lbs) tom weights. Vertical net openings and depths were monitored with either a Simrad FS70 third-wire netsounder or a Furuno CN24 acoustic-link netsonde attached to the headrope. A Simrad ITI unit was used as a backup. The AWT's vertical net opening averaged 21.1 m and ranged from 15.6 to 28.0 m. The bottom trawl vertical net opening averaged 2.1 m and ranged from 2.0 to 2.4 m. Detailed trawl gear specifications are described in Honkalehto et al. (2002). A small-mesh (12 mm) recapture (also called 'pocket') net was permanently attached 10 meshes aft of the leading edge of the third bottom panel of the AWT intermediate, 19.4 m forward of the

codend, to sample escapement. The net recaptures organisms that escape through the larger meshes of the trawl. Catch in the recapture net was recorded independently from the catch in the codend. These data are being used in ongoing research to estimate the trawl selectivity of the AWT and to gauge escapement of juvenile pollock and other small fishes (Williams et al. 2011). Recapture net data were not used to adjust trawl codend catches or other estimates reported here.

The AWT also included a stereo camera-trawl (CamTrawl) system used on nearly all hauls to autonomously collect stereo images to identify species and estimate their length as they pass through the trawl (Williams et al. 2010a, b). The CamTrawl consists of two cameras, strobes, and associated electronics mounted within a frame attached to the midsection of an AWT just forward of the codend. The CamTrawl was also used to enumerate age-0 pollock which were not retained in the codend, to estimate the potential impact of age-0s contribution to the age 1+ pollock backscatter (Appendix II).

A Methot frame trawl was used to sample backscatter with a frequency response consistent with that from euphausiids. This trawl (described in Methot [1986]) had a rigid square frame measuring 2.3 m on each side, which formed the mouth of the net. Mesh sizes were 2 by 3 mm in the body of the net and 1 mm in the codend. A 1.8 m dihedral depressor was suspended below the frame and a 45 kg lead weight was attached to the bottom of the frame to generate additional downward force. A calibrated General Oceanics flowmeter was attached in the mouth of the trawl. The number of flowmeter revolutions, the net mouth opening, and time in the water were used to determine the volume of water filtered during the haul. The trawl was towed from the stern on a single cable fed through a block on the A-frame. Trawl depths were monitored using a Simrad ITI acoustic link temperature-depth sensor attached to the bottom of the Methot frame. All survey operations were conducted as specified in NOAA protocols for fisheries acoustics

surveys and related sampling[1], and the acoustic units used are defined in MacLennan et al. (2002).

Physical oceanographic measurements were made throughout the cruise. Temperature-depth profiles were obtained at trawl sites with a Sea-Bird Electronics temperature-depth probe (SBE-39) attached to each trawl headrope. These temperature profile data were subsequently averaged by geographic area and 1-m vertical depth bins. Conductivity-temperature-depth (CTD) measurements were made with a Sea-Bird SBE 911*plus* CTD at calibration sites and throughout the survey to describe EBS shelf temperature features associated with pollock and euphausiids. CTD casts were made at the closest point along a survey transect to 16 of 19 nominal station locations selected to provide a systematic, representative set of water column observations (P. Stabeno, PMEL, pers. commun.) to complement SBE profiles. Three nominal stations in the Russian EEZ were not sampled. A cast was also made wherever the ship stopped surveying for the night if it was more than 20 nautical miles (nmi) from another nighttime cast. This sampling strategy is repeatable each survey year with minimal impact on other survey operations. Salinity bottle samples (e.g., one bottle every other day, alternating at surface and bottom of cast) were collected from the casts to calibrate the CTD conductivity sensor. Sea surface temperature data were measured using the ship's Sea-Bird Electronics sea surface temperature system (SBE 38, accuracy ± 0.002° C) located near the ship's bow, approximately 1.4 m below the surface. At times when the SBE-38 was not operating, sea surface temperatures were taken from a Furuno T-2000 temperature probe (accuracy ± 0.2 °C) located amidships 1.4 m below the surface. During this summer season, the SBE 38 was used 95% of the time and the Furuno was used 5% of the time. These and other environmental data were recorded using the ship's Scientific Computing Systems (SCS). Surface water temperatures were plotted as 1 nautical mile (nmi) averages along the vessel's cruise track, contours are generated using integrated distance-weighting (IDW) in ArcGIS 10.

[1] National Marine Fisheries Service (NMFS) 2013. NOAA protocols for fisheries acoustics surveys and related sampling (Alaska Fisheries Science Center), 23 p. Prepared by Midwater Assessment and Conservation Engineering Program, Alaska Fish. Sci. Center, Natl. Mar. Fish. Serv., NOAA. Available online: http://www.afsc.noaa.gov/RACE/midwater/AFSC%20AT%20Survey%20Protocols_Feb%202013.pdf.

Survey Design

The survey design initially consisted of 28 north-south oriented parallel transects spaced 20 nmi apart over the Bering Sea shelf from 162° W (west of Port Moller, Alaska) to about 178° 53 W, excluding Russian waters. The initial design also included a northern extension with similar spacing (Fig. 1). To add an element of randomization to this systematic transect design, the longitudinal position of the first transect was offset by a random distance in the range of ± 20 nmi (i.e., the inter-transect distance), and then subsequent transects were offset by 20 nmi from that point (Rivoirard et al. 2000). The initial plan was amended with the following three changes: 1) due to an engine malfunction during leg 2, the remaining northern extension transect spacing was increased from 20 nmi apart to 25-40 nmi depending on proximity to completed 20 nmi spaced transects in the core area, and 2) an additional leg (3b) was added to the survey. Finally, 3) A second *Oscar Dyson* engine malfunction during leg 3b forced us to drop the final three transects (Figs. 1 and 2). Echo integration and trawl information were collected during daylight hours (typically between 0600 and 2400 local time). Daytime Methot trawls targeted suspected macrozooplankton backscatter to support an acoustic-trawl estimate of Bering Sea euphausiid ('krill') density.

Nighttime hours were devoted to special projects, which included collection of additional physical oceanographic data, additional trawl hauls for species identification, and deployment of specialized sampling devices. The latter included tests of a lowered target strength (TS) measurement package (dropTS). In addition to these nighttime projects, AFSC scientists from the Recruitment Processes Alliance (RPA) participated on Leg 3b to collect data on juvenile groundfish, including Methot and bongo net tows. Two drifters were also deployed for Pacific Marine Environmental Laboratory (PMEL) researchers during the survey.

Trawl catches were sampled to identify the species composition, length, and other biological characteristics of animals in acoustically observed aggregations. A portion of the pollock captured in midwater and bottom trawls was sampled to determine length and sex composition, sexual maturity, body weight, and to collect otoliths for age determination. If mixtures of juveniles and adult pollock were encountered in a haul, the predominant size groups were sub-

sampled separately. Approximately 50 to 400 individuals were randomly sampled for length, and about 20 to 50 were also sampled for body weight, maturity, sex and age. Fork lengths (FL) were measured to the nearest millimeter with an electronic measuring board (Towler and Williams 2010). An electronic motion-compensating scale (Marel M60) was used to weigh individual walleye pollock specimens to the nearest 2 g. Maturity was determined by visual gonad inspection and fish were categorized as immature, developing, mature/pre-spawning, spawning, or post-spawning[2]. Walleye pollock otoliths were stored in individually marked vials of glycerol-thymol solution. Otoliths were read by AFSC scientists in the Age and Growth Program following the survey.

Additional biological samples were taken from most species in the catch. For select species or broader taxonomic groups, 25-100 lengths, and 10-75 lengths paired with individual weights (i.e., length-weights), were taken depending on species and dominance in the catch. These included young-of-the-year (age-0) pollock, forage fishes (e.g., capelin, eulachon, herring, sand lance, northern smoothtongue, myctophids), Pacific cod, rockfishes, and large jellyfishes. For all other species except sessile invertebrates caught in bottom trawls, either 10 length-weights were collected (organisms weighing ≥ 5 g) or else 10 individuals were weighed in aggregate and then length was measured individually (organisms weighing < 5 g). Fork lengths were measured for all fish species, except for Pacific viperfish and myctophids, where total length (TL) and standard length (SL), were measured, respectively. Shrimp carapace lengths, squid mantle lengths, and jellyfish bell diameters were also measured.

Pocket net catch data were recorded independently from the catch in the codend. Pocket net catches were sorted to species for fishes or broader taxonomic groups for invertebrates, subsampled if necessary, counted, and weighed. Twenty or more lengths were measured for each fish species caught in pocket nets. Trawl station and biological measurements were digitally recorded directly into a database using the Catch Logger for Acoustic Midwater Surveys (CLAMS), a customized software program developed by MACE scientists.

[2] ADP Code Book. 2016. Unpublished document. Resource Assessment and Conservation Engineering Division, Alaska Fisheries Science Center, 7600 Sand Point Way NE, Seattle WA 98115.

CamTrawl images were viewed and annotated with age-0 pollock counts if present. Age-0 pollock encountered during this survey are small and not well retained in the AWT. However, they can be detected in CamTrawl stereo camera images, particularly in near-surface waters (Williams et al., 2010b). This led to concern that backscatter from age-0 pollock not retained in the trawl would be interpreted as being from older fish, leading to over-estimates of the abundance of age-1^+ pollock. A simple sensitivity analysis was performed to better quantify the potential impact of backscatter from age-0 pollock that were not retained in the trawl on estimates of age-1^+ pollock. By assessing the ratio of age-0 pollock to age-1^+ pollock in CamTrawl images in 10 m layers, and using a worst-case estimate of trawl selectivity (i.e., assuming that age-0 pollock act as passive particles exhibiting no herding behavior, and that all age-1^+ pollock entering the trawl mouth are retained), an upper bound of the effect was calculated. Survey-wide, these calculations indicated that age-0 pollock accounted for no more than 3.4% of the backscatter identified as pollock in the survey area (see Appendix II for details). These calculations were taken to mean that the effects of poorly sampling age-0 pollock on the survey estimates of older pollock are minor for this survey. In large part, this is because age-0 pollock tend to be distributed shallower than older pollock during daytime when the survey is conducted. Given that even the upper-bound estimate of the impact of backscatter from age-0 pollock on the abundance estimate of larger pollock is negligible, no further corrections were pursued.

Additionally, an automated image processing routine was used to extract length estimates for pollock seen in the CamTrawl images (Chuang et al., 2011). Lengths obtained from CamTrawl were used primarily in comparisons with physically measured fish lengths from the codend to evaluate the accuracy of the imaged-based lengths.

Methot catches were transferred to a ~ 0.5 × 1 m rectangular plastic tub. Large organisms such as jellyfishes and small fishes were removed, identified to the lowest taxonomic group possible, weighed, and body lengths or diameters (jellyfishes) measured. The remainder of the catch was placed on a 1-mm mesh screen to remove as much seawater as possible and weighed. A subsample of this zooplankton mixture was then weighed and sorted into broad taxonomic

groups, while a second subsample was weighed and preserved in a 5% buffered formalin solution for more detailed enumeration at the Polish Sorting Center in Szczecin, Poland. These results will be reported elsewhere.

Several special projects required additional sampling. Pollock ovaries were collected from all maturity stages of females for a reproductive biology study, along with gonad and liver weight measurements (M. Dorn/S. Neidetcher, AFSC). Pacific cod fin clips were collected for genetic studies (I. Spies, AFSC). Pollock specimens were frozen for observer training (B. Mason, AFSC). When time allowed at night, a pollock catch-related mortality study was attempted. This involved hook-and-line fishing for adult pollock specimens which were then held for several days in a live tank (A. McCarthy, AFSC). Methot tows and euphausiid samples were taken as part of an ongoing study of euphausiid acoustical properties and net avoidance (P. Ressler, AFSC).

Data Analysis

Acoustic backscatter at 38 kHz was classified as age-1+ walleye pollock (≥ 8 cm), non-pollock fishes, a mixture containing age-1+ pollock, a mixture containing primarily age-0 pollock, or an undifferentiated mixture (primarily plankton and small fishes). Backscatter was integrated over 0.5 nmi horizontal elementary distance sampling units (EDSUs) by 10 m vertical resolution cells (*i*) to within 0.5 m of the bottom and exported to a database. Classification was based on catch composition from nearby hauls as well as on the appearance and vertical distribution characteristics of the aggregations. In an EBS shelf region representing about 10% of the core survey area located just north of the Pribilof Islands, a two-part filter was applied where it was difficult to separate age 1+ pollock backscatter from that of co-occurring acoustic targets, which exhibited near-resonant scattering at 18 kHz. These targets were not retained in our trawls. The first part of the filter consisted of a frequency-response criterion to remove near-resonant targets. Specifically, data were averaged into 5 ping by 5 m deep cells; those cells where the 18-120 kHz frequency response was > 1 standard deviation above the expected frequency response for pollock were removed by the filter (i.e., cases where $Sv_{18kHz} - Sv_{120kHz} > 4.8$ dB were excluded;

see De Robertis et al. 2010). The second part of the filter changed the integration threshold applied to the full-resolution sample data from -70 to -60 dB re 1 m^2, which served to exclude low-intensity backscatter unlikely to be from pollock.

Walleye pollock abundance was estimated by combining acoustic and trawl information. In previous surveys, backscatter from regions classified as pollock was assumed to be entirely from pollock. In this survey, new methods (De Robertis et al. 2017) were adopted that account for the backscatter from other, non-pollock species in the catch. Acoustic backscatter was assigned to strata based on the appearance and vertical distribution of the aggregations. Strata containing backscatter not considered to be from pollock (e.g., the near-surface mixture of unidentifiable backscatter) were excluded from further analyses. Trawls targeting the species of interest (in this case pollock) were associated with a stratum. For example, if juvenile pollock were consistently found at shallow depths and adult pollock layers were consistently found at deeper depths in the same area, the backscatter dominated by juveniles would be assigned to a shallow stratum (A) and the backscatter dominated by adults would be assigned to a deep stratum (B). Hauls that sampled juvenile aggregations would be assigned to stratum A, and hauls that sampled the adult layer would be assigned to stratum B.

Backscatter that was primarily attributed to age 1+ pollock was further apportioned between pollock and other co-occurring acoustic taxa using TS-to-length relationships from the literature and the catch composition at the geographically nearest haul location within each stratum. TS relationships were used for fishes with swim bladders, fishes without swim bladders, jellyfish, squid, and pelagic crustaceans (Stienessen et al. 2019). The general approach was to apply generic TS relationships for rare species. However, if a species was relatively abundant (defined as contributing > 5% of the numbers or weight to the total catch during the survey), a more specific TS to length relationship was used, if available. Pollock and *Chrysaora* jellyfish each contributed > 5% by weight to the survey catches and species-specific TS relationships were applied (Appendix III, Table 1).

Pollock abundance was computed for each 0.5 nmi EDSU based on the following approach. The

echosounder measures backscattering strength, which is integrated vertically to produce the nautical area scattering coefficient, s_A (units of m^2 nmi^{-2}; MacLennan et al. 2002). The backscattering from an individual fish is referred to as its backscattering cross-section, σ_{bs} (m^2), or in logarithmic terms as its target strength, TS (dB re 1 m^2), where,

$$TS = 10 \log10 \sigma_{bs} . \qquad \text{Eqn. (1)}$$

The estimated TS-to-length relationship for walleye pollock (Foote and Traynor 1988, Traynor 1996) is

$$TS = 20 \log10 (L)-66 , \qquad \text{Eqn. (2)}$$

where L = FL in centimeters.

The numbers of fish of species *s* and of length *l* ($N_{s,l}$) captured in each haul *h* were used to compute the proportion of acoustic backscatter associated with each species and length. First the number of individuals in the catch were converted to a proportion ($P_{s.l,h}$)

$$P_{s,l,h} = \frac{N_{s,l,h}}{\sum_{s,l,} N_{s,l,h}} ,$$

where $\sum_{s,l,} P_{s,l,h} = 1$. Eqn. (3)

The mean backscattering cross section (an areal measure of acoustic scattering in m^2 – MacLennan et al., 2002) of species *s* of length class *l* is

$$\sigma_{bs_{s,l}} = 10^{(0.1 \cdot TS_{s,l})} , \qquad \text{Eqn. (4)}$$

where TS is the target strength (dB re m^2) computed using the relationships in Appendix III, Table 1 and Equation 2.

The proportion of backscatter from species s of length class l in haul h ($PB_{s,l,h}$) is computed from the proportion of individuals of species s and length class l estimated from haul h ($P_{s,l,h}$) and their backscattering cross section,

$$PB_{s,l,h} = \frac{P_{s,l,h} \cdot \sigma_{bs_{s,l}}}{\sum_{s,l,}(P_{s,l,h} \cdot \sigma_{bs_{s,l}})} \quad . \qquad \text{Eqn. (5)}$$

The measured nautical area backscattering coefficient (s_A) at interval i was allocated to species and length as follows:

$$s_{A_{s,l,i}} = s_{A_i} \cdot PB_{s,l,h} \ , \qquad \text{Eqn. (6)}$$

where haul h is the nearest haul within a stratum assigned to represent the species composition in a given 0.5 nmi along-track interval i . The nearest geographic haul was determined by using great-circle distance to find the nearest trawl location (defined as the location where the net is at depth and begins to catch fish) out of the pool of hauls assigned to the same stratum (see above for details) closest to the start of interval i.

The abundance of pollock of length l in interval i was estimated from the area represented by that interval (A_i, nmi^2), the mean areal backscatter attributed to pollock (i.e., $s = pk$) in given length/size class l ($s_{A_{pk,l,i}}$, m^2 nmi^{-2}), and mean backscattering cross-section of pollock at that size ($\sigma_{bs_{pk,l}}$ m^2):

Numbers at length l: $N_{pk,l} = \sum_i \left(\frac{s_{A,pk,l,i}}{4\pi\sigma_{bs_{pk,l,i}}} \cdot A_i \right)$. Eqn. (7)

Biomass at length l: $B_{pk,l} = \Sigma_i \, (W_{pk,l} \times N_{pk,l,i})$, Eqn. (8)

where $W_{pk,l}$ is the mean pollock weight-at-length in each 1 cm length interval. $W_{pk,l}$ was estimated from the trawl information when five or more walleye pollock were measured within a length

interval. Otherwise, weight-at-length was estimated using a linear regression of the natural log-transformed length-weight data, including a correction for bias attributable to back-transformation (De Robertis and Williams 2008).

The abundance at age was computed from $Q_{pk,l,,j}$, the proportion of j-aged pollock of length l as follows:

Numbers at age j: $N_{pk,j} = \Sigma_i (Q_{pk\ l,,j} \times N_{pk,l})$ Eqn. (9)

Biomass at age j: $B_{pk,j} = \Sigma_i (Q_{pk,l,,j} \times B_{pk,l})$. Eqn. (10)

The abundances across the survey area were estimated by adding the estimates for all length or age classes. Due to geographic growth differences, walleye pollock are typically larger, and heavier at age, east than west of 170° W (Traynor and Nelson 1985, Honkalehto et al. 2002). Therefore biomass was estimated by multiplying numbers-at-length by pollock mean weight-at-length using two length-weight strata, one for east and one for west of 170° W. Pollock abundance by length was converted into abundance- and biomass-at-age using two age-length keys, one each for east and west of 170° W. Ages were estimated for lengths where no age structures were available using Gaussian simulations of pollock length distributions occurring for each age bin within the age-length key (see Jones et al. 2017). Walleye pollock distribution and abundance were summarized by sub-areas east and west of 170° W, the Steller sea lion Conservation Area (SCA), and the northern extension area (Fig. 1).

For comparison with previous surveys, pollock estimates were also computed with the traditional analysis methods in EBS AT surveys prior to 2018 (Honkalehto et al. 2008, 2018). Walleye pollock length compositions from AT survey hauls were combined into regional length strata (27 in 2018) based on geographic proximity, length composition similarities, and backscatter characteristics. Estimates of biomass at length were computed in the same way as is detailed above except that 1) the traditional method apportioned 100% of the backscatter visually classified as pollock to pollock, whereas the newer method apportions backscatter based on the geographically nearest haul species composition, and 2) hauls are not grouped into regional

length strata in the newer method. Given that pollock dominate midwater scatterers, and that the population is generally dominated by several geographically contiguous age classes in the EBS, the two methods are expected to produce similar results. In 2018, the traditional method resulted in pollock abundance and biomass estimates that were very similar to the newer methods (-0.8% and 1.2% difference in numbers and biomass, respectively) and are not reported here.

Historically, AT survey results on the U.S. EBS shelf were presented for the water column between 16 m and 3 m off the seafloor. The analysis did not extend deeper than 3 m above the seafloor because 1) diverse catches in bottom trawl survey suggested that pollock may not dominate the backscatter close to the seafloor, and 2) the annual bottom trawl (BT) survey samples to a nominal depth of 2.5-3.0 m above the seafloor in the U.S. EEZ (Conner and Lauth 2017, Ianelli et al. 2016, Lauth and Conner 2014). An approach was developed (Lauffenburger et al. 2017) to estimate the acoustic contribution of pollock relative to other species in the diverse region between 0.5 and 3 m off bottom using a combination of AT and BT data and first applied to EBS survey results in 2016 (Honkalehto et al. 2018). This report presents AT survey results with the upper and lower water column combined, from 16 m depth to 0.5 m off-bottom.

The vertical distribution of pollock was computed by plotting the mean biomass in each 10 m depth bin, at the midpoint of each bin, relative to 1) the surface and 2) the sea floor. The overall mean weighted depth (mwd) and the mean weighted distance off the seafloor were computed for adult pollock (≥ 30 cm FL), and juvenile pollock (< 30 cm FL) east and west of 170° W in the U.S. EEZ as follows:

$$mwd = \frac{\sum_d (B_d \times d)}{\sum_d (B_d)}, \qquad \text{Eqn. (11)}$$

where B is biomass (kg), and d is either depth or distance from the seafloor (m) for each depth bin-EDSU combination.

Relative errors in the core survey area biomass and abundance estimates associated with spatial structure in the acoustic data were derived using a one-dimensional (1D) geostatistical method (Petitgas 1993, Williamson and Traynor 1996, Walline 2007). "Relative estimation error" is defined as the ratio of the square root of the 1-D estimation variance ($variance_{sum}$) to the biomass estimate (i.e., the sum of biomass over all transects, $biomass_{sum}$, kg):

$$Relative\ estimation\ error_{1\text{-}D} = \frac{\sqrt{variance_{sum}}}{biomass_{sum}} \quad . \qquad \text{Eqn. (12)}$$

Geostatistical methods were used for error computation because they account for the observed spatial structure in fish distribution. These errors quantify the sampling variability (Rivoirard et al. 2000). Other sources of error (e.g., availability to the survey, target strength, biases associated with trawl sampling) are not included in the estimate. Error estimates were computed for the water column from 16 m to within 3 m off bottom, between 3 m and 0.5 m off bottom, and for the whole water column (16 m to within 0.5 m off bottom).

Unsampled area

Due to an unforeseen ship failure, the final three transects of the 2018 AT survey could not be completed (red transects in Fig. 2). This 6,016 nmi^2 "unsampled area" (filled polygon in Fig. 2) extended from 10 nmi from the *Oscar Dyson's* last transect out to the 200 m depth contour and is a relatively small fraction of the survey area sampled in 2018 (92,283 nmi^2). In other words, about 6.1% of the normal survey area was missed.

To estimate the fraction of pollock in this unsampled area, we opportunistically used acoustic data that were collected by NOAA's 2018 eastern Bering Sea BT survey vessels for another purpose (estimating the AVO pollock backscatter index; Honkalehto et al. 2011), trawl data from adjacent areas surveyed by *Oscar Dyson* during the AT survey, and bottom trawl information from the BT survey hauls. The small area at the "shelf break" (> 200 m depth) normally covered

by the AT survey in this region was omitted since this area was not covered by the bottom trawl vessels.

The 38 kHz acoustic data from the two chartered BT vessels FV *Vesteraalen* and FV *Alaska Knight* inside the unsampled area were identified (Fig. 2). The vessels were equipped with Simrad ES60 echosounders and ES38B 38 kHz transducers. Data collected during daytime at speeds > 4 knots were processed in Echoview using equivalent methods as for the *Oscar Dyson* survey data. This resulted in 435 nmi of trackline in the unsampled area on 27-29 July 2018. The repeating 'triangle wave' error present in ES60 data were removed (Honkalehto et al. 2011). The average of two sphere calibrations conducted before and after the 2018 BT survey was applied in data post-processing, and regions consistent with backscatter from walleye pollock were identified. The 38 kHz backscatter consistent with pollock was exported every 0.5 nmi along the vessel track from 16 m below the sea surface to 0.5 m above the sounder-detected bottom. Abundance was estimated by averaging the available backscatter observations in the unsampled area, estimating the density of pollock (i.e., fish nmi^{-2}), and extrapolating this point estimate of density over the unsampled area.

Abundance (*N*, total number of pollock in the unsampled area) was computed as follows:

$$N = \frac{\overline{s_A}}{4\pi\hat{\sigma}_{bs,PK}} PB_{pk} A \quad , \qquad \text{Eqn. (13)}$$

where $\overline{s_A}$ is the mean nautical area scattering coefficient in the unsampled area (MacLennan et al. 2002) attributed to pollock, and PB_{pk} is the proportion of this backscatter estimated to be from pollock. $\overline{s_A}$ was estimated as the average over all 0.5 nmi segments in the unsampled area, and $\hat{\sigma}_{bs,PK}$ is the mean backscattering cross section of pollock (see De Robertis et al. 2017).

As in the AT survey, different methods are used to estimate abundance > 3 m from the seafloor and < 3 m from the seafloor. For > 3 m from the seafloor, 10 AT survey AWTs conducted on 15-20 August on adjacent transects 24 and 25 (Fig. 1) were used to estimate $\hat{\sigma}_{bs,PK}$.

No pelagic trawls were available in the unsampled area to quantify acoustic scatters > 3 m from the seafloor. The size distribution estimated in the *Dyson* acoustic-trawl survey on two transects adjacent to the unsampled area (transects 24, 25; Fig. 1) was assumed to be the same as in the unsampled area and was applied to the unsampled area. The proportion of backscatter in areas classified as age-1+ pollock PB_{pk} was estimated as the average value from these 10 hauls (PB_{pk} = 0.994) using the methods described in equations 5-8. This value was used in equation 13 above to convert the BT survey acoustic backscatter to estimates of pollock abundance. The abundance at length and age were computed with the same methods as the AT survey. In the near-bottom 0.5 to 3 m layer, the method of Lauffenburger et al. (2017) was applied, but with the acoustic data from the bottom trawl vessels substituted for that from the *Oscar Dyson* to estimate $\overline{s_A}$. In this method, the bottom trawl hauls conducted during the 2018 bottom trawl survey and a statistical model are used to estimate PB_{pk} and $\hat{\sigma}_{bs,PK}$.

RESULTS AND DISCUSSION

Calibration

Initial acoustic system settings for the survey were based on results from the 7 June calibration (Table 1). The end-of-cruise sphere 38 kHz calibration on 25 August exhibited a small difference (0.26 dB) from the initial calibration. This was slightly larger than the discrepancy typically observed on most surveys (< 0.2 dB). However, this discrepancy is small in an absolute sense and within previous reports of repeat calibration precision for this transducer (Knudsen et al. 2009). There was no evidence of equipment malfunction during this or subsequent surveys. Acoustic data were thus processed using an average of the pre- and post-cruise (linearized) gain values. Using the average of both calibrations resulted in a change of 6.3% compared backscatter values processed with either the pre- or post-cruise gains.

Water Temperature

The mean sea surface temperature (SST) during the 2018 survey was 8.5° C (range 5.2°-10.6° C; Fig. 3, upper panel). This was cooler than 2016 (mean SST 11.4°C , range 7.4°-14.0° C), and 2014 (mean SST 9.6° C, range 6.4°- 12.4° C), but still much warmer than relatively cold

conditions experienced during the 2006-2012 surveys (means between 4.9° - 6.8° C). Seasonal warming of surface waters typically leads to maximum SST in August, (Overland et al. 1999) and the warmest surface temperatures observed in the 2018 EBS survey were in Pervenets Canyon in late August. Surface temperatures were coolest north of the Pribilof Islands in late June.

Bottom temperatures in 2018 from CTD casts were higher than all recent years with the exception of the 2016 survey (mean bottom temperature 3.7 vs. 3.9° C in 2016; Fig. 3, lower panel). A region of bottom temperatures < 2° observed previously in the Bering Sea (i.e., termed cold-pool by Wyllie-Echeverria and Wooster 1998) was present but was limited to a small area south of St. Lawrence Island; much farther north than in past years. Temperature-depth profiles from trawl headrope sensors indicate that the water column was vertically stratified with a thermocline at roughly 20-40 m from the surface. The EBS shelf region west of 170° W was somewhat more vertically stratified than east of 170°W (Fig. 4). Trawl headrope temperatures below the thermocline in the northwest portion of the survey area were > 2° C. Temperatures in this layer were cooler, but > 0° C in 2014, and well below 0° C in recent cold years (2007-2012). The AFSC BT survey, which started earlier than the AT survey, measured similar surface and bottom temperature increases in 2018 compared with prior survey years (R. Lauth, AFSC, personal communication).

Trawl Sampling

Biological data and specimens were collected from 119 trawl hauls (Table 2, Fig. 1). The majority of these hauls (107) targeted backscatter during daytime for species classification during the survey: 97 hauls were conducted with an AWT, 3 with a bottom trawl, and 7 with a Methot trawl. The remaining 12 hauls were either nighttime bongo net tows (6) targeting larval fish or nighttime Methot tows (6) targeting euphausiids. CamTrawl image data were successfully collected during 83 AWT hauls. Biological information collected for walleye pollock and other species is presented by haul in Tables 3-7.

Walleye pollock was the most abundant species in AWT midwater haul catches by weight (83.6%) and by number (90.2%), followed by northern sea nettle jellyfish (*Chrysaora melanaster*; 12.4% by weight and 4.5% by number; Table 3). Pollock was the most abundant species by weight (31.3%; Table 4) and snow crab (*Chionoecetes opilio*) the most abundant by number in AT survey bottom trawl catches, followed by Pacific cod (*Gadus macrocephalus*; 16.5% by weight and 1.4% by number; Table 4). Methot hauls were dominated by weight by northern sea nettles (57.4%) and euphausiids (37.8%), and numerically by euphausiids (98%; Table 5).

Nearly 37,000 lengths were measured and nearly 7,000 specimen weights were collected for all species during the AT survey (Tables 3-5). Of those, over 32,000 lengths, 5,100 weights, and 2,800 otoliths were walleye pollock (Table 6). Most adult pollock (≥ 34 cm; 82% of males and females) sampled were in the developing maturity stage (Fig. 5). Four females (0.2%) were in a spawning stage of maturity (two west of 170° W, two in the northern extension survey area). Walleye pollock mean weight-at-length for fish greater than 55 cm tended to be less in 2018 than those in 2004-2016, and fish over 45 cm in the northern extension survey area were slightly thinner than those in the core survey area (Fig. 6).

Acoustic Backscatter

About 35% of the total acoustic backscatter observed in the core survey area between 16 m below the surface and 3 m off bottom (the midwater layer) during the 2018 survey was attributed to age 1+ walleye pollock. This was lower than the fraction of pollock observed in 2016 (52%), 2014 (45%) and 2012 (56%), and much less than that observed in 2010 (82%; Honkalehto et al. 2018; Honkalehto and McCarthy 2015; Honkalehto et al. 2013, 2012). The low fraction of backscatter attributed to pollock in 2018 could be partly due to the lack of observations in the unsampled area (see Fig. 2); the western-most transects tend to have fewer and lower density non-pollock backscatter layers compared with transects to the east. In the northern extension area, about 38% of the backscatter was attributed to pollock. Pollock were observed in a variety of aggregations including near-bottom layers, small dense schools (cherry balls) in midwater, and diffuse aggregations of individual fish. The remaining non-pollock midwater backscatter was

attributed to an undifferentiated plankton-fishes mixture (60%), or in a few isolated areas, to rockfishes (*Sebastes* spp.) or other fishes (2%). The near-bottom analysis (Lauffenburger et al. 2017) attributed ~ 60.5% of the backscatter in the near-bottom zone in the core survey area to pollock, and 93.7% of the backscatter in the near-bottom of the northern extension area to pollock in 2018. The near-bottom backscatter attributed to pollock in the 2016 survey was 71.6%. The northern extension area contributed about 8.7% more pollock backscatter to the survey over the total in the core survey area.

Abundance Estimates

A total of 5.57 billion midwater walleye pollock weighing 2.50 million t (Tables 7-9) were estimated in the core survey area on the U.S. Bering Sea shelf in 2018. This estimate is for midwater pollock to within 0.5 m of the bottom using AT methodology, and includes the estimate for the area that could not be sampled due to the vessel breakdown (described in next section). This 2018 biomass estimate represents a ~48% decrease compared to the 2016 (4.83 million t) and 2014 (4.73 million t) biomass estimates. It is similar to the biomass estimates in 2010 and 2012 (2.64 million t and 2.30 million t, respectively; Table 7). The relative estimation error for the walleye pollock biomass estimate to within 0.5 m off bottom was 0.039, indicating a patchier distribution of pollock than observed in 2016 (0.019). Pollock were observed throughout the surveyed area between the 100- and 200-m isobaths (Fig. 7). East of 170° W, pollock abundance was 1.28 billion fish, weighing 0.74 million t (27% of total midwater biomass including the northern extension and unsampled area biomass, Fig. 8). This was less than half of the pollock biomass observed east of the Pribilof Islands in the AT survey in 2016 (1.80 million t, Table 7). In the U.S. EEZ core survey area west of 170° W, pollock numbered 4.29 billion and weighed 1.75 million t, which was 64% of total midwater biomass (Table 7, Fig. 8).

The majority of the pollock biomass in the survey was found in the region to the south and west of St. Matthew Island (Fig. 7). Pollock biomass decreased inside the SCA from 0.54 million t in 2016 to 0.23 million t in 2018. Estimates for the entire survey and the SCA correlate well (r^2 = 0.79, $p < 0.001$) throughout the 1994-2018 time series (Table 7). The pollock estimate in the

northern extension area was 492 million fish weighing 0.24 million metric tons, contributing an additional 9% by number and weight compared with the amount of pollock estimated within the core survey area (Fig. 8). In the northern extension, fish were sparsely but evenly distributed between the 50- and 100-m isobaths.

Unsampled Area

The abundance estimate for the unsampled area (0.5 m from the seafloor to 16 m from surface) was 616 million pollock with a biomass of 178,194 t. When expressed as the proportion of the total in the core AT survey area (i.e., the traditional survey area excluding the northern extension), the estimated biomass in the unsampled area was 7.1% of that in the core survey area (11.1% in terms of numbers). This compares well to the proportion of the survey area that was unsampled (6.1% of the core AT survey area), and suggests that pollock were not disproportionately present in the unsampled area. These estimates are included in the pollock numbers and biomass estimates presented above for the core survey area.

Pollock Length and Age Composition

Pollock modal lengths tended to decline to the west (Fig. 8), and length compositions differed between midwater and near bottom layers (Fig. 9). East of 170° W, pollock ranged between 8 and 72 cm FL with a mode of 43 cm (Tables 8, 9; Fig. 8). Very few fish smaller than 30 cm were observed east of 170° W. In the U.S. EEZ core survey area west of 170° W, pollock ranged from 8 to 75 cm FL with multiple modes observed at 17, 26 and 42 cm FL (Tables 8, 9; Fig. 8). Near-bottom juvenile pollock were smaller compared to midwater juveniles throughout the survey area in 2018 (mode of 15 cm near the bottom compared to 17.5 cm in midwater), and adults were larger (mode of 45 cm compared to 42 cm; Fig. 9). Within the northern extension of the survey area fish were slightly longer than in the core survey area (mode of 42 cm with a long right tail), and a few much smaller fish were also seen (mode of 14 cm; Fig. 8).

Five-year-olds (2013 year class) dominated the pollock population in the core survey area, followed by 6-year-olds (2012 year class; Table 10, Fig. 10). One-year-old pollock were not abundant numerically over all but were almost as abundant as the dominant 5-year-olds in the

near-bottom layer (Fig. 11). Five-year-olds were dominant in terms of biomass in the core survey area (46% vs. 23% for 5- and 6-year-olds, respectively; Table 10). East of 170° W, 5-year-olds dominated, with 6-year-old fish a close second (44% and 34 % of biomass, respectively; Fig. 10). West of 170° W, 5-year-old pollock were even more abundant (48% of biomass; Fig. 10) with 6-year-old fish comprising 18% of the biomass. In the northern extension area, 5-year-olds comprised 37% and 6-year-olds comprised 23% of the pollock biomass.

Length and Weight at Age

Mean length- and weight-at-age of pollock were plotted against mean data from combined AT surveys between 2004 and 2016 (Fig. 12). The results show similar patterns to the mean weight-at-length plot (Fig. 6). East of 170° W, fish age 4 and older appear to be shorter (Fig. 12a) and lighter at a given age (Fig. 12b) in 2018 than in the earlier surveys. As is typical for EBS shelf pollock, length-at-age tended to be greater in the east than in the west, even though data were collected up to 6 weeks earlier east of 170° W. This east west difference supports the use of two age-length keys to convert abundance-at-length to abundance-at-age (see Methods). Comparing mean weight-at-age for 2018 with those from 2006 to 2016 showed that weight-at-age were 25-30% lighter for fish < 10 years old in 2018 than they have been historically for the entire EBS survey.

Pollock Vertical Distribution

The vertical distribution of adult and juvenile pollock in the core survey area sampled by the *Oscar Dyson* exhibited subtle differences to one another (Fig. 13). The estimated mean biomass-weighted depth for adult pollock (≥ 30 cm FL) was 79 m in the core region east of 170° W, 14 m deeper than was observed in 2016. Mean biomass-weighted depth was 97 m in the core region west of 170° W. Note that bottom depths gradually increase to the west, which could partially explain the difference in mean depth between areas. Additionally, vertical distribution by size could not be analyzed for the unsampled area west of 170° W in 2018 (Fig. 2), reducing both the area covered and the overall mean depth of the water column compared with prior survey years. Thus mean weighted fish depths in the west were not strictly comparable to those observed in prior surveys. The mean biomass-weighted depth for juveniles (< 30 cm FL, ~ages 1 and 2) west

of 170° W (relatively few juveniles were observed east of 170° W) was 106 m, 9 m deeper than adults (97 m). More than 83% of adults across the shelf were found within 50 m of the bottom (mean weighted depth off bottom 31 m; 40 m east and 26 m west of 170° W), whereas for juveniles west of 170° W, the proportion within 50 m of bottom was higher (91%; mean off-bottom depth 27 m). This may occur (i.e., juveniles deeper, but approximately the same height off bottom) because of differences in bathymetry in the survey area. That is, greater proportions of juveniles compared to adults generally tended to occur farther to the west where bottom depths are relatively deeper (Fig. 13). Finally, although adult biomass increased towards the bottom, juvenile biomass peaked at about 15 m off bottom and then decreased towards the seafloor (Fig. 13).

Historical Population Trends

Spatial distribution of pollock and non-pollock backscatter were evaluated over the period 2006-2018. Earlier spatial patterns (1999-2004) when the survey was also conducted in early summer (June-July) are presented in prior publications (e.g., Honkalehto et al. 2008, 2009, 2010, 2012, 2013; Honkalehto and McCarthy 2015). Pollock population numbers and biomass estimates were also examined from 1994 to highlight patterns emerging with the addition of results from the most recent surveys (e.g., 2014, 2016, 2018).

Pollock spatial distribution trends in midwater were compared for 2006 through 2018 survey years (Fig. 14). Pollock backscatter was relatively low and concentrated west of 170° W from 2006 to 2012. In 2014, pollock backscatter increased east of the Pribilof Islands, resulting in a more widely distributed spatial pattern which continued with even higher backscatter in 2016. The highest pollock backscatter observed in 2018 was distributed west of 170° W along the shelf between 58° N and 62° N, and also just southeast of the Pribilof Islands (Fig. 14). A broad region of more dispersed, low-density pollock backscatter was also observed farther inshore on the shelf between the 100- and 50-m isobaths north of the Pribilofs in 2018.

Temporal patterns in pollock numbers and biomass at length and age since 1994 were examined for pollock between 0.5 m off-bottom and near-surface (Figs. 15-16, and Tables 8-10). Since

2014, the 2012 year class (44-46 cm, 6-year-olds in 2018, the second most abundant 6-year-old cohort in the time series since 1994) and the 2013 year class (42-43 cm, 5-year-olds in 2018), have grown to dominate the midwater abundance. Older year classes have generally contributed less of the total abundance in the AT survey since about 2006 compared to earlier surveys (1994+). For example, the formerly strong 2008 year class (~49-54 cm, 10-year-olds) though present in 2018, only accounted for about 1% of the total numbers.

The EBS pollock population tends to depend on the success of strong year classes at roughly a 3-5 year frequency (Ianelli et al. 2017). Years with good age-1 recruitment are evident in recent AT survey results (e.g., 1997, 2007- 2010, and 2014) by the presence of relatively large numbers of 1-2 year-olds (Table 10; Figs. 15, 16). In 2018, age-1 fish made up just 8% of the population in the core survey area, which suggests that 2018 was not a year of strong age-1 pollock recruitment. Two-year-old pollock comprised 9% of the population numbers. One-year-old pollock were observed in slightly higher numbers in the northern extension area (12% of the population numerically).

Pollock biomass estimates for the stock portion in midwater, near-bottom, and combined were plotted for the U.S. EEZ core survey area between 1994 and 2018 (Fig. 17). The midwater biomass averaged 2.51 million t over this time series. The near-bottom biomass averaged 0.63 million t, which represented about 21% of the average combined biomass of 3.14 million t since 1994. The near-bottom biomass ranged from 12% (2010) to 30% in (2009) of the combined biomass over the time series. In 2018, the near-bottom estimate was 15% of the combined estimate of 2.50 million t. When these new, near-bottom survey estimates were added to the midwater estimates, the combined values were 14 to 43% higher than midwater estimates alone over the 1994-2018 time series.

The non-pollock portion of observed acoustic backscatter at 38 kHz ("non-pollock backscatter") is assumed to represent a temporally-varying mixture of largely unidentified zooplankton and fishes. This backscatter has varied spatially over the AT survey time series. Most non-pollock backscatter (at 38 kHz) has been observed in the upper part of the water column above the

thermocline (Honkalehto et al. 2008). Non-pollock backscatter observed in 2018, a warm year, consisted of three patches; one on the west side of Bristol Bay on transects 1 and 2, the second on the mid-shelf between Unimak Pass and Nunivak Island, and the third south of St. Matthew Island and northwest of the Pribilofs (Fig. 18). Non-pollock backscatter observed in 2004 covered large portions of the survey area on the middle shelf from the Alaska Peninsula to Cape Navarin, Russia (see Honkalehto et al. 2018, Fig. 20). It diminished during years of relatively cold Bering Sea conditions between 2006 and 2010 and has been more widespread in recent years (Fig. 18). Concentrations were observed near the Pribilof Islands in some years (e.g., 2007, 2008, 2012, 2014, and 2016), and in 2018. This backscatter information should be interpreted with caution because the biological composition of the scatterers is unknown.

An Acoustic-trawl Index of Euphausiid Biomass in the EBS

Euphausiids, principally *Thysanoessa inermis* and *T. raschii*, are among the most important prey items for walleye pollock in the Bering Sea (e.g., Livingston 1991, Lang et al. 2000, Brodeur et al. 2002). Acoustic data at four frequencies (18, 38, 120, and 200 kHz) and Methot trawl sampling (2004-2018) were used to classify euphausiid backscatter and create an index of euphausiid biomass on the Bering Sea shelf from 2004 to the present using methods described elsewhere (De Robertis et al. 2010, Ressler et al. 2012). In 2018, 7 Methot trawls targeted suspected euphausiid backscatter during daytime and 6 oblique Methot trawls were conducted at night as part of a study of euphausiid acoustical properties and net avoidance. Preliminary results show that the spatial distribution and relative magnitude of the euphausiid backscatter was patchy across the survey area, with highest backscatter appearing near the edges of Pribilof canyon, near Unimak Pass, and across shallower regions of the southeastern shelf (Fig. 19). Summertime euphausiid density increased in the eastern Bering Sea from 2004 to 2009, then subsequently declined in 2010 through 2016, when the lowest value in the time series was reported (Fig. 20). Euphausiid density increased slightly in summer 2018 from 2016 but remains relatively low. The 2018 value is similar to what was observed in 2004, a year with very low euphausiid densities according to data from many sources (Fig. 20; reviewed in Hunt et al. 2016).

ACKNOWLEDGMENTS

The authors thank the officers and crew of the NOAA ship *Oscar Dyson* for their proficient field support. They thank the MACE lead scientists and staff for excellent field work and data analysis support, the NOAA Teacher at Sea (TAS) Program and our TINRO (Pacific branch of the Federal State Budget Scientific Institution "Russian Federal Research Institute of Fisheries and oceanography") colleagues for their collaboration.

CITATIONS

Bodholt, H. 2002. The effect of water temperature and salinity on echo sounder measurements. ICES Symposium on Acoustics in Fisheries, Montpellier 10–14 June 2002.

Bodholt, H., and H. Solli. 1992. Split beam techniques used in Simrad EK500 to measure target strength, p. 16-31. *In* World Fisheries Congress, May 1992, Athens, Greece.

Brodeur, R., M. Wilson, L. Ciannelli, M. Doyle, and J. Napp. 2002. Interannual and regional variability in distribution and ecology of juvenile pollock and their prey in frontal structures of the Bering Sea. Deep-sea Res. II 49: 6051-6067.

Conner, J., and R. Lauth. 2017. Results of the 2016 eastern Bering sea continental shelf bottom trawl survey of groundfish and invertebrate resources. U.S. Dep. Commer., NOAA Tech. Memo. NMFS-AFSC 352, 159 p.

Chuang, M., J. Hwang, K. Williams, and R. Towler. 2011. Automatic fish segmentation via double local thresholding for trawl-based underwater camera systems. *In* Image Processing (ICIP), 2011 18th IEEE International Conference on (pp. 3145-3148). IEEE.

Demer, D., and S. Conti. 2005. New target-strength model indicates more krill in the Southern Ocean. ICES J. Mar. Sci. 62: 25-32.

Demer, D.A., Berger, L., Bernasconi, M., Bethke, E., Boswell, K., Chu, D., Domokos, R., et al. 2015. Calibration of acoustic instruments. ICES Coop. Res. Rep. 326, 133 p.

De Robertis, A., D. McKelvey, and P. Ressler. 2010. Development and application of an empirical multifrequency method for backscatter classification. Can. J. Fish. Aquat. Sci. 67:1459-1474.

De Robertis, A., and K. Williams. 2008. Weight-length relationships in fisheries studies: the standard allometric model should be applied with caution. Trans. Am. Fish. Soc. 137:707-719.

De Robertis, A., and K. Taylor. 2014. *In situ* target strength measurements of the scyphomedusa *Chrysaora melanaster*. Fish. Res. 153:18-23.

De Robertis, A., K. Taylor, C. Wilson, and E. Farley. 2017. Abundance and distribution of Arctic cod (*Boreogadus saida*) and other pelagic fishes over the U.S. continental shelf of the northern Bering and Chukchi seas. Deep-sea Res. II 135: 51-65.

De Robertis, A., N. Lawrence-Slavas, R. Jenkins, R., I. Wangen, C. W. Mordy, C. Meinig, M. Levine, and H. Tabisloa. 2019. Long-term measurements of fish backscatter from Saildrone unmanned surface vehicles and comparison with observations from a noise-reduced research vessel. ICES J. Mar. Sci. DOI: 10.1093/icesjms/fsz124.

Foote, K. 1987. Fish target strengths for use in echo integrator surveys. J. Acoust. Soc. Am. 82(3): 981-987.

Foote, K.G., and J. Traynor. 1988. Comparison of walleye pollock target-strength estimates determined from in situ measurements and calculations based on swimbladder form. J. Acoust. Soc. Am. 83: 9-17.

Gauthier, S., and J. K. Horne. 2004. Acoustic characteristics of forage fish species in the Gulf of Alaska and Bering Sea. Can. J. Fish. Aquat. Sci. 61: 1839-1850.

Honkalehto, T., W. Patton, S. de Blois, and N. Williamson. 2002. Echo integration-trawl survey results for walleye pollock (*Theragra chalcogramma*) on the Bering Sea shelf and slope during summer 2000. U.S. Dep. Commer., NOAA Tech. Memo. NMFS-AFSC-126, 66 p.

Honkalehto, T., N. Williamson, D. Jones, A. McCarthy, and D. McKelvey. 2008. Results of the echo integration-trawl survey of walleye pollock (*Theragra chalcogramma*) on the U.S. and Russian Bering Sea Shelf in June and July 2007. U.S. Dep. Commer., NOAA Tech. Memo. NMFS-AFSC-190, 53 p.

Honkalehto, T., D. Jones, A. McCarthy, D. McKelvey, M. Guttormsen, K. Williams, and N. Williamson. 2009. Results of the echo integration-trawl survey of walleye pollock (*Theragra chalcogramma*) on the U.S. and Russian Bering Sea shelf in June and July 2008. U.S. Dep. Commer., NOAA Tech. Memo. NMFS-AFSC-194, 56 p.

Honkalehto, T., A. McCarthy, P. Ressler, S. Stienessen, and D. Jones. 2010. Results of the acoustic-trawl survey of walleye pollock (*Theragra chalcogramma*) on the U.S. and Russian Bering Sea shelf in June - August 2009 (DY0909). AFSC Processed Rep. 2010-03, 57 p. Alaska Fish. Sci. Cent., NOAA, Natl. Mar. Fish. Serv., 7600 Sand Point Way NE, Seattle WA 98115.

Honkalehto, T., P. Ressler, R. H. Towler, and C. D. Wilson. 2011. Using acoustic data from fishing vessels to estimate walleye pollock (*Theragra chalcogramma*) abundance in the eastern Bering Sea. Can. J. Fish. Aquat. Sci. 68:1231-1242.

Honkalehto, T., A. McCarthy, P. Ressler, K. Williams, and D. Jones. 2012. Results of the acoustic-trawl survey of walleye pollock (*Theragra chalcogramma*) on the U.S. and Russian Bering Sea shelf in June - August 2010 (DY1006). AFSC Processed Rep. 2012-01, 57 p. Alaska Fish. Sci. Cent., NOAA, Natl. Mar. Fish. Serv., 7600 Sand Point Way NE, Seattle WA 98115.

Honkalehto, T., A. McCarthy, P. Ressler, and D. Jones. 2013. Results of the acoustic-trawl survey of walleye pollock (*Theragra chalcogramma*) on the U.S. and Russian Bering Sea shelf in June - August 2012 (DY1207). AFSC Processed Rep. 2013-02, 60 p. Alaska Fish. Sci. Cent., NOAA, Natl. Mar. Fish. Serv., 7600 Sand Point Way NE, Seattle WA 98115.

Honkalehto, T., and A. McCarthy. 2015. Results of the acoustic-trawl survey of walleye pollock (*Theragra chalcogramma*) on the U.S. and Russian Bering Sea shelf in June - August 2014 (DY1407). AFSC Processed Rep. 2013-02, 60 p. Alaska Fish. Sci. Cent., NOAA, Natl. Mar. Fish. Serv., 7600 Sand Point Way NE, Seattle WA 98115.

Honkalehto, T., A. McCarthy, and N. Lauffenburger. 2018. Results of the acoustic-trawl survey of walleye pollock (*Gadus chalcogrammus*) on the U.S. Bering Sea shelf in June - August 2016 (DY1608). AFSC Processed Rep. 2018-03, 78 p. Alaska Fish. Sci. Cent., NOAA, Natl. Mar. Fish. Serv., 7600 Sand Point Way NE, Seattle WA 98115.

Hunt Jr., G., P. Ressler, G. Gibson, A. DeRobertis, K. Aydin, M. Sigler, I. Ortiz, E. Lessard, B. Williams, A. Pinchuk, and T. Buckley. 2016. Euphausiids in the eastern Bering Sea: A synthesis of recent studies of euphausiid production, consumption and population control. Deep-sea Res. Pt. II: Top. Stud. Oceanogr. 134:204-222.

Ianelli, J., S. Kotwicki, T. Honkalehto, K. Holsman, and B. Fissel, 2017. Assessment of the walleye pollock stock in the eastern Bering Sea, p. 55-184 *In* Stock assessment and fishery evaluation report for the groundfish resources of the Bering Sea/Aleutian Islands regions. N. Pac. Fish. Mgmt. Counc., 605 W. 4th Ave., Anchorage, AK 99501-2252.

Ianelli, J., T. Honkalehto, S. Barbeaux, B. Fissel, and S. Kotwicki. 2016. Assessment of the walleye pollock stock in the eastern Bering Sea, p. 55-180. *In* Stock assessment and fishery evaluation report for the groundfish resources of the Bering Sea/Aleutian Islands regions. N. Pac. Fish. Mgmt. Counc., 605 W. 4th Ave., Anchorage, AK 99501-2252.

Jech, M., K. Foote, D. Chu, and L. Hufnagle. 2005. Comparing two 38-kHz scientific echosounders. ICES J. Mar. Sci. 62: 1168-1179.

Jones, D., A. De Robertis, and N. Williamson. 2011. Statistical combination of multifrequency sounder-detected bottom lines reduces bottom integrations. U.S. Dep. Commer., NOAA Tech. Memo. NMFS-AFSC-219, 13 p.

Jones, D. T., S. Stienessen, and N. Lauffenburger. 2017. Results of the acoustic-trawl survey of walleye pollock (*Gadus chalcogrammus*) in the Gulf of Alaska, June-August 2015 (DY2015-06). AFSC Processed Rep. Alaska Fish. Sci. Cent., NOAA, Natl. Mar. Fish. Serv., 7600 Sand Point Way NE, Seattle WA 98115.

Kang, D., T. Mukai, K. Iida, D. Hwang, and J.-G. Myoung. 2005. The influence of tilt angle on the acoustic target strength of the Japanese common squid (*Todarodes pacificus*). ICES J. Mar. Sci. 62: 779-789.

Knudsen, H. P. 2009. Long-term evaluation of scientific-echosounder performance. ICES J. Mar. Sci. 66: 1335-1340.

Lang, G.M., R.D. Brodeur, J.M. Napp, and R. Schabetsberger. 2000. Variation in groundfish predation on juvenile walleye pollock relative to hydrographic structure near the Pribilof Islands, Alaska. ICES J. Mar. Sci. 57:265-271.

Lauffenburger, N., A. De Robertis, S. Kotwicki. 2017. Combining bottom trawls and acoustics in a diverse semipelagic environment: What is the contribution of walleye-pollock (*Gadus chalcogrammus*) to near-bottom acoustic backscatter in the eastern Bering Sea? Can. J. Fish. Aquat. Sci. 74:256-264.

Lauth, R., and J. Conner. 2014. Results of the 2011 eastern Bering Sea continental shelf bottom trawl survey of groundfish and invertebrate fauna. U.S. Dep. Commer., NOAA Tech. Memo. NMFS-AFSC-227, 176 p.

Levine, M., and De Robertis, A. 2019. Don't work too hard: subsampling leads to efficient analysis of large acoustic datasets. Fish. Res. 219: 105323.

Livingston, P. 1991. Walleye pollock, p. 9-30. *In* P.A. Livingston (ed.), Groundfish food habits and predation on commercially important prey species in the eastern Bering Sea, 1984-1986. U.S. Dep. Commer., NOAA Tech. Memo. NMFS-F/NWC-207, 240 p.

MacLennan, D. N., P. G. Fernandes, and J. Dalen. 2002. A consistent approach to definitions and symbols in fisheries acoustics. ICES J. Mar. Sci. 59: 365–369.

Methot, R. D. 1986. Frame trawl for sampling pelagic juvenile fish. CalCOFI Rep. Vol. XXVII: 267-278.

Mordy, C., E. Cokelet, A. De Robertis, R. Jenkins, C. Kuhn, N. Lawrence-Slavas, C. Berchok, et al. 2017. Saildrone surveys of oceanography, fish and marine mammals in the Bering Sea. Oceanography 30(2):113-116.

Overland, J.E., S.A. Salo, L.H. Kantha, and C.A. Clayson. 1999. Thermal stratification and mixing on the Bering Sea shelf, p. 129-146 *In* T.R. Loughlin and K. Ohtani (eds.), Dynamics of the Bering Sea: a summary of physical, chemical and biological characteristics and a synopsis of research on the Bering Sea. Sydney, British Columbia and Fairbanks, Alaska: North Pacific Marine Science Organization (PICES), and University of Alaska Sea Grant College Program AK-SG-99-03.

Petitgas, P. 1993. Geostatistics for fish stock assessments: a Review and an acoustic application. ICES J. Mar. Sci. 50:285-298.

Ressler, P. H., A. De Robertis, J. D. Warren, J. N. Smith, and S. Kotwicki. 2012. Developing an acoustic index of euphausiid abundance to understand trophic interactions in the Bering Sea ecosystem. Deep-sea Res. II. 65-70 (2012): 184-195.

Rivoirard, J., J. Simmonds, K. G. Foote, P. Fernandez, and N. Bez. 2000. Geostatistics for estimating fish abundance. Blackwell Science, Ltd., Oxford, U.K., 206 p.

Simrad. 2008. Simrad ER60 scientific echo sounder manual Version Rev.C. Simrad Subsea A/S, Strandpromenaden 50, Box 111, N-3191 Horten, Norway.

Stevenson, D. E., and R. Lauth. 2018. Bottom trawl surveys in the northern Bering Sea indicate recent shifts in the distribution of marine species. Polar Biol. 42(2): 407-421. https://doi.org/10.1007/s00300-018-2431-1.

Stienessen, S., and N. Lauffenburger. 2019. Results of the acoustic-trawl surveys for walleye pollock in the Gulf of Alaska, February-March 2018 (DY1801 and DY1803). AFSC Processed Rep. Alaska Fish. Sci. Cent., NOAA, Natl. Mar. Fish. Serv., 7600 Sand Point Way NE, Seattle WA 98115.

Towler, R., and K. Williams. 2010. An inexpensive millimeter-accuracy electronic length measuring board. Fish. Res. 106:107-111.

Traynor, J. J. 1996. Target strength measurements of walleye pollock (*Theragra chalcogramma*) and Pacific whiting (*Merluccius productus*). ICES J. Mar. Sci. 64:559-569.

Traynor, J. J., and M.O. Nelson. 1985. Results of the U.S. hydroacoustic survey of pollock on the continental shelf and slope, p. 192-200. *In* R.G. Bakkala and K. Wakabayashi (eds.), Results of cooperative U.S.-Japan groundfish investigations in the Bering Sea during May-August 1979. Int. North Pac. Fish. Comm. Bull. 44.

Walline, P. D. 2007. Geostatistical simulations of eastern Bering Sea walleye pollock spatial distributions, to estimate sampling precision. ICES J. Mar. Sci. 64:559-569.

Williams, K., C. N. Rooper, and R. Towler. 2010a. Use of stereo camera systems for assessment of rockfish abundance in untrawlable areas and for recording pollock behavior during midwater trawls. Fish. Bull., U.S. 108: 352-362.

Williams, K., R. Towler, and C. Wilson. 2010b. Cam-trawl: A combination trawl and stereo-camera system. Sea Technol. 51(12):45-50.

Williams, K., A. E. Punt, C. D. Wilson, and J. K. Horne. 2011. Length-selective retention of walleye pollock, *Theragra chalcogramma*, by midwater trawls. ICES J. Mar. Sci. 68: 119-129.

Williamson, N., and J. Traynor. 1996. Application of a one-dimensional geostatistical procedure to fisheries acoustic surveys of Alaskan pollock. ICES J. Mar. Sci. 53:423-428.

Wyllie-Echeverria, T., and W. Wooster. 1998. Year-to-year variations in Bering Sea ice cover and some consequences for fish distributions. Fish. Oceanogr. 7: 159−170.

TABLES AND FIGURES

Table 1. -- Simrad EK60 38 kHz acoustic system description and settings used during the summer 2018 acoustic-trawl survey of walleye pollock in the eastern Bering Sea, results from standard sphere acoustic system calibrations conducted in association with the surveys, and final analysis parameters.

		Initial system settings	7 June Captain's Bay Unalaska	25 Aug. Kalsin Bay Kodiak	Final analysis parameters
Echosounder		Simrad EK60	--	--	Simrad ER60
Transducer		ES38B	--	--	ES38B
Frequency (kHz)		38	--	--	38
Transducer depth (m)		9.15	--	--	9.15
Pulse length (ms)		0.512	--	--	0.512
Transmitted power (W)		2000	--	--	2000
Angle sensitivity	Along	22.76	--	--	22.76
	Athwart	21.37	--	--	21.37
2-way beam angle (dB)		-20.74	--	--	-20.74
Gain (dB)		22.09	22.09	21.89	21.99
s_A correction (dB)		-0.59	-0.59	-0.66	-0.62
Integration gain (dB)		21.49	21.49	21.23	21.36
3 dB beamwidth	Along	6.64	6.67	6.70	6.69
	Athwart	7.20	7.21	7.10	7.16
Angle offset	Along	-0.03	-0.04	-0.03	-0.04
	Athwart	-0.06	-0.06	-0.05	-0.06
Post-processing sv threshold (dB)		-70	--	--	--
Measured standard sphere TS (dB)		--	-40.71	-42.63	--
Sphere range from transducer (m)		--	40.84	19.36	--
Absorption coefficient (dB/m)		0.009978	0.0100	0.0089	0.0100
Sound velocity (m/s)		1470.0	1468.5	1486.7	1470.0
Water temp at transducer (°C)		--	5.2	10.3	--

Note: Gain and beam pattern terms are defined in Demer et al., 2015.

Table 2. -- Trawl stations, catch data summary, and drop TS stations from the summer 2018 eastern Bering sea shelf walleye pollock acoustic trawl survey aboard the NOAA ship *Oscar Dyson*.

Haul	area	Gear[a]	Date	Time	Duration	Start position		Depth (m)		Temp. (°C)		Walleye pollock		Other
no.		type	(GMT)	(GMT)	(minutes)	Lat. (N)	Long. (W)	footrope	bottom	headrope	surface[b]	(kg)	number	(kg)
1	U.S. east of 170°	AWT	8-Jun	7:59	23.37	56 58.64	-160 -55.22	48.4	68.07	4.84	5.5	69.7	117	52.2
2	U.S. east of 170°	AWT	9-Jun	0:08	28.6	56 43.43	-161 -32.52	78.0	87.1	4.31	6.69	519.4	968	86.0
3	U.S. east of 170°	AWT	9-Jun	19:35	28.7	56 6.00	-162 -11.78	67.9	76.84	4.89	6.8	307.9	531	283.1
4	U.S. east of 170°	Methot	10-Jun	4:27	30.77	55 45.19	-162 -49.49		61.98		7.69			43.8
5	U.S. east of 170°	AWT	10-Jun	18:32	40.35	56 44.18	-162 -45.71	60.5	67.36	4.77	6.7	252.6	483	197.4
6	U.S. east of 170°	AWT	11-Jun	6:54	52.67	55 46.31	-163 -23.47	68.9	89.34	4.38	7.58	178.7	279	163.2
7	U.S. east of 170°	AWT	11-Jun	20:50	40.95	55 19.58	-163 -59.18	64.6	72.99	5.47	7.58	111.2	167	672.9
8	U.S. east of 170°	Methot	12-Jun	2:37	30.57	55 52.00	-163 -58.94	70.5	93.56		7.8			21.5
9	U.S. east of 170°	AWT	12-Jun	7:26	41.75	56 31.99	-163 -57.40	50.1	79.5	4.18	7.47	281.9	517	73.2
10	U.S. east of 170°	DropTS	12-Jun	10:01	73.02	56 34.57	-164 -0.77		67.37		6.65			
11	U.S. east of 170°	DropTS	12-Jun	12:15	54	56 34.64	-164 -0.70		67.45		6.67			
12	U.S. east of 170°	AWT	13-Jun	0:23	25.68	56 13.64	-164 -34.57	84.4	89.42	3.84	8.55	184.1	351	108.4
13	U.S. east of 170°	AWT	13-Jun	3:57	17.42	55 55.36	-164 -34.28	79.4	94.69	3.94	10.35	378.6	769	131.6
14	U.S. east of 170°	DropTS	13-Jun	10:16	98.9	55 22.16	-164 -32.94		49.75		8.75			
15	U.S. east of 170°	AWT	13-Jun	15:57	23.48	55 16.57	-164 -33.80	89.4	101.83	4.96	8.55	506.4	813	450.1
16	U.S. east of 170°	AWT	14-Jun	3:14	25.45	55 1.13	-165 -8.39	107.3	112.07	4.85	8.07	354.3	531	1,654.0
17	U.S. east of 170°	AWT	14-Jun	7:35	20.93	55 16.11	-165 -8.83	103.8	112.07	5.22	8.66	258.6	355	44.0
18	U.S. east of 170°	DropTS	14-Jun	10:16	102.87	55 11.69	-165 -9.13		59.92		8.6			
19	U.S. east of 170°	AWT	15-Jun	0:13	60.85	56 40.18	-165 -11.53	71.6	75.91	3.9	8.5	329.8	640	191.4
20	U.S. east of 170°	DropTS	15-Jun	10:07	72.38	57 10.26	-165 -49.19		69.98		8.13			
21	U.S. east of 170°	AWT	16-Jun	1:41	21.5	55 2.39	-165 -45.08	59.9	128.61	5.77	7.5	157.2	238	140.1
22	U.S. east of 170°	DropTS	16-Jun	10:16	68.25	54 16.26	-166 -3.53		107.74		6.12			
23	U.S. east of 170°	AWT	16-Jun	16:37	21.02	54 10.43	-166 -17.02	149.9	163.52	4.91	6	613.7	791	346.3
24	U.S. east of 170°	AWT	16-Jun	20:08	33.97	54 12.14	-166 -16.25	120.2	393.11	5.06	6.13	77.9	106	3.7
25	U.S. east of 170°	AWT	17-Jun	5:25	22.35	55 29.78	-166 -21.34	103.3	129.3	4.6	7.44	312.8	463	0.0
26	U.S. east of 170°	DropTS	17-Jun	10:35	31.4	55 41.29	-166 -23.59		12.19		7.7			
27	U.S. east of 170°	DropTS	17-Jun	11:42	25.15	55 41.67	-166 -24.86		25.45		7.7			
28	U.S. east of 170°	AWT	17-Jun	17:46	29.42	56 6.61	-166 -22.66	102.5	116.88	4.64	7.99	149.3	240	32.9
29	U.S. east of 170°	AWT	17-Jun	23:01	20.35	56 31.54	-166 -24.50	84.1	94.02	4.3	7.7	352.2	662	26.6
30	U.S. east of 170°	AWT	18-Jun	7:33	30.8	57 37.01	-166 -28.72	42.0	67.76	3.99	8.08	109.0	223	10.5
31	U.S. east of 170°	AWT	18-Jun	21:58	39.48	56 19.01	-166 -59.23	40.8	113.65	6.97	7.92	4.5	8	81.1
32	U.S. east of 170°	DropTS	19-Jun	10:25	110.88	54 37.55	-166 -54.38		356.19		6.94			
33	U.S. east of 170°	AWT	19-Jun	17:30	34.62	55 8.94	-167 -30.49	145.0	194.1	4.39	7.45	108.8	146	1.4
34	U.S. east of 170°	AWT	19-Jun	23:25	15.1	55 43.22	-167 -32.45	110.9	135.37	4.49	7.8	1,141.1	1,740	5.3
35	U.S. east of 170°	AWT	20-Jun	5:37	19.63	56 29.83	-167 -36.95	100.8	110.97	4.43	8.09	537.2	861	7.9
36	U.S. east of 170°	DropTS	20-Jun	10:52	0.03	56 42.34	-167 -32.24				7.8			
37	U.S. east of 170°	AWT	20-Jun	17:28	32.93	57 2.77	-167 -40.66	58.7	76.27	4.73	7.94	174.6	373	5.1

Table 2. -- Cont.

Haul	Area	Gear[a]	Date	Time	Duration	Start position				Depth (m)		Temp. (°C)		Walleye pollock		Other
no.		type	(GMT)	(GMT)	(minutes)	Lat. (N)		Long. (W)		footrope	bottom	headrope	surface[b]	(kg)	number	(kg)
38	U.S. east of 170°	AWT	21-Jun	4:32	30.48	57	56.92	-168	-22.9	55.8	69.7	4.4	8.37	283.4	618	9.7
39	U.S. east of 170°	DropTS	21-Jun	10:00	176.3	57	30.53	-168	-20.5		216.0		6.93			
40	U.S. east of 170°	AWT	21-Jun	17:59	22.72	56	50.96	-168	-16.5	83.3	92.8	4.44	7.6	348.1	731	1.9
41	U.S. east of 170°	AWT	22-Jun	0:51	5.85	55	51.58	-168	-10.1	125.8	139.7	4.39	7.83	259.6	336	1.1
42	U.S. east of 170°	AWT	22-Jun	5:19	27.97	55	28.82	-168	-6.73	160.8	170.6	4.49	8.2	466.9	615	2.8
43	U.S. east of 170°	DropTS	22-Jun	9:36	139.33	55	40.61	-168	-46.5				7.77			
44	U.S. east of 170°	AWT	22-Jun	16:18	33.53	55	39.35	-168	-44.4	247.2	260.3	4.34	7.7	91.8	138	74.0
45	U.S. east of 170°	AWT	22-Jun	22:54	40.17	56	24.61	-168	-50.4	114.9	119.8	4.46	7.75	255.1	370	4.8
46	U.S. east of 170°	AWT	23-Jun	3:28	29.73	56	46.13	-168	-52.9	91.1	97.3	4.43	7.71	335.7	683	1.1
47	U.S. east of 170°	AWT	23-Jun	7:47	15.55	57	13.65	-168	-56.3	51.3	75.2	4.52	7.6	238.3	540	1.3
48	U.S. east of 170°	DropTS	23-Jun	10:02	65.13	57	13.06	-168	-55.5				7.68			
49	U.S. east of 170°	AWT	24-Jun	1:47	46.53	58	15.07	-169	-41.6	50.4	70.7	3.68	6.6	356.4	885	7.2
50	U.S. east of 170°	DropTS	24-Jun	9:57	7.97	56	57.59	-169	-30.8				6.4			
51	U.S. east of 170°	AWT	24-Jun	16:58	19.02	56	48.95	-169	-31.1	63.8	75.2	5.07	7.15	413.8	784	18.9
52	U.S. east of 170°	AWT	24-Jun	22:58	24.43	56	26	-169	-28			4.52	7	806.8	1,335	4.1
53	U.S. west of 170°	AWT	25-Jun	6:04	30.12	56	10.2	-170	-2.34	113.9	120.4	4.48	6.97	356.8	487	5.4
54	U.S. west of 170°	DropTS	25-Jun	9:24	123.43	56	9.288	-170	-1.81				6.87			
55	U.S. west of 170°	AWT	25-Jun	17:12	25.1	56	30.72	-170	-4.84	98.5	103.3	4.61	7.29	223.1	319	0.5
56	U.S. west of 170°	AWT	26-Jun	8:01	36.77	58	31.64	-170	-23.8	50.4	74.8	3.44	6.51	313.9	710	9.2
57	U.S. west of 170°	DropTS	26-Jun	10:27	63.95	58	31.57	-170	-21.5				6.5			
58	U.S. west of 170°	AWT	26-Jun	18:45	40.65	59	16.31	-170	-31	60.9	68.4	3.33	6.45	362.7	867	12.3
59	U.S. west of 170°	AWT	27-Jun	1:01	20.63	59	42.47	-170	-34	60.8	66.4	2.99	6.68	275.4	809	9.4
60	U.S. west of 170°	Methot	27-Jun	4:05	29.92	59	55.19	-170	-35.5	51.4	65.6		7			18.3
61	EBS N. Extension	AWT	3-Jul	8:26	1.67	60	4.98	-170	-38.3	42.8	55.5	5.73	8.1	44.8	114	3.4
62	EBS N. Extension	AWT	3-Jul	17:54	37.95	60	26.59	-170	-42.1	54.5	51.9	2.87	8.08	414.5	766	4.0
63	EBS N. Extension	83/112	4-Jul	2:26	5.62	61	40.75	-170	-52.5	49.7	41.2	1.75	8.17	335.1	520	267.9
64	EBS N. Extension	83/112	4-Jul	6:21	15.25	62	13.06	-170	-59.1	44.8	36.5	2.04	7.81	154.1	223	695.4
65	EBS N. Extension	83/112	4-Jul	15:07	15.25	62	46.52	-171	-4.3	45.0	45.5	1.66	7.59	128.3	371	392.1
66	EBS N. Extension	AWT	5-Jul	3:10	30.43	61	28.93	-171	-33.6	42.8	55.3	4.14	8.8	106.2	155	3.2
67	EBS N. Extension	Methot	5-Jul	16:47	30.48	60	20.42	-171	-21	58.5	66.4		8.92			11.9
68	U.S. west of 170°	AWT	5-Jul	21:26	45.87	59	53.71	-171	-16.1	65.3	71.1	2.71	8.72	367.8	784	17.1
69	U.S. west of 170°	AWT	6-Jul	8:54	44.38	58	6.18	-170	-57.4	76.6	86.3	3.5	8.2	195.2	404	21.1
70	U.S. west of 170°	DropTS	6-Jul	12:17	73.32	58	7.176	-170	-56.3		73.1		8.2			
71	U.S. west of 170°	AWT	6-Jul	20:16	29.7	57	9.756	-170	-49.6	69.3	83.4	5.76	9.05	430.5	868	18.3
72	U.S. west of 170°	AWT	26-Jul	4:25	30.9	56	19.95	-170	-39.6	108.5	120.5	4.53	9.38	127.8	202	2.0
73	U.S. west of 170°	AWT	26-Jul	19:06	16.4	56	40.97	-171	-19	68.3	117.9	4.73	9.9			5.3
74	U.S. west of 170°	AWT	27-Jul	4:11	26.52	58	13.19	-171	-35.4	92.4	96.7	3.58	10.29	544.3	955	17.3
75	U.S. west of 170°	Methot	27-Jul	9:28	29.52	58	38.41	-171	-39.7	29.8	93.1		10			6.4

Table 2. -- Cont.

Haul	Area	Gear[a]	Date	Time	Duration	Start position		Depth (m)		Temp. (°C)		Walleye pollock		Other
no.		type	(GMT)	(GMT)	(minutes)	Lat. (N)	Long. (W)	footrope	bottom	headrope	surface[b]	(kg)	number	(kg)
76	U.S. west of 170°	AWT	27-Jul	20:11	45.77	59 30.48	-171 -50.46	73.8	78.4	3.34	10.2	480.2	938	2.3
77	U.S. west of 170°	AWT	28-Jul	7:42	39.47	59 10.85	-172 -25.48	88.3	92.4	3.44	10.1	245.5	473	4.5
78	U.S. west of 170°	DropTS	28-Jul	12:13	31.53	59 10.87	-172 -23.54		56.7		10.01			
79	U.S. west of 170°	AWT	28-Jul	18:32	16.27	58 43.16	-172 -19.55		100.7		10.1	671.7	1,302	1.4
80	U.S. west of 170°	Methot	29-Jul	0:20	23.43	58 2.21	-172 -12.77	93.2	104.0		10.03			3.4
81	U.S. west of 170°	AWT	29-Jul	6:54	23.27	57 9.50	-172 -1.80	70.9	113.5	4.55	10.1	0.7	1	19.8
82	U.S. west of 170°	AWT	29-Jul	20:36	25.43	56 32.40	-171 -55.51	149.6	153.7	4.35	9.8	297.4	451	1.1
83	U.S. west of 170°	AWT	30-Jul	3:15	12.92	56 33.79	-172 -30.74	219.1	341.6	4.32	9.69	144.7	227	16.5
84	U.S. west of 170°	AWT	30-Jul	17:20	30.45	57 25.20	-172 -43.94	78.3	118.4	4.79	9.53			77.4
85	U.S. west of 170°	AWT	30-Jul	23:59	20.48	58 15.67	-172 -53.70	100.5	107.8	3.61	9.69	910.4	1,568	2.6
86	U.S. west of 170°	AWT	31-Jul	6:04	15.67	58 54.45	-173 -1.79	102.4	108.9	3.42	9.5	306.9	593	3.9
87	U.S. west of 170°	AWT	31-Jul	19:26	16.32	59 34.28	-173 -12.15	92.1	97.5	3.36	9.3	624.8	1,366	4.2
88	U.S. west of 170°	AWT	1-Aug	4:48	45.95	61 4.22	-173 -32.77	71.6	76.1	4.45	9.66	465.9	897	76.4
89	EBS N. Extension	DropTS	1-Aug	13:19	30.62	60 47.48	-172 -30.27		45.3		9			
90	EBS N. Extension	AWT	1-Aug	19:17	45.8	61 28.04	-172 -41.82	61.2	66.4	2.83	9.64	580.7	1,575	57.6
91	EBS N. Extension	AWT	2-Aug	5:02	40.05	62 58.35	-173 -3.80	61.9	66.7	2.66	10.38	150.5	261	85.4
92	EBS N. Extension	DropTS	2-Aug	12:36	45.88	62 53.14	-174 -13.70		66.9		10.18			
93	EBS N. Extension	AWT	2-Aug	19:02	30.55	62 14.28	-174 -3.70	59.4	65.9	2.07	9.7	269.7	507	333.8
94	U.S. west of 170°	AWT	3-Aug	3:56	12.5	61 10.22	-174 -14.95	75.7	80.6	2.6	10.09	581.1	1,230	34.4
95	U.S. west of 170°	Methot	3-Aug	6:36	31.98	61 1.78	-174 -12.76	72.9	83.1		10.1			7.9
96	U.S. west of 170°	DropTS	3-Aug	12:40	52.35	60 58.06	-174 -14.99		58.6		10			
97	U.S. west of 170°	AWT	3-Aug	20:21	29.72	60 23.65	-174 -3.97	77.3	88.7	3.55	10	13.8	25	53.5
98	U.S. west of 170°	AWT	4-Aug	3:44	14.92	59 28.32	-173 -49.43	101.4	108.5	3.36	9.8	705.1	1,323	3.3
99	U.S. west of 170°	AWT	4-Aug	7:41	29.98	59 2.93	-173 -43.43	110.4	117.5	3.48	9.79	300.9	549	17.9
100	U.S. west of 170°	DropTS	4-Aug	12:26	65.42	59 3.06	-173 -41.39		60.2		9.8			
101	U.S. west of 170°	AWT	4-Aug	19:55	61.18	58 32.02	-173 -34.49	116.2	122.1	3.79	9.79	106.9	182	33.4
102	U.S. west of 170°	AWT	5-Aug	8:08	51.27	56 56.69	-173 -14.83	140.6	149.3	4.37	9.61	9.2	12	6.0
103	U.S. west of 170°	AWT	5-Aug	18:46	15.72	56 40.09	-173 -10.25	196.6	258.2	4.39	9.77	360.2	411	25.9
104	U.S. west of 170°	AWT	6-Aug	3:37	43.07	57 37.99	-173 -59.93	128.3	133.7	4.33	9.87	146.3	210	828.5
105	U.S. west of 170°	DropTS	6-Aug	12:54	45.83	58 4.84	-174 -6.80		23.2		9.98			
106	U.S. west of 170°	AWT	6-Aug	17:37	28.75	58 16.63	-174 -8.71	125.4	132.2	4.03	9.8	276.8	420	26.9
107	U.S. west of 170°	AWT	6-Aug	22:11	3.28	58 39.89	-174 -14.68	147.2	154.4	3.95	9.9	1,045.8	1,715	29.0
108	U.S. west of 170°	AWT	7-Aug	3:52	16.2	59 19.75	-174 -26.03	103.8	121.0	3.5	10	148.9	265	13.4
109	U.S. west of 170°	AWT	7-Aug	8:12	9.53	59 45.31	-174 -32.73	78.5	115.2	3.76	10.1	297.9	603	12.0
110	U.S. west of 170°	DropTS	7-Aug	12:29	45.92	59 44.31	-174 -33.03		62.0		10.1			
111	U.S. west of 170°	AWT	7-Aug	18:50	7.48	60 12.22	-174 -40.40	90.9	104.3	3.29	10.2	1,241.0	2,559	26.7
112	U.S. west of 170°	AWT	7-Aug	23:57	13.82	60 49.69	-174 -50.71	85.4	95.3	3.11	10.3	557.6	1,134	13.9
113	U.S. west of 170°	AWT	8-Aug	6:32	50.18	61 45.49	-175 -6.33	77.3	85.9	2.05	9.93	806.4	2,068	6.9

Table 2. -- Cont.

Haul	Area	Gear[a]	Date	Time	Duration	Start position				Depth (m)		Temp. (°C)		Walleye pollock		Other
no.		type	(GMT)	(GMT)	(minutes)	Lat. (N)		Long. (W)		footrope	bottom	headrope	surface[b]	(kg)	number	(kg)
114	U.S. west of 170°	DropTS	8-Aug	12:31	64.83	61	45.22	-175	-6.43		78.8		9.9			
115	U.S. west of 170°	AWT	8-Aug	18:54	30.5	62	19.03	-175	-16.49	59.9	79.1	3.76	10.08	597.8	1,544	39.7
116	U.S. west of 170°	AWT	9-Aug	4:00	15.52	61	30.08	-175	-42.85	85.1	97.0	2.53	10.1	751.2	1,624	7.6
117	U.S. west of 170°	AWT	9-Aug	7:42	13.02	61	7.36	-175	-37.18	69.7	102.0	2.94	10.02	156.6	338	6.9
118	U.S. west of 170°	AWT	9-Aug	19:39	17.72	60	26.42	-175	-24.74	91.7	109.9	2.96	10.2	870.3	1,878	15.5
119	U.S. west of 170°	AWT	10-Aug	0:39	6.58	59	54.53	-175	-15.27	101.1	120.0	3.02	10.8	513.9	1,067	5.3
120	U.S. west of 170°	AWT	10-Aug	6:13	3.4	59	15.97	-175	-4.10	109.0	133.2	3.33	10.3	203.5	382	17.7
121	U.S. west of 170°	AWT	16-Aug	7:59	35.55	59	6.01	-175	-1.26	124.8	130.7	3.5	10.2	100.2	176	7.7
122	U.S. west of 170°	Bongo	16-Aug	11:04	0.2	59	0.55	-174	-59.39		129.6		10.12			
123	U.S. west of 170°	Methot	16-Aug	12:54	20.95	59	2.09	-174	-58.75		129.0	9.73	10.1			
124	U.S. west of 170°	AWT	17-Aug	0:06	22.48	58	31.30	-175	-30.40	137.4	145.2	3.93	10.43	32.8	53	30.6
125	U.S. west of 170°	AWT	17-Aug	7:12	21.82	59	27.80	-175	-47.53	122.0	137.2	2.77	10.6	864.6	1,720	11.5
128	U.S. west of 170°	Methot	17-Aug	12:46	17.18	59	25.33	-175	-41.27		136.5	9.96	10.5			
129	U.S. west of 170°	AWT	17-Aug	17:53	8.05	59	37.71	-175	-50.06	126.5	137.4	2.84	10.41	679.8	4,255	18.2
130	U.S. west of 170°	AWT	18-Aug	3:44	12.5	60	51.64	-176	-13.51	99.8	115.3	2.61	10.1	573.9	1,288	26.7
131	U.S. west of 170°	AWT	18-Aug	7:59	29.5	61	14.07	-176	-21.19	102.6	110.0	2.44	10.1	375.7	1,080	6.0
132	U.S. west of 170°	Bongo	18-Aug	10:27	11.37	61	12.31	-176	-29.98		112.2		10			
133	U.S. west of 170°	Methot	18-Aug	11:58	15.95	61	10.96	-176	-34.10	22.2	113.5		10			
134	U.S. west of 170°	Methot	18-Aug	18:18	30.57	61	32.03	-176	-23.27	96.3	105.8		10			6.0
135	U.S. west of 170°	AWT	18-Aug	20:25	30.45	61	32.05	-176	-23.13	98.9	106.1	2.39	10	615.9	2,510	16.9
136	U.S. west of 170°	AWT	19-Aug	5:02	20.8	61	19.30	-177	-4.69	112.6	119.7	2.22	10.1	412.1	2,744	9.2
137	U.S. west of 170°	Bongo	19-Aug	8:18	12.83	61	4.66	-177	-0.32		122.7		10.1			
138	U.S. west of 170°	Methot	19-Aug	10:45	9.7	61	3.43	-177	-6.30	21.0	124.8		10.09			
139	U.S. west of 170°	Bongo	19-Aug	13:22	0.07	61	5.69	-176	-53.50		119.9		10.1			
140	U.S. west of 170°	Methot	19-Aug	13:27	20.65	61	5.56	-176	-53.90	19.2	120.2		10.1			
141	U.S. west of 170°	AWT	19-Aug	18:24	24.5	60	47.27	-176	-53.23	110.4	126.1	2.33	10.14	846.6	2,024	11.7
142	U.S. west of 170°	AWT	19-Aug	23:26	12.73	60	21.05	-176	-44.73	126.4	137.8	2.22	10.41	719.8	4,368	13.6
143	U.S. west of 170°	AWT	20-Aug	3:10	4.63	60	5.84	-176	-39.20	125.2	140.8	2.13	10.5	441.6	1,055	36.7
144	U.S. west of 170°	AWT	20-Aug	8:09	18.38	59	32.93	-176	-28.06	125.2	135.7	2.64	10.5	462.5	843	36.4
145	U.S. west of 170°	Bongo	20-Aug	10:41	14.88	59	31.64	-176	-23.10		135.4		10.4			
146	U.S. west of 170°	Bongo	20-Aug	13:28	13.95	59	31.54	-176	-32.12		137.2		10.4			

[a]AWT = Aleutian wing trawl, 83-112 = eastern bottom trawl, Methot = Methot trawl, Marinovich = small mesh midwater trawl
[b]shipboard sensor at 1.4 m depth.

Table 3.--Catch by species, and numbers of individual length and weight measurements taken from 97 Aleutian wing (midwater) trawls during the summer 2018 acoustic-trawl survey of walleye pollock on the eastern Bering Sea shelf.

		Catch				Individual measurements	
Species name	Scientific name	Weight (kg)	%	Number	%	Length	Weight
walleye pollock	*Gadus chalcogrammus*	36,056.0	83.4	78662	52.9	31,432	4,997
Northern sea nettle	*Chrysaora melanaster*	5,343.6	12.4	6745	4.5	1308	628
Pacific ocean perch	*Sebastes alutus*	800.6	1.9	1468	1.0	292	81
northern rockfish	*Sebastes polyspinis*	451.4	1.0	673	0.5	84	25
chum salmon	*Oncorhynchus keta*	135.7	0.3	72	<0.1	72	71
Aequorea sp.	*Aequorea sp.*	131.4	0.3	468	0.3	72	67
walleye pollock Age 0	*Gadus chalcogrammus*	83.2	0.2	55459	37.3	1190	
yellowfin sole	*Limanda aspera*	37.8	0.1	82	0.1	82	67
jellyfish unid.	*Scyphozoa (class)*	28.6	0.1	3730	2.5	228	45
lions mane	*Cyanea capillata*	25.4	0.1	143	0.1	66	65
Pacific herring	*Clupea pallasii*	20.6	<0.1	84	0.1	84	51
smooth lumpsucker	*Aptocyclus ventricosus*	18.0	<0.1	9	<0.1	9	3
Pacific cod	*Gadus macrocephalus*	17.4	<0.1	7	<0.1	7	7
Alaska plaice	*Pleuronectes quadrituberculatus*	12.5	<0.1	15	<0.1	15	14
flathead sole	*Hippoglossoides elassodon*	10.0	<0.1	14	<0.1	14	14
egg yolk jelly	*Phacellophora camtschatica*	8.9	<0.1	39	<0.1	34	30
northern rock sole	*Lepidopsetta polyxystra*	8.6	<0.1	21	<0.1	21	21
Aurelia sp.	*Aurelia sp.*	7.1	<0.1	592	0.4	45	32
chinook salmon	*Oncorhynchus tshawytscha*	5.9	<0.1	3	<0.1	3	3
arrowtooth flounder	*Atheresthes stomias*	4.5	<0.1	5	<0.1	5	5
yellow Irish lord	*Hemilepidotus jordani*	1.9	<0.1	2	<0.1	2	2
Okhotsk snailfish	*Liparis ochotensis*	1.6	<0.1	1	<0.1	1	1
squid unid.	*Cephalopoda (class)*	1.1	<0.1	149	0.1	76	64
chrysaora jellyfish	*Chrysaora sp.*	1.0	<0.1	3	<0.1		
prowfish	*Zaprora silenus*	0.7	<0.1	69	<0.1	67	46
eulachon	*Thaleichthys pacificus*	0.5	<0.1	6	<0.1	6	6
Alaska skate	*Bathyraja parmifera*	0.5	<0.1	1	<0.1	1	1
magistrate armhook squid	*Berryteuthis magister*	0.5	<0.1	1	<0.1	1	1
capelin	*Mallotus villosus*	0.4	<0.1	29	<0.1	29	26
butterfly sculpin	*Hemilepidotus papilio*	0.3	<0.1	1	<0.1	1	1
comb jelly unid.	*Ctenophora (phylum)*	0.2	<0.1	3	<0.1		
isopod unid.	Isopoda (order)	0.1	<0.1	65	<0.1		
shrimp unid.	Malacostraca (class)	0.1	<0.1	21	<0.1	13	2
crested sculpin	*Blepsias bilobus*	0.1	<0.1	1	<0.1	1	1
California market squid	*Doryteuthis opalescens*	0.0	<0.1	1	<0.1	1	
Total		43,216.2		148,642		35,262	6,377

Table 4.--Catch by species, and numbers of individual length and weight measurements taken from three 83-112 bottom trawls during the summer 2018 acoustic-trawl survey of walleye pollock on the eastern Bering sea shelf.

		Catch				Individual measurements	
Species name	Scientific name	Weight (kg)	%	Number	%	Length	Weight
walleye pollock	*Gadus chalcogrammus*	617.6	31.3	1113	11.4	772	187
Pacific cod	*Gadus macrocephalus*	325.0	16.5	136	1.4	70	70
Alaska plaice	*Pleuronectes quadrituberculatus*	231.3	11.7	272	2.8	58	23
snow crab	*Chionoecetes opilio*	222.1	11.3	4079	41.7	65	10
whelk unid.	Gastropoda (class)	148.2	7.5	1440	14.7		
snail unid.	Gastropoda (class)	99.8	5.1	957	9.8		
yellowfin sole	*Limanda aspera*	85.2	4.3	181	1.9	71	30
Pacific herring	*Clupea pallasii*	61.2	3.1	277	2.8	46	21
Northern sea nettle	*Chrysaora melanaster*	43.6	2.2	78	0.8	39	21
Alaska skate	*Bathyraja parmifera*	30.9	1.6	6	0.1	6	3
hermit crab unid.	Paguridae (family)	28.0	1.4	407	4.2		
sea star unid.	Asteroidea (class)	22.1	1.1	284	2.9		
empty gastropod shells	Gastropoda (class)	15.3	0.8	141	1.4		
rock sole unid.	*Lepidopsetta (*genus*)*	9.3	0.5	51	0.5	44	17
Bering flounder	*Hippoglossoides robustus*	7.5	0.4	68	0.7	68	28
northern rock sole	*Lepidopsetta polyxystra*	5.5	0.3	93	0.9	10	10
basketstar	*Gorgonocephalus eucnemis*	4.5	0.2	18	0.2		
plain sculpin	*Myoxocephalus jaok*	3.7	0.2	7	0.1	7	6
shorthorn (=warty) sculpin	*Myoxocephalus scorpius*	2.9	0.1	3	<0.1	3	3
Pacific lyre crab	*Hyas lyratus*	2.5	0.1	27	0.3	1	
sponge unid.	Porifera (phylum)	2.5	0.1	89	0.9		
bivalve unid.	Bivalvia (class)	1.4	0.1	22	0.2		
snailfish unid.	Liparidae (family)	0.9	<0.1	1	<0.1	1	
great sculpin	*Myoxocephalus polyacanthocephalus*	0.7	<0.1	2	<0.1	2	2
arrowtooth flounder	*Atheresthes stomias*	0.7	<0.1	1	<0.1	1	
longhead dab	*Limanda proboscidea*	0.2	<0.1	1	<0.1	1	1
skate egg case unid.	Rajidae (family)	0.2	<0.1	1	<0.1		
sturgeon poacher	*Podothecus accipenserinus*	0.1	<0.1	7	0.1	7	5
capelin	*Mallotus villosus*	0.1	<0.1	11	0.1	11	6
saffron cod	*Eleginus gracilis*	0.1	<0.1	1	<0.1	1	1
prickleback unid.	Stichaeidae (family)	<0.1	<0.1	1	<0.1	1	1
sculpin unid.	Cottidae (family)	<0.1	<0.1	1	<0.1	1	1
shrimp unid.	Malacostraca (class)	<0.1	<0.1	1	<0.1		
Total		1,972.9		9,777		1,286.0	446

Table 5.--Catch by species, and numbers of individual length and weight measurements taken from 13 Methot trawls during the summer 2018 acoustic-trawl survey of walleye pollock on the eastern Bering Sea shelf.

		Catch				Individual measurements	
Species name	Scientific name	Weight (kg)	%	Number	%	Length	Weight
Northern sea nettle	*Chrysaora melanaster*	68.4	57.4	214	0.0	171	70
euphausiid unid.	Euphausiacea (order)	37.8	31.8	739,033	98.0		
Aequorea sp.	*Aequorea* sp.	6.1	5.1	95	0.0	24	24
Aurelia sp.	*Aurelia* sp.	3.9	3.3	217	0.0	102	52
jellyfish unid.	Scyphozoa (class)	0.9	0.8	1,416	0.2	5	5
Staurophora mertensi	*Staurophora mertensi*	0.6	0.5	18	0.0		
isopod unid.	Isopoda (order)	0.5	0.4	493	0.1		
lions mane	*Cyanea capillata*	0.4	0.3	9	0.0	9	9
Crab larvae	Crab larvae	0.2	0.2	10,719	1.4		
Hydromedusa (unid.)	Hydromedusa (class)	0.1	0.1	770	0.1		
walleye pollock Age 0	Gadus chalcogrammus	0.1	0.1	422	0.1	34	
fish larvae unid.	Actinopterygii (class)	0.1	0.1	102	0.0		
flatfish larvae	Pleuronectiform larvae	0.0	0.0	232	0.0	30	
squid unid.	Cephalopoda (class)	0.0	0.0	2	0.0		
poacher unid.	Agonidae (family)	0.0	0.0	3	0.0		
Total		119.2		753,744		375	160

Table 6. -- Number of walleye pollock biological samples and measurements collected from trawl codends and CamTrawl images during the summer 2018 acoustic-trawl survey of the eastern Bering sea shelf.

Haul	Walleye pollock age 1+						Age-0	CamTrawl Autolengths
no.	Lengths	Weights	Maturity	Otoliths	Gonad wts	Ovaries	Lengths	Age1+
1	117	51	51	31	6	6		18
2	297	52	50	32	5	5		76
3	340	62	51	37	5	5		49
5	320	51	51	32	2	2		77
6	279	50	50	30	5	5		27
7	167	50	50	30	2	2		74
9	517	55	52	25	5	4		44
12	351	64	50	40	3	3		60
13	394	50	49	35	2	1		130
15	275	50	50	35				233
16	329	50	50	35	1	1		104
17	355	55	55	35				59
19	399	53	48	38				102
21	238	50	50	35				195
23	315	50	50	35	1	1		94
24	106	50	50	35	1	1		40
25	290	51	51	36	3	2		115
28	240	50	50	35				52
29	383	54	50	39				119
30	223	50	50	34				22
31	8	8	8	8				5
33	146	50	50	30				51
34	363	50	50	35	1	1		300
35	334	50	50	30				200
37	373	50	50	30	1	2		64
38	411	55	54	35	8	8		57
40	343	50	50	25	1	1		122
41	336	50	50	25	1	1		90
42	273	50	50	25	1	1		162
44	138	50	50	25	2	2		31
45	370	49	49	25	3			204
46	394	50	50	25	2	1		176
47	540	50	50	25				56
49	413	53	52	28	2	3		
51	317	50	50	25	1			
52	337	50	50	25	1			226
53	311	50	50	25				188
55	290	50	50	25				124
56	401	51	50	26				53
58	482	52	51	31	4	4		
59	809	52	52	27	7	6		35
61	114	48	48	25	12	12		16
62	326	50	50	25	11	10		31
63	352	65	40	20	5	5		
64	204	51	43	25	1	1		

Table 6. -- Cont.

Haul no.	Walleye pollock age 1+ Lengths	Weights	Maturity	Otoliths	Gonad wts	Ovaries	Age-0 lengths	Camtrawl Autolengths Age1+
65	216	71	50	30	6	5		
66	155	40	40	20	5	5		
68	325	50	50	25	2	2		64
69	404	57	55	27				24
71	301	50	50	25	3	3		47
72	202	50	50	30	2	2		54
73							94	
74	353	52	51	32	1		10	52
75							4	
76	461	54	54	30	2	2	1	
77	473	57	51	37	3	3		103
79	328	66	66	30	2	1	11	158
80							30	
81	1	1	1	1			77	
82	343	64	64	30				129
83	227	50	50	30	2	2	30	
84							80	
85	398	50	50	30	3	3		300
86	499	52	50	32			3	151
87	387	58	58	30	3	3		
88	299	50	50	30	2	1		
90	553	93	93	30	7	5	1	61
91	261	50	50	30	3	2		
93	338	60	60	30	2			
94	340	50	50	30	1		3	60
97	25	25	25		1		35	9
98	305	50	50	30	2	2	44	235
99	324	50	50	30			27	40
101	182	50	50	30			43	139
102	12	12	12	12	1	1	61	1
103	411	50	50	29	7	6	47	62
104	210	56	52	34	4	3	6	81
106	420	54	54	30	2	2	26	
107	388	65	65	30			30	254
108	265	52	52	30	1	1	39	117
109	374	50	50	30	2	2	1	59
111	359	52	52	32				99
112	337	50	50	30	1	1	40	85
113	394	80	80	30	7	4		43
115	476	69	69	31	4	3	36	112
116	340	59	57	38	6	5		91
117	338	50	50	30	1	1		32
118	357	52	52	30	1		12	205
119	343	50	50	30	4	1	40	126
120	382	50	50	30	2	2	19	41
121	176	57	51	37	8	8	21	20
124	53	53	53	30	6	6	66	30
125	446	85	76	34	10	8	30	197
129	554	56	55	24	3	3	52	300

Table 6. -- Cont.

Haul no.	Walleye pollock age1+ Lengths	Weights	Maturity	Otoliths	Gonad wts	Ovaries	Age-0 lengths	Camtrawl Autolengths Age1+
130	368	50	50	30	6	6		166
131	453	82	51	32	10	10	14	67
135	461	60	40	30	3	3	11	125
136	494	80	32	30	4	3	80	181
141	410	51	50	29	2	1		284
142	682	62	46	30	2	3	40	300
143	353	65	65	30	2	2	27	131
144	328	50	49	30	9	8	33	78
Total	31,383	5,052	4,835	2,793	249	214	1,210	8,561

Table 7. -- Walleye pollock biomass estimates between near surface and 0.5 m off bottom from summer acoustic-trawl surveys in the standard U.S. EEZ portion of the Bering Sea shelf, 1994-2018. Relative estimation error for the biomass is indicated. Estimates for 2018 include the 'unsampled area' west of 170° W, but do not include the northern extension area.

Date		Area (nmi)^2	Biomass, million metric tons (top) and percent of total (bottom)			Total Biomass to within 0.5 m off bottom (million metric tons)	Relative estimation error to 3m	Relative estimation error to 0.5m
			SCA	E170-SCA	W170			
1994	9 Jul-19 Aug	78,251	0.378	0.656	2.595	3.629	0.047	0.040
			10.4	18.1	71.5			
1996	20 Jul-30 Aug	93,810	0.272	0.490	2.182	2.945	0.039	0.032
			9.3	16.6	74.1			
1997	17 Jul-4 Sept	102,770	0.274	0.853	2.463	3.591	0.037	0.029
			7.6	23.7	68.6			
1999	7 Jun-5 Aug	103,670	0.323	0.758	3.060	4.141	0.055	0.044
			7.8	18.3	73.9			
2000	7 Jun-2 Aug	106,140	0.457	0.717	2.452	3.626	0.032	0.028
			12.6	19.8	67.6			
2002	4 Jun -30 Jul	99,526	0.755	0.946	2.605	4.306	0.031	0.027
			17.5	22.0	60.5			
2004	4 Jun -29 Jul	99,659	0.546	0.920	2.543	4.010	0.037	0.031
			13.6	23.0	63.4			
2006	3 Jun -25 Jul	89,550	0.144	0.342	1.387	1.873	0.039	0.033
			7.7	18.3	74.0			
2007	2 Jun -30 Jul	92,944	0.136	0.244	1.898	2.278	0.045	0.038
			6.0	10.7	83.3			
2008	2 Jun -31 Jul	95,374	0.122	0.087	1.197	1.406	0.076	0.056
			8.7	6.2	85.2			
2009	9 Jun -7 Aug	91,414	0.153	0.057	1.115	1.325	0.088	0.069
			11.5	4.3	84.1			
2010	5 Jun -7 Aug	92,849	0.098	0.193	2.351	2.642	0.060	0.054
			2.9	4.8	92.3			
2012	7 Jun -10 Aug	96,852	0.195	0.320	1.782	2.296	0.042	0.034
			7.7	7.5	84.8			
2014	12 Jun -13 Aug	94,361	0.561	1.462	2.707	4.730	0.046	0.034
			12.4	29.1	58.6			
2016	12 Jun -17 Aug	100,674	0.540	1.267	3.022	4.829	0.021	0.019
			11.2	26.2	62.6			
2018	12 Jun -22 Aug	92,283	0.231	0.513	1.755	2.499	0.044	0.039
			9.3	20.5	70.2			

Table 8. -- Numbers-at-length estimates (millions) of walleye pollock between near surface and 0.5 m off bottom from acoustic- trawl surveys in the U.S. EEZ, 1994-2018. Estimates for 2018 include the 'unsampled area' west of 170° W, but do not include the northern extension area.

Length (cm)	1994	1996	1997	1999	2000	2002	2004	2006	2007	2008	2009	2010	2012	2014	2016	2018
0	0.00	0.00	0.00	0.00	0.00	0.00	0.00	0.00	0.00	0.00	0.00	0.00	0.00	0.00	0.00	0.00
1	0.00	0.00	0.00	0.00	0.00	0.00	0.00	0.00	0.00	0.00	0.00	0.00	0.00	0.00	0.00	0.00
2	0.00	0.00	0.00	0.00	0.00	0.00	0.00	0.00	0.00	0.00	0.00	0.00	0.00	0.00	0.00	0.00
3	0.00	0.00	0.00	0.00	0.00	0.00	0.00	0.00	0.00	0.00	0.00	0.00	0.00	0.00	0.00	0.00
4	0.00	0.00	0.00	0.00	0.15	0.26	0.22	0.02	0.00	0.00	0.00	0.00	0.01	0.00	0.00	0.00
5	0.05	0.00	0.00	0.00	0.07	0.02	0.02	0.00	0.00	0.00	0.00	0.00	0.05	0.00	0.00	0.00
6	0.00	0.00	0.08	0.10	0.00	0.10	0.02	0.02	0.00	0.00	0.00	0.00	0.03	0.00	0.00	0.00
7	0.00	0.00	0.11	0.00	0.01	0.01	0.39	0.06	0.00	0.00	0.00	0.00	0.14	0.00	0.00	0.00
8	0.09	0.92	0.44	0.10	0.37	0.35	0.04	0.19	0.13	0.04	0.05	0.02	0.11	0.02	0.00	0.36
9	0.88	4.08	6.84	2.65	1.99	1.59	0.34	1.00	0.56	0.08	5.55	0.07	0.90	1.11	0.00	0.00
10	13.03	37.16	34.61	12.80	9.00	4.66	1.01	4.64	33.39	0.36	49.62	0.03	2.65	6.55	0.23	0.15
11	28.89	121.09	80.17	49.50	17.99	13.16	1.64	11.78	272.01	2.37	229.48	1.19	13.61	31.85	4.10	1.35
12	68.85	145.99	127.72	82.55	31.38	23.05	6.58	68.05	687.06	6.46	778.77	10.00	21.56	111.17	10.71	4.48
13	127.85	183.06	475.72	92.36	58.73	49.19	10.84	155.10	1,375.05	14.62	1,125.84	70.38	24.01	533.37	24.52	16.44
14	222.15	197.60	1,569.42	121.92	86.62	134.64	15.93	132.81	1,544.54	19.85	1,102.29	270.84	32.77	986.66	29.51	37.33
15	284.21	261.15	3,108.27	112.84	86.88	237.04	12.21	98.01	831.16	12.68	1,054.48	521.40	29.16	1,179.46	31.25	64.87
16	225.51	297.18	3,460.58	82.20	106.12	210.83	16.61	33.81	577.18	7.44	542.00	805.03	27.02	960.52	25.58	97.11
17	154.98	358.60	2,254.69	49.23	61.10	116.03	8.85	11.88	312.10	9.13	269.03	704.05	16.32	580.36	18.57	99.91
18	157.24	220.79	1,333.33	26.85	26.11	41.51	8.61	4.74	118.32	51.41	85.57	305.46	10.89	304.26	13.03	91.92
19	241.03	118.32	574.52	60.45	32.55	42.31	8.12	5.68	135.74	130.18	84.55	156.26	26.29	105.18	20.73	39.45
20	401.25	68.72	184.48	172.67	51.92	64.68	11.64	11.96	119.49	266.07	57.65	175.83	81.46	72.44	33.16	18.86
21	629.82	41.79	78.29	277.46	99.17	166.56	25.81	18.54	145.81	403.19	79.27	229.36	192.45	104.32	69.40	12.52
22	813.04	73.42	85.72	345.58	142.19	296.17	39.09	33.30	148.36	441.53	109.03	375.56	315.66	211.40	140.77	19.20
23	803.67	66.63	157.46	313.70	191.42	492.82	51.05	38.57	130.24	569.34	137.34	630.16	394.80	439.23	177.28	37.46
24	783.13	77.64	265.96	239.06	192.65	744.37	52.88	35.59	143.92	447.79	114.23	939.70	361.31	1,023.80	204.95	66.21
25	591.59	56.67	415.98	179.59	213.35	868.44	42.34	31.07	93.11	357.94	116.71	1,171.12	293.33	1,735.79	161.09	92.85
26	383.75	48.04	467.77	202.91	192.24	840.11	35.00	26.31	67.09	242.47	116.23	1,175.11	227.24	1,981.88	129.70	131.32
27	205.41	42.54	530.36	269.95	191.58	724.27	29.41	23.04	51.52	116.56	132.01	932.11	196.19	1,528.29	119.12	109.33
28	133.16	68.83	429.73	321.35	173.47	522.16	32.31	26.61	35.41	80.95	143.15	579.77	211.48	954.24	149.79	92.09
29	144.93	91.55	303.00	431.36	168.75	498.87	72.32	31.05	23.00	105.29	186.30	274.59	266.37	490.86	174.72	48.16
30	150.38	129.00	182.57	445.93	171.64	514.11	93.69	36.35	20.28	130.42	210.24	132.14	309.04	328.09	294.56	23.81
31	191.82	191.69	122.05	427.45	173.62	600.42	153.03	43.49	17.34	120.90	257.29	90.55	284.31	220.01	468.12	17.88
32	243.93	248.56	84.00	423.18	172.67	552.03	154.63	47.14	36.53	137.43	248.13	104.62	230.67	166.88	632.95	18.01
33	248.60	350.49	74.23	383.16	195.22	544.84	182.48	53.27	47.76	118.91	201.86	115.35	196.40	153.67	750.24	26.21
34	302.87	415.27	86.19	406.88	231.20	433.83	187.63	71.43	63.82	113.17	154.59	130.45	213.08	124.88	731.02	31.30
35	311.77	465.89	100.81	430.76	342.76	300.33	240.47	86.03	77.74	83.98	108.45	164.59	265.86	173.42	695.98	54.13
36	344.53	485.58	180.84	451.20	374.74	259.15	305.92	117.09	68.05	42.78	88.48	237.12	342.28	194.52	533.66	94.01
37	363.75	407.88	286.92	416.33	429.39	236.72	434.14	124.64	85.73	31.10	65.12	295.12	414.07	252.07	434.38	165.97
38	329.97	343.56	396.86	436.74	388.28	259.06	484.60	135.66	81.89	28.93	46.65	393.10	446.64	273.38	504.73	237.80
39	322.84	263.91	497.97	391.30	362.70	249.53	551.43	127.91	93.47	38.42	39.81	417.32	405.05	288.89	729.40	321.87

Table 8. -- Cont.

Length (cm)	1994	1996	1997	1999	2000	2002	2004	2006	2007	2008	2009	2010	2012	2014	2016	2018
40	345.38	227.12	477.29	334.19	322.82	252.20	527.07	143.31	119.80	31.22	34.70	384.72	347.72	254.97	1,008.03	421.77
41	305.56	186.30	412.11	276.24	360.94	237.82	543.01	154.61	130.18	33.73	29.41	299.23	229.90	259.62	983.89	490.24
42	328.15	177.54	346.78	287.88	359.93	227.97	526.62	178.41	167.24	46.18	30.32	216.86	156.12	277.86	740.50	511.76
43	330.64	173.84	257.47	327.24	371.39	232.85	511.97	189.44	221.95	52.51	27.09	147.00	96.85	397.29	489.25	482.69
44	306.44	160.58	199.11	395.76	351.86	241.25	464.78	207.31	227.37	63.10	22.34	102.25	90.18	416.67	353.00	371.65
45	329.50	148.39	150.12	407.55	348.58	246.17	405.30	197.80	261.97	68.96	25.23	69.80	80.70	476.66	273.53	300.04
46	281.11	135.05	122.52	383.94	323.58	240.11	318.36	190.10	258.78	89.53	27.69	51.35	88.00	411.95	210.73	234.52
47	234.24	129.67	105.92	305.40	301.79	237.92	262.03	173.14	228.85	87.69	30.17	30.95	82.39	341.88	177.44	175.46
48	196.29	135.22	94.87	253.77	238.90	226.10	223.21	161.44	195.52	97.44	43.69	20.63	78.41	256.74	151.04	137.42
49	106.78	116.27	74.62	172.51	186.15	206.48	178.46	128.81	168.47	81.18	46.62	17.24	65.59	198.48	121.92	104.34
50	94.55	103.51	76.69	133.03	147.41	181.98	140.70	113.80	142.48	72.54	43.36	20.08	54.21	148.51	100.93	70.69
51	59.48	103.34	63.61	103.78	111.64	159.27	111.20	90.13	111.49	69.70	42.36	18.09	38.50	118.36	75.41	55.47
52	52.77	86.92	65.70	76.68	80.45	133.13	101.30	79.80	85.57	58.82	41.73	18.39	33.96	89.98	55.43	42.09
53	34.42	72.52	63.06	63.57	56.36	120.47	77.25	59.54	65.50	44.73	37.81	16.52	27.05	70.67	42.07	29.65
54	30.52	60.60	53.48	57.25	39.81	87.71	59.66	47.25	58.24	39.98	35.03	19.61	27.06	52.88	31.81	18.98
55	38.53	44.55	50.78	41.08	30.30	66.04	42.56	32.50	38.32	31.73	30.47	16.07	19.13	40.06	22.00	15.73
56	26.53	31.65	43.41	31.64	25.39	59.22	35.50	28.06	31.89	26.88	24.70	14.91	17.12	31.31	17.18	10.60
57	27.49	23.60	35.42	32.55	19.51	35.37	23.78	21.94	24.39	21.71	20.22	14.53	13.68	27.25	13.94	6.57
58	19.35	22.67	33.90	22.03	15.67	30.77	16.26	16.81	16.21	18.67	19.82	13.88	14.55	25.80	7.94	5.39
59	15.41	17.43	29.51	16.50	12.65	19.65	14.68	12.87	12.50	15.04	11.80	9.73	12.15	21.83	6.10	3.31
60	14.76	15.70	24.81	15.61	7.71	18.37	11.06	8.94	9.02	14.20	12.11	11.25	12.34	15.60	4.58	2.04
61	17.26	17.33	24.07	15.26	7.14	11.73	8.49	8.04	5.49	8.07	10.40	10.16	9.63	14.92	3.22	2.00
62	10.06	11.13	16.47	10.51	6.41	9.78	6.24	4.47	5.54	9.68	8.11	7.31	10.31	11.52	3.57	1.01
63	9.37	9.21	13.11	6.31	4.93	5.76	4.98	3.62	4.25	6.56	5.13	5.51	6.08	8.26	3.38	1.11
64	6.22	10.00	13.08	5.66	4.56	5.13	1.92	3.83	3.54	4.55	4.91	5.96	7.23	6.01	1.99	0.99
65	7.29	8.16	12.01	6.04	2.80	4.60	1.53	1.80	2.23	3.59	6.32	3.86	4.22	5.98	1.56	0.66
66	3.93	6.98	8.10	5.58	2.18	3.15	1.49	1.95	1.97	2.62	4.97	3.24	3.88	3.78	1.28	0.28
67	4.16	3.82	8.57	3.04	1.01	1.62	0.91	1.00	1.47	1.91	2.96	2.58	2.44	1.85	1.41	0.23
68	3.82	3.33	6.23	3.13	1.58	1.53	0.81	0.69	0.89	1.71	1.92	2.77	2.90	1.48	0.43	0.12
69	1.29	2.49	5.63	2.56	1.70	0.60	0.23	0.40	0.48	0.65	2.05	1.01	1.19	1.78	1.05	0.10
70	3.10	2.62	1.96	1.87	0.48	1.59	0.28	0.37	1.23	0.87	1.38	1.02	2.03	1.53	0.31	0.34
71	2.52	1.69	1.80	1.60	0.24	0.10	0.27	0.28	0.57	0.43	0.99	0.29	0.87	0.46	0.51	0.04
72	1.80	1.61	2.87	1.23	0.91	0.18	0.15	0.55	0.28	0.78	0.89	0.89	0.68	0.89	0.29	0.15
73	0.95	0.88	2.74	1.39	0.57	0.08	0.13	0.12	0.23	0.32	0.94	0.94	0.55	0.63	0.33	0.00
74	0.39	1.09	0.92	1.53	0.44	0.04	0.11	0.13	0.28	0.37	0.58	0.41	0.56	0.10	0.13	0.04
75	0.73	0.28	1.38	0.56	0.06	0.18	0.11	0.05	0.05	0.20	0.54	0.13	0.38	0.17	0.12	0.03
76	0.34	0.42	0.58	0.25	0.11	0.05	0.02	0.02	0.15	0.12	0.19	0.20	0.20	0.13	0.07	0.00
77	0.16	0.35	0.26	0.39	0.08	0.00	0.02	0.05	0.05	0.05	0.29	0.03	0.01	0.08	0.04	0.00
78	0.67	0.46	0.16	0.18	0.25	0.11	0.07	0.01	0.01	0.05	0.32	0.17	0.06	0.04	0.00	0.00
79	0.10	0.11	0.05	0.66	0.06	0.06	0.04	0.08	0.08	0.08	0.09	0.03	0.06	0.15	0.00	0.01
80	0.11	0.47	0.42	0.02	0.02	0.09	0.08	0.03	0.01	0.05	0.15	0.05	0.01	0.00	0.00	0.00

Table 8. -- Cont.

Length (cm)	1994	1996	1997	1999	2000	2002	2004	2006	2007	2008	2009	2010	2012	2014	2016	2018
81	0.00	0.04	0.04	0.10	0.03	0.00	0.00	0.00	0.04	0.01	0.06	0.01	0.00	0.00	0.00	0.00
82	0.01	0.00	0.00	0.00	0.00	0.00	0.00	0.00	0.03	0.06	0.01	0.00	0.00	0.00	0.00	0.00
83	0.00	0.00	0.00	0.08	0.01	0.00	0.01	0.00	0.01	0.00	0.00	0.00	0.00	0.00	0.00	0.00
84	0.00	0.00	0.28	0.00	0.00	0.00	0.03	0.00	0.00	0.00	0.00	0.00	0.00	0.00	0.00	0.00
85	0.00	0.00	0.00	0.00	0.00	0.00	0.00	0.00	0.00	0.00	0.00	0.00	0.00	0.00	0.00	0.00
86	0.00	0.00	0.00	0.00	0.00	0.00	0.00	0.00	0.00	0.00	0.00	0.00	0.00	0.01	0.00	0.00
87	0.00	0.00	0.00	0.00	0.00	0.00	0.00	0.00	0.00	0.00	0.00	0.00	0.00	0.00	0.00	0.00
88	0.00	0.00	0.42	0.00	0.00	0.00	0.00	0.00	0.00	0.00	0.00	0.00	0.00	0.00	0.00	0.00
89	0.00	0.00	0.00	0.00	0.00	0.00	0.00	0.00	0.00	0.00	0.00	0.00	0.00	0.00	0.00	0.00
90	0.00	0.00	0.00	0.00	0.00	0.00	0.00	0.00	0.00	0.03	0.00	0.00	0.00	0.00	0.00	0.00
91	0.00	0.00	0.00	0.00	0.00	0.00	0.00	0.00	0.00	0.00	0.00	0.00	0.00	0.00	0.00	0.00
92	0.00	0.00	0.00	0.00	0.00	0.00	0.00	0.00	0.00	0.00	0.00	0.00	0.00	0.00	0.00	0.00
93	0.00	0.00	0.00	0.00	0.00	0.00	0.00	0.00	0.00	0.00	0.00	0.00	0.00	0.00	0.00	0.00
94	0.00	0.00	0.00	0.00	0.00	0.00	0.00	0.00	0.00	0.00	0.00	0.00	0.00	0.00	0.00	0.00
95	0.00	0.00	0.00	0.00	0.00	0.00	0.00	0.00	0.00	0.00	0.00	0.00	0.00	0.00	0.00	0.00
Total	14,471	10,135	22,856	13,465	10,726	15,352	9,898	5,916	12,049	7,248	10,639	14,978	9,504	21,527	14,236	7,588

Table 9. -- Biomass-at-length estimates (metric tons) of walleye pollock between near surface and 0.5 m off bottom on the Bering Sea shelf from acoustic-trawl surveys in the U.S. EEZ, 1994-2018. Estimates for 2018 include the 'unsampled area' west of 170° W, but do not include the northern extension area.

Length (cm)	1994	1996	1997	1999	2000	2002	2004	2006	2007	2008	2009	2010	2012	2014	2016	2018
0	0	0	0	0	0	0	0	0	0	0	0	0	0	0	0	0
1	0	0	0	0	0	0	0	0	0	0	0	0	0	0	0	0
2	0	0	0	0	0	0	0	0	0	0	0	0	0	0	0	0
3	0	0	0	0	0	0	0	0	0	0	0	0	0	0	0	0
4	0	0	0	0	0	0	0	0	0	0	0	0	0	0	0	0
5	0	0	0	0	0	0	0	0	0	0	0	0	0	0	0	0
6	0	0	0	0	0	0	0	0	0	0	0	0	0	0	0	0
7	0	0	0	0	0	0	1	0	0	0	0	0	0	0	0	0
8	0	4	2	0	1	1	0	1	0	0	0	0	0	0	0	1
9	4	23	37	16	10	8	2	4	2	0	28	0	4	5	0	0
10	91	281	256	104	61	28	7	28	219	2	360	0	16	40	2	1
11	270	1,215	791	535	173	113	14	106	2,566	20	2,067	11	110	273	38	12
12	840	1,897	1,641	1,158	369	275	72	844	7,563	71	9,324	128	221	1,249	130	51
13	2,006	3,019	8,004	1,577	956	843	164	2,503	19,660	206	17,310	1,133	320	8,027	372	237
14	4,495	4,077	34,384	2,410	1,729	3,099	292	2,427	26,524	333	21,843	5,636	525	18,392	564	654
15	7,004	6,837	85,531	2,699	2,253	6,756	264	2,262	18,307	280	25,813	13,265	616	27,502	711	1,442
16	6,769	9,222	114,075	2,588	3,442	7,274	464	967	15,222	199	16,311	25,321	675	27,156	704	2,611
17	5,521	13,368	86,128	1,853	2,382	4,750	300	417	10,119	294	10,231	26,389	494	19,562	632	3,179
18	6,702	9,734	59,251	1,234	1,209	1,960	342	188	4,536	1,974	3,728	13,367	380	12,368	507	3,596
19	12,039	6,109	29,021	3,311	1,781	2,386	384	275	6,275	5,963	4,254	7,612	1,224	4,862	935	1,767
20	23,333	4,124	10,888	10,938	3,264	4,220	669	680	6,478	14,140	3,289	10,030	4,294	3,940	1,728	998
21	42,266	2,887	5,130	20,225	7,184	12,493	1,758	1,196	9,837	24,645	5,378	15,491	11,995	6,531	4,248	761
22	62,526	5,837	6,455	28,741	11,814	25,297	3,017	2,517	11,704	32,036	8,898	29,824	22,556	15,854	10,147	1,340
23	70,370	6,031	13,544	29,585	18,070	47,914	4,575	3,357	11,567	48,182	12,703	56,891	33,393	40,231	14,277	3,189
24	77,654	7,974	26,036	25,342	20,503	82,205	5,306	3,414	14,652	42,991	11,701	97,519	34,830	107,654	19,388	6,053
25	66,095	6,563	46,007	21,330	25,530	108,639	4,784	3,256	10,401	38,588	14,295	137,876	31,659	208,917	16,952	10,034
26	48,092	6,246	58,154	26,937	25,685	118,576	4,630	3,254	8,218	29,442	15,561	154,478	27,511	268,514	15,461	15,955
27	28,741	6,191	73,891	39,827	28,501	114,279	4,311	3,101	7,058	15,860	20,709	136,677	26,913	229,990	16,237	15,207
28	20,786	11,106	66,832	52,503	28,599	90,626	5,235	4,067	5,414	12,244	24,266	95,842	32,214	156,588	22,865	14,283
29	25,147	16,397	52,498	77,806	30,720	94,182	13,154	5,244	3,873	17,623	36,696	49,748	45,820	87,140	29,423	8,485
30	28,768	25,506	35,139	88,380	34,370	105,352	18,582	6,750	3,786	24,023	45,015	25,498	57,946	65,285	54,211	4,461
31	40,527	41,794	26,065	92,792	38,166	134,142	33,511	9,478	3,653	24,936	61,499	19,804	60,177	47,306	97,204	3,711
32	56,300	59,505	19,673	100,309	41,474	134,207	37,002	11,133	8,880	30,941	64,575	25,186	53,026	39,658	146,117	4,107
33	62,710	91,811	19,026	98,899	51,177	144,432	48,814	13,657	12,493	29,640	57,511	30,961	48,978	39,982	189,582	6,578
34	83,137	118,782	24,146	114,113	65,965	125,435	54,037	19,913	18,290	30,110	47,709	38,852	57,920	35,480	202,239	8,662
35	93,093	145,111	30,624	130,942	106,254	94,857	74,888	26,162	24,288	25,085	36,107	53,442	78,365	54,296	211,040	16,273
36	111,770	164,314	59,987	148,312	125,738	88,738	104,382	38,508	22,864	14,013	31,512	83,627	110,151	67,122	177,907	31,810
37	127,765	149,556	103,683	147,694	155,814	87,938	158,135	43,278	31,527	10,968	24,312	112,574	145,297	93,558	158,509	60,329
38	125,329	136,254	155,037	166,856	151,890	102,392	190,999	51,543	32,608	11,057	19,268	164,348	166,411	109,874	205,775	93,195
39	132,793	112,891	210,473	160,602	152,550	106,073	233,905	52,742	39,916	15,815	17,034	185,257	162,947	124,097	326,182	134,966
40	152,852	104,709	217,378	147,011	146,310	114,928	242,198	62,716	54,211	13,948	16,046	184,912	150,795	118,113	488,727	188,431
41	145,985	92,210	202,379	130,152	175,511	115,887	266,935	72,298	62,927	15,977	14,930	153,430	106,728	129,328	510,035	232,454
42	169,722	94,449	183,338	145,202	187,652	118,500	278,043	90,396	85,610	22,805	16,364	118,269	77,816	147,493	404,861	260,909
43	185,272	98,874	145,766	175,891	207,166	130,045	293,120	101,116	122,933	28,499	15,722	85,093	51,439	226,061	278,963	262,627
44	185,591	98,004	120,762	226,679	209,380	142,984	283,390	119,469	132,865	36,132	13,706	62,972	51,064	251,442	211,592	216,695
45	214,772	96,739	97,398	247,924	219,831	155,379	261,913	120,086	163,870	42,291	15,922	45,438	49,145	305,366	172,062	187,318
46	195,473	93,794	84,948	248,327	217,158	161,830	216,423	122,478	173,624	57,807	19,237	35,918	56,727	279,948	138,048	153,464

Table 9. -- Cont.

Length (cm)	1994	1996	1997	1999	2000	2002	2004	2006	2007	2008	2009	2010	2012	2014	2016	2018
47	173,200	96,094	78,123	209,154	213,598	170,074	188,150	118,641	161,437	60,404	22,227	22,660	57,400	245,570	120,580	121,219
48	153,689	107,418	74,823	184,248	179,554	171,830	167,232	116,175	147,234	69,589	34,241	16,401	58,517	194,558	109,272	98,731
49	88,569	97,638	62,740	132,810	148,018	167,289	141,308	98,496	132,770	62,462	38,243	14,408	51,596	158,686	92,502	79,095
50	83,148	92,238	68,685	108,375	123,586	155,037	117,891	93,920	120,184	59,474	38,136	17,633	44,612	125,349	80,166	56,209
51	55,185	97,997	60,519	88,882	98,525	144,191	98,605	77,277	98,584	59,265	39,191	17,095	34,071	106,584	63,152	45,915
52	52,440	87,262	65,963	69,597	74,341	127,714	93,852	71,798	80,469	54,043	41,163	18,147	31,059	86,313	48,637	36,108
53	35,799	77,023	66,981	60,723	55,660	123,107	76,076	57,657	64,036	44,146	38,345	17,011	26,851	70,807	38,607	27,385
54	33,903	67,818	60,322	57,665	40,395	93,999	61,923	48,287	61,937	40,768	37,559	21,471	28,334	56,082	31,158	18,368
55	45,443	52,792	60,228	43,511	32,790	74,528	45,881	35,087	43,248	34,816	33,799	18,484	21,209	44,836	23,195	16,125
56	33,152	39,789	54,774	35,710	28,601	70,647	41,003	30,769	37,668	32,029	29,747	18,351	19,369	36,801	18,504	11,616
57	36,409	31,448	47,671	38,505	23,095	44,433	29,158	25,900	30,748	26,597	26,094	18,338	16,582	33,153	16,155	7,620
58	27,226	32,050	48,692	27,710	19,294	40,789	20,297	21,109	21,175	24,696	25,620	18,620	18,475	33,496	9,674	6,604
59	22,375	25,896	44,548	21,398	16,589	27,151	20,070	17,064	17,530	20,413	17,428	14,058	15,754	30,298	8,170	4,215
60	22,572	23,971	39,384	21,588	10,569	26,475	15,636	12,766	13,245	20,994	18,434	17,278	17,581	22,543	6,183	2,767
61	27,582	28,464	40,468	22,192	10,131	17,805	12,951	11,748	8,398	12,472	16,842	16,458	14,229	22,397	4,688	2,803
62	16,927	19,266	29,484	16,320	9,654	15,392	9,625	6,909	8,921	15,934	13,378	12,166	16,237	18,914	5,512	1,516
63	16,711	16,409	22,950	10,128	7,897	9,592	8,246	5,816	7,388	11,027	9,112	9,718	9,816	13,689	5,455	1,736
64	11,610	18,653	24,530	9,839	7,473	8,896	3,186	6,427	6,331	8,011	9,027	11,023	12,219	10,706	3,380	1,593
65	14,074	15,930	23,557	10,586	4,846	8,524	2,706	3,215	4,182	6,587	12,251	7,545	7,708	10,872	2,813	1,199
66	7,984	14,271	16,646	10,170	3,995	5,863	2,800	3,633	3,950	4,939	10,200	6,818	7,293	7,613	2,333	498
67	8,805	8,133	18,334	5,807	1,995	3,213	1,795	1,925	2,995	3,936	6,206	5,606	4,843	3,760	2,811	425
68	8,351	7,438	14,003	6,263	3,140	3,106	1,682	1,417	1,964	3,567	4,168	6,406	5,920	3,228	894	229
69	2,790	5,815	13,197	5,338	3,560	1,291	477	878	1,065	1,437	4,677	2,336	2,489	3,770	2,273	198
70	7,106	6,371	4,807	3,850	832	3,460	601	814	2,997	1,967	3,241	2,506	4,381	3,522	681	754
71	6,355	4,285	4,616	3,613	558	232	620	667	1,378	1,051	2,514	713	2,022	1,104	1,152	91
72	4,616	4,262	7,661	2,889	2,157	441	342	1,306	755	1,935	2,259	2,323	1,731	2,167	687	348
73	2,536	2,430	7,609	3,406	1,405	204	327	298	622	840	2,591	2,668	1,380	1,677	805	349
74	1,138	3,118	2,677	3,912	1,095	106	284	331	782	966	1,649	1,189	1,519	292	338	350
75	2,063	828	4,144	1,477	154	478	308	130	144	553	1,571	385	1,022	504	328	351
76	1,070	1,292	1,821	705	295	133	45	46	471	359	566	641	576	408	191	352
77	523	1,120	844	1,123	225	1	60	137	167	149	928	108	26	245	122	353
78	0	0	0	0	0	0	0	0	0	0	0	0	0	0	0	354
79	2,115	1,546	545	547	755	330	223	32	36	158	1,064	600	197	133	0	355
80	358	389	191	1,968	188	199	135	246	260	267	285	99	192	505	0	356
81	0	0	0	0	0	0	0	0	0	0	0	0	0	0	0	357
82	419	1,704	1,544	61	51	290	265	99	19	162	538	176	34	0	0	358
83	8	155	141	342	115	0	0	3	160	29	211	32	7	0	0	359
84	58	0	0	0	0	0	0	0	109	219	23	6	2	0	0	360
85	0	0	0	295	30	0	40	0	44	13	1	0	0	0	0	361
86	0	0	0	0	1	0	0	0	0	0	0	0	0	42	0	362
87	0	0	0	0	0	0	0	0	0	0	0	5	0	0	0	363
88	0	0	2,051	0	0	0	0	0	0	0	0	0	0	0	0	364
89	0	0	0	0	0	0	0	0	0	0	0	0	0	0	0	365
90	0	0	0	0	0	0	0	0	0	169	0	0	0	0	0	366
91	0	0	0	0	0	0	0	0	0	9	0	0	0	0	0	367
92	0	0	0	0	0	0	0	0	0	0	0	0	0	0	0	368
93	0	0	0	0	0	0	0	0	0	0	0	0	0	0	0	369
94	0	0	0	0	0	0	0	0	0	0	0	0	0	0	0	370
95	0	0	0	0	0	0	0	0	0	0	0	0	0	0	0	371
Total	4,541,756	3,532,672	4,060,362	5,276,344	4,731,550	5,291,306	5,106,746	2,546,664	3,181,077	1,761,633	1,496,794	2,798,777	2,617,972	6,043,333	5,545,455	3,207,574

Table 10. -- Estimated numbers-at-age (millions, top panel) and biomass-at-age (thousand metric tons, bottom panel) for walleye pollock observed between near surface and 0.5 m off bottom in the U.S. EEZ from summer Bering Sea shelf acoustic-trawl surveys 1994-2018. Estimates for 2018 include the 'unsampled area' west of 170° W, but do not include the northern extension area.

Age	1994	1996	1997	1999	2000	2002	2004	2006	2007	2008	2009	2010	2012	2014	2016	2018
0	2.1	0.0	0.0	0.0	0.0	0.0	0.0	0.0	0.0	0.0	0.0	0.0	0.0	0.0	0.0	0.0
1	1140.1	1800.3	13226.8	607.2	460.4	796.4	83.1	524.7	5775.3	70.9	5196.8	2567.9	177.3	4750.8	173.8	450.0
2	4969.1	566.7	2881.0	1780.0	1322.0	4943.9	313.5	217.0	1040.6	2914.8	815.8	6404.1	1988.7	8655.1	1037.9	516.6
3	1424.5	552.2	440.5	3717.1	1230.1	3385.1	1216.9	291.2	345.1	1047.0	1734.1	983.6	1692.9	969.5	4496.1	248.6
4	1818.6	2741.1	535.6	1809.7	2588.0	1294.9	3122.6	654.1	477.8	166.0	281.3	2294.9	2710.2	1161.0	4476.4	621.2
5	2251.8	915.0	2330.3	651.9	1011.8	660.6	1634.3	783.4	793.7	160.8	76.7	445.9	279.7	1118.7	715.5	2267.5
6	389.1	633.5	546.4	397.5	326.6	935.3	567.1	658.6	729.4	287.6	94.1	73.1	366.7	1769.6	348.1	944.1
7	108.6	585.0	313.0	1548.0	308.4	538.4	287.7	390.2	406.9	234.9	128.9	33.2	113.1	740.1	392.2	198.4
8	95.9	141.7	290.4	526.3	949.6	140.4	282.7	144.9	240.8	136.1	110.8	36.9	35.7	170.1	420.3	111.8
9	56.2	38.6	75.1	180.0	277.6	162.4	120.9	74.8	97.7	101.8	76.7	37.8	24.9	78.8	95.7	107.3
10	67.1	28.2	27.8	141.6	134.1	304.5	68.5	58.6	39.3	32.0	44.2	28.9	28.7	31.5	30.7	74.9
11	30.3	22.4	30.9	48.2	60.3	103.6	58.9	32.8	37.2	30.1	25.2	26.0	25.1	12.6	18.0	19.7
12	51.1	39.5	35.2	20.5	35.6	45.4	77.0	21.7	18.8	19.0	11.3	13.1	17.9	13.9	5.8	5.5
13	20.6	13.9	38.9	10.3	7.0	20.2	37.4	16.5	9.2	10.9	10.1	8.0	16.2	14.1	3.6	2.9
14	17.6	24.8	18.7	7.8	4.6	12.2	12.5	19.8	9.6	5.6	5.5	4.9	5.1	7.7	2.2	0.0
15	10.0	10.3	26.1	4.2	4.3	1.5	9.3	10.0	10.5	5.8	3.9	3.3	4.1	6.9	2.9	0.1
16	15.5	12.5	16.1	3.7	2.0	1.1	1.0	6.7	5.0	8.2	3.7	1.3	1.5	4.5	0.2	0.5
17	7.7	6.0	18.8	4.9	2.0	0.8	0.1	2.2	1.1	3.7	2.6	1.0	0.9	3.5	0.3	0.0
18	0.0	4.9	2.6	1.7	1.4	1.3	0.1	0.4	1.6	1.9	2.7	2.2	0.4	1.7	0.0	0.3
19	0.7	2.2	2.6	4.5	0.1	1.2	0.0	2.5	1.1	2.5	1.8	1.0	1.0	1.0	0.0	0.2
20	0.2	0.0	2.7	0.9	0.2	0.4	0.1	0.1	0.2	0.4	2.4	0.5	0.5	0.4	0.0	0.0
21+	0.3	0.0	0.0	0.1	0.1	1.0	0.0	0.1	1.4	0.1	1.2	0.6	1.3	1.1	0.0	0.2
Total	12,477	8,139	20,860	11,466	8,726	13,351	7,894	3,910	10,042	5,240	8,630	12,968	7,492	19,513	12,220	5,570

Age	1994	1996	1997	1999	2000	2002	2004	2006	2007	2008	2009	2010	2012	2014	2016	2018
0	0.0	0.0	0.0	0.0	0.0	0.0	0.0	0.0	0.0	0.0	0.0	0.0	0.0	0.0	0.0	0.0
1	28.4	52.5	434.8	13.6	11.6	24.2	2.0	9.9	106.4	1.4	105.5	80.9	3.3	117.9	4.5	13.6
2	440.2	43.0	380.1	171.4	147.6	652.0	36.0	21.8	91.0	243.3	80.1	751.3	184.4	1,163.9	106.3	60.3
3	334.5	124.0	114.0	873.2	294.7	868.6	338.2	70.2	96.9	224.3	414.7	218.1	345.6	219.4	1,196.8	54.8
4	724.4	908.6	205.9	691.6	1,018.9	517.8	1,448.2	247.7	211.5	68.3	120.0	1,017.8	1,028.0	459.4	2,165.0	246.2
5	1,297.6	451.5	1,107.3	304.5	547.0	373.5	936.9	414.3	464.3	92.4	46.8	257.8	157.4	612.6	379.9	1,159.8
6	256.1	433.2	345.9	239.3	204.3	634.3	396.6	428.0	508.2	199.8	74.6	55.6	269.5	1,215.2	218.3	564.7
7	79.2	497.6	254.8	1,013.9	217.0	424.0	222.9	297.3	325.9	190.3	118.8	33.7	96.2	550.9	276.1	131.6
8	87.9	129.3	292.1	387.5	705.1	126.2	238.7	122.8	213.6	128.4	112.7	42.9	36.0	166.8	326.2	83.2
9	63.4	41.9	89.4	161.5	219.5	160.0	112.6	69.8	95.5	99.2	84.1	47.0	30.9	85.2	79.0	86.8
10	83.0	35.1	35.3	139.6	123.2	307.7	66.6	58.2	43.4	37.8	55.1	39.2	37.2	37.1	31.2	67.8
11	41.3	32.7	44.9	53.8	66.5	110.8	60.3	33.7	41.7	37.3	33.1	35.9	32.9	17.7	21.7	19.4
12	74.7	61.8	57.1	24.3	36.7	50.7	81.3	25.4	22.5	23.5	17.3	20.0	24.4	19.5	8.5	5.7
13	31.2	22.9	66.5	16.4	8.9	25.5	40.8	20.5	12.5	15.2	16.7	13.6	23.7	21.8	5.7	3.0
14	28.5	42.8	32.6	13.3	7.0	17.7	15.0	25.1	13.9	8.7	9.9	8.7	8.5	11.9	3.8	0.0
15	19.2	16.8	45.0	7.1	7.2	2.2	12.1	12.3	14.1	8.3	6.7	6.0	6.9	11.2	4.7	0.1
16	25.0	24.7	29.8	6.2	3.3	1.9	1.4	8.3	7.2	13.1	7.3	2.5	2.9	6.8	0.4	0.9
17	12.4	12.1	37.2	9.6	3.6	1.5	0.1	3.1	2.3	5.8	5.6	2.2	1.8	5.1	0.5	0.0
18	0.0	10.0	5.5	2.9	2.5	2.1	0.2	0.8	2.8	3.6	5.5	4.7	0.8	2.6	0.0	0.6
19	0.8	4.1	5.5	9.6	0.3	2.3	0.0	3.2	2.1	3.8	3.5	2.1	1.7	1.8	0.0	0.4
20	0.6	0.0	5.3	1.6	0.5	0.7	0.1	0.2	0.3	0.8	3.8	1.2	1.1	0.8	0.0	0.0
21+	0.8	0.0	0.0	0.3	0.3	1.9	0.0	0.3	1.8	0.3	2.9	1.3	2.5	2.3	0.0	0.5
Total	3,629	2,945	3,589	4,141	3,626	4,306	4,010	1,873	2,278	1,405	1,325	2,642	2,296	4,730	4,829	2,499

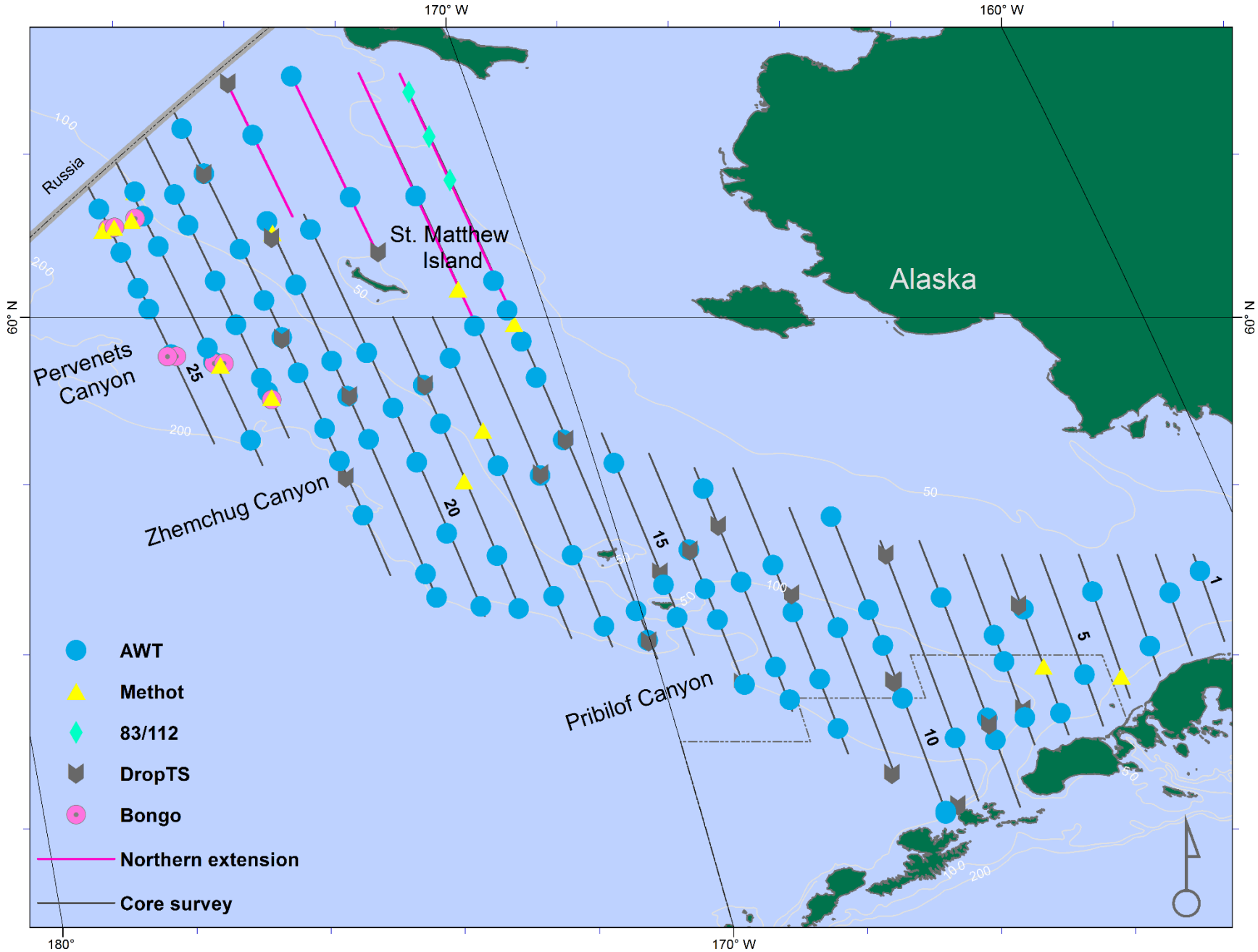

Figure 1.-- Transect lines with locations of Aleutian wing trawls, Methot trawls, 83-112 trawls, Drop-TS deployments, and Bongos during the summer 2018 acoustic-trawl survey of walleye pollock on the eastern Bering Sea shelf. Transect numbers are noted on transects. Steller sea lion conservation area is outlined in dashed line.

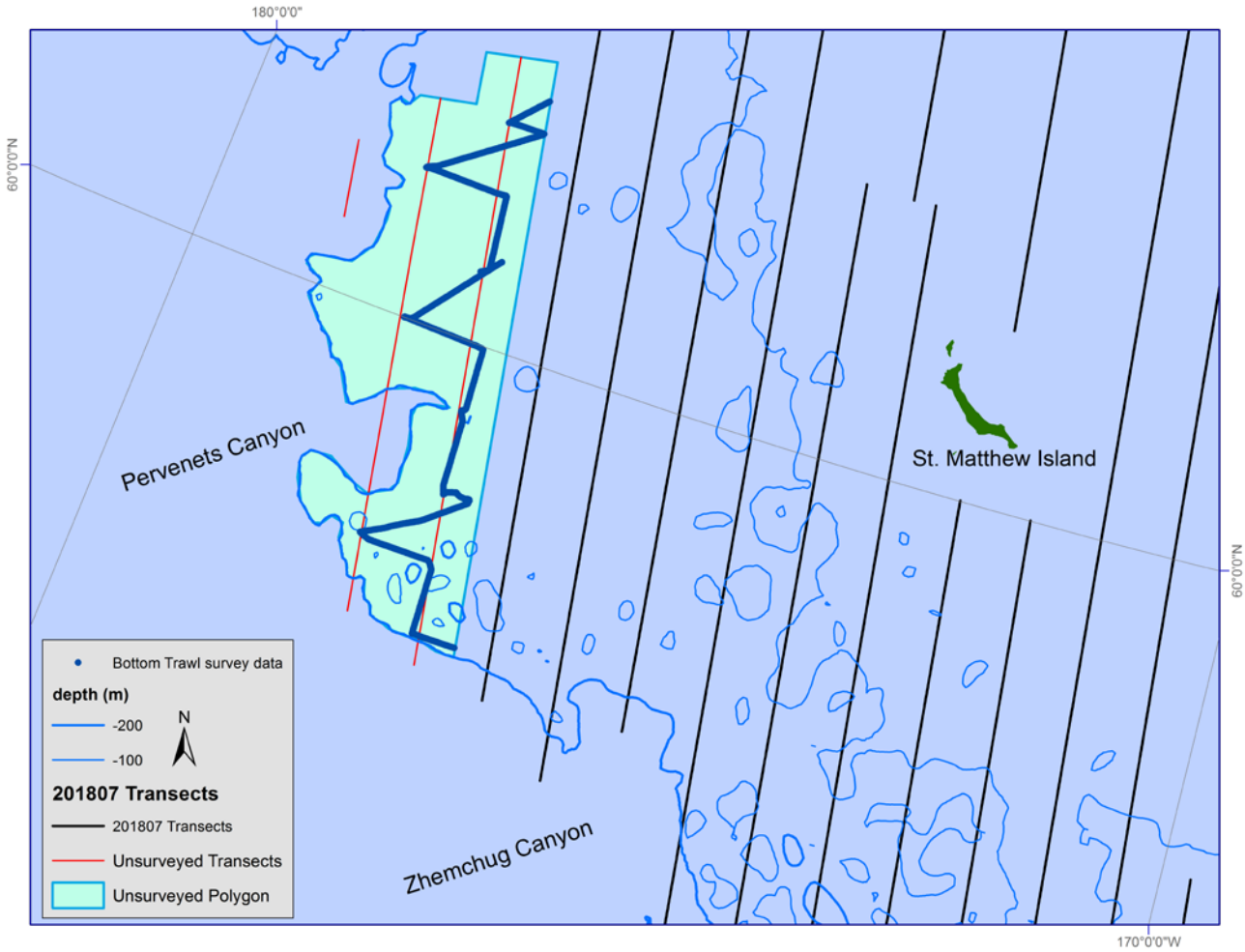

Figure 2. Map of survey area showing completed transects (black lines), unsurveyed transects (red lines), unsurveyed polygon (green shading), and the tracks of the bottom trawl vessels (thick blue line) inside the unsampled area that were used to estimate acoustic backscatter in this area. The 100 and 200 m contours are shown.

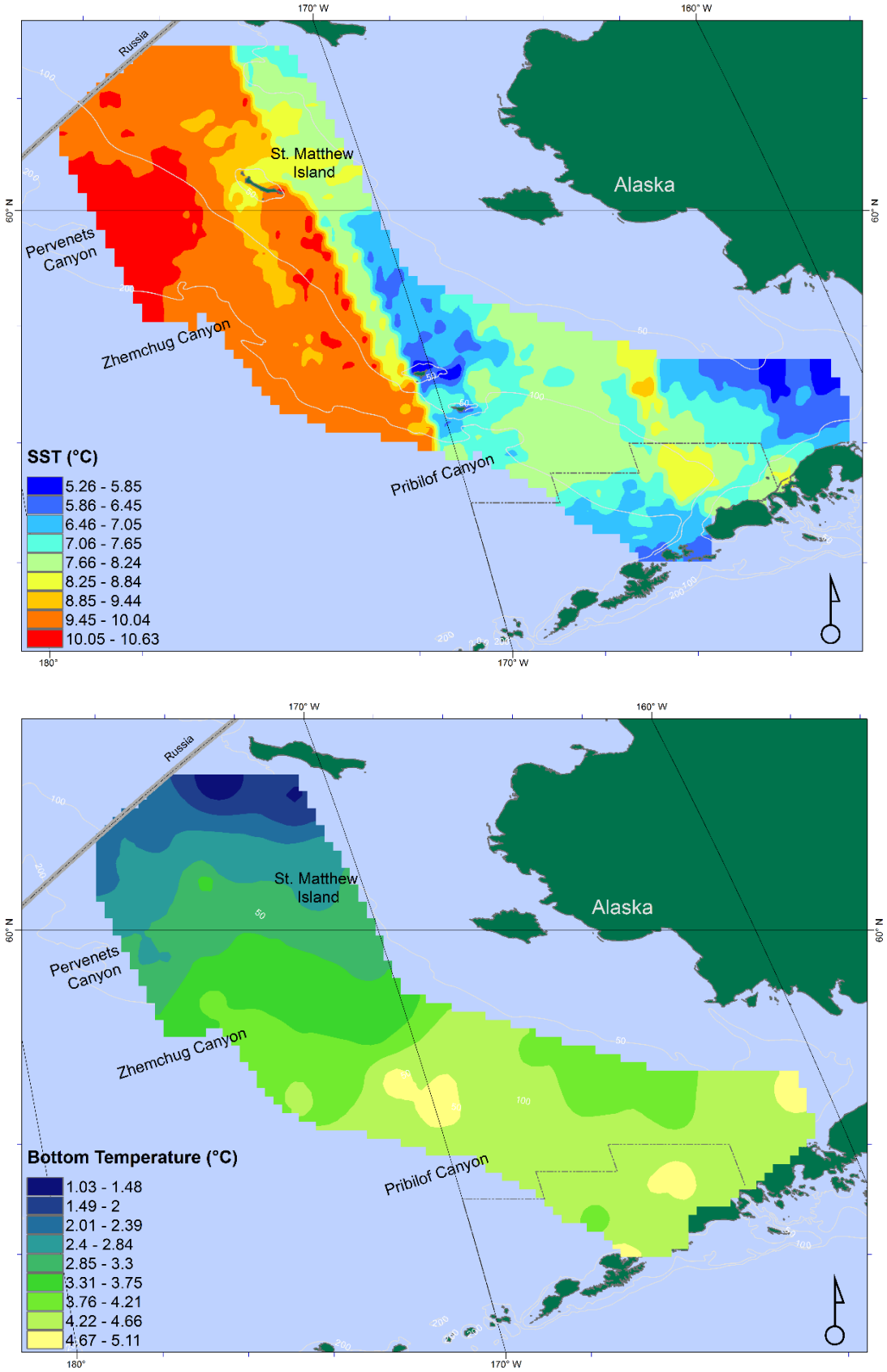

Figure 3. -- Temperature (°C) a) measured at the sea surface using shipboard surface temperature sensors along survey transects averaged at 10 nautical mile resolution, and b) at the bottom using conductivity-temperature-depth profilers (CTDs, n = 59), during the summer 2018 acoustic-trawl survey of the eastern Bering Sea shelf. Contours generated with IDW.

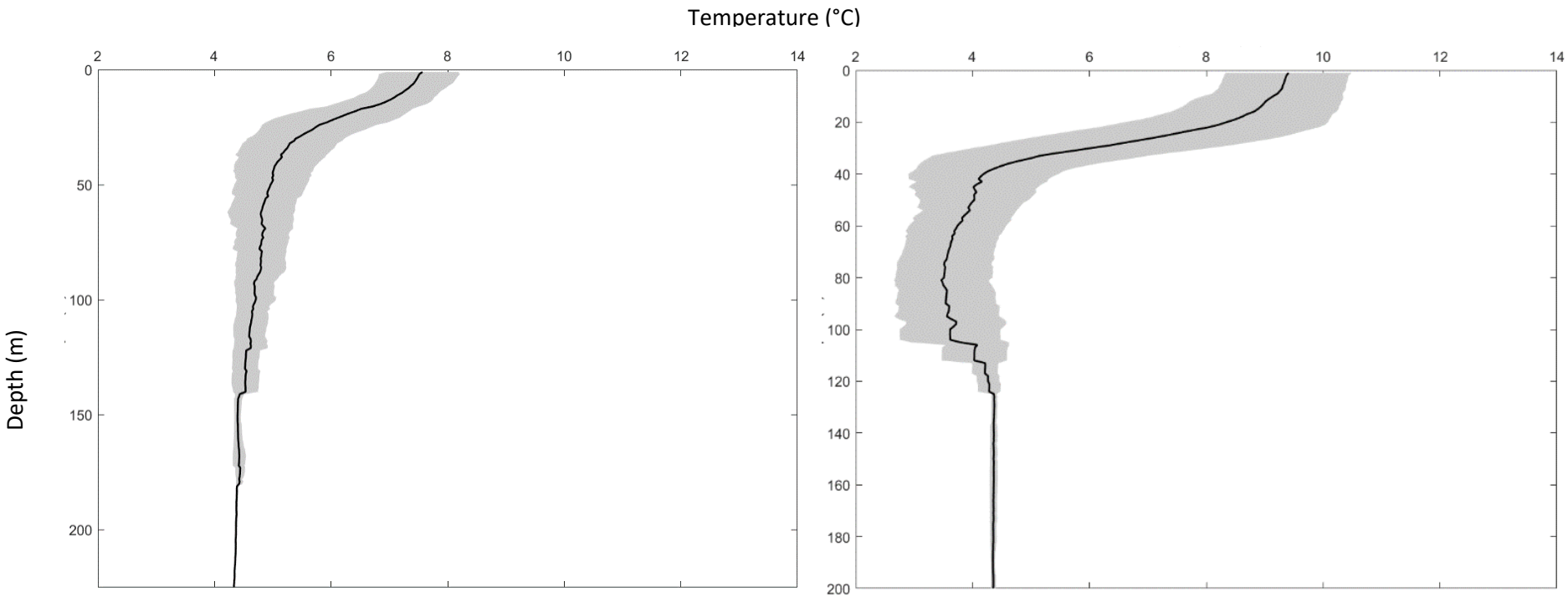

Figure 4. -- Mean water temperature (°C; solid line) by 1-m depth intervals for trawl haul locations during the summer 2018 eastern Bering Sea acoustic-trawl survey. Data were collected with a Sea-Bird Electronics temperature-depth probe (SBE-39) attached to the trawl headrope. Gray region represents minimum and maximum temperatures observed. Profiles are shown for trawls east of 170 °W (n = 54; left) and west of 170 °W in the U.S. EEZ (n = 86; right).

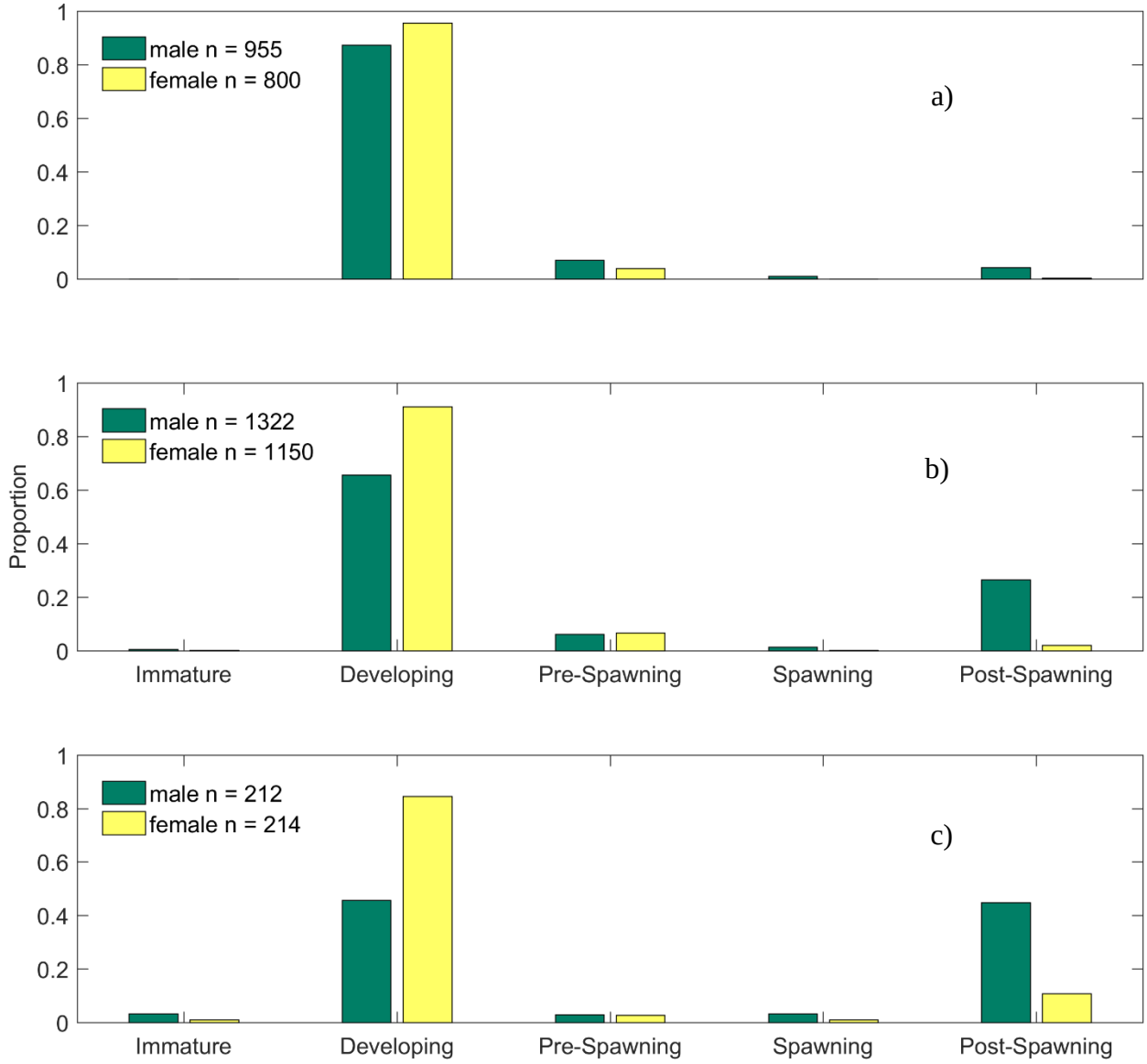

Figure 5. -- Maturity stages by sex for walleye pollock ≥ 34 cm observed during the summer 2018 eastern Bering Sea shelf acoustic-trawl survey in the core survey area a) east and b) west of 170° W, and c) in the northern extension area outside of the core survey area.

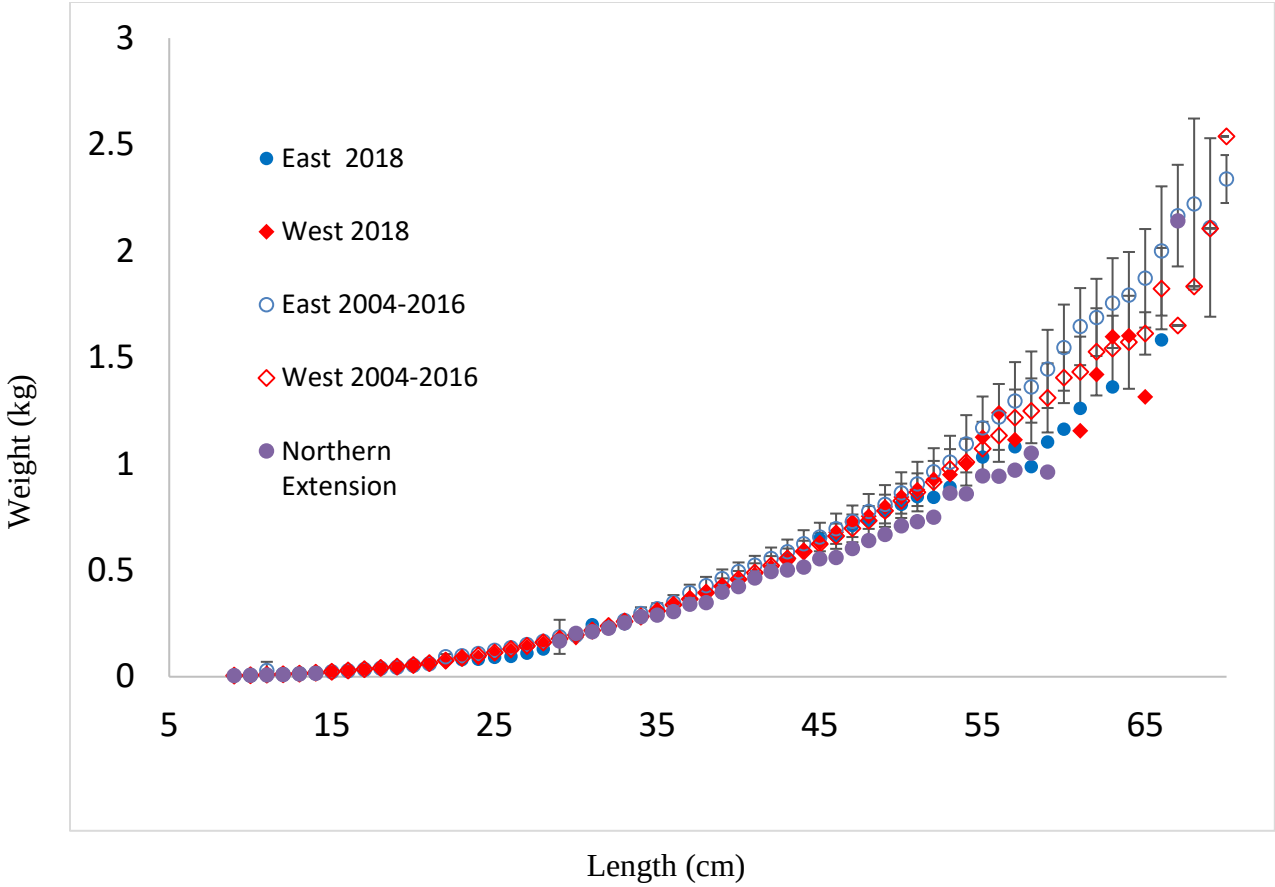

Figure 6. -- Mean weight-at-length for walleye pollock measured in the core survey area east and west of 170°W, and in the northern extension area during the summer 2018 eastern Bering Sea shelf acoustic-trawl survey, plotted against mean values for 2004, 2006-2010, 2012, 2014 and 2016. Error bars represent ± 1 standard deviation around the 2004-2016 data points.

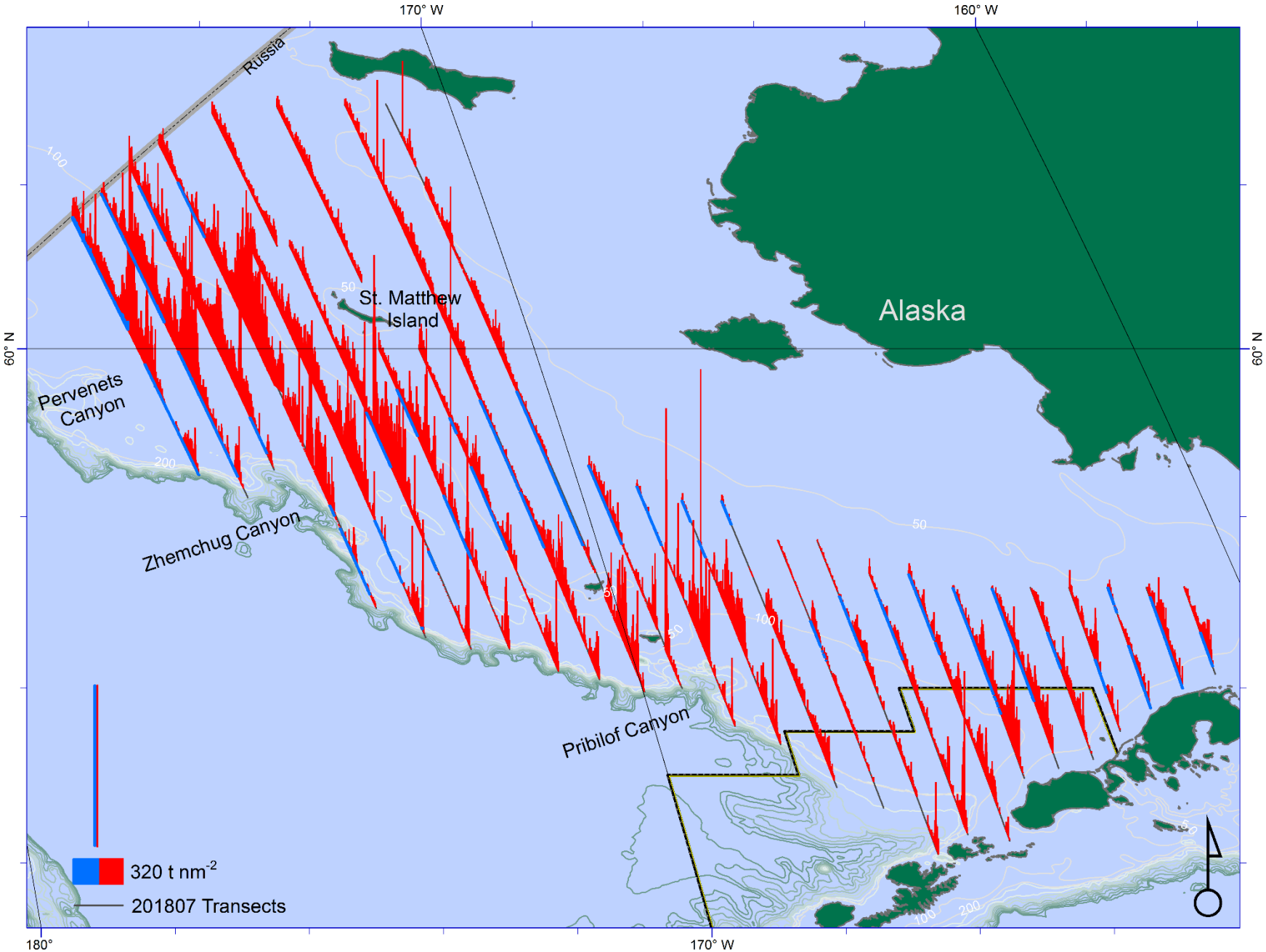

Figure 7.–Estimated walleye pollock biomass per sq. nmi for the summer 2018 acoustic-trawl survey for 16 m from surface to 0.5 m off bottom. Fish ≤ 20 cm FL (blue), and > 20 cm FL (red) are indicated. The Steller sea lion Conservation Area (SCA) is outlined in black.

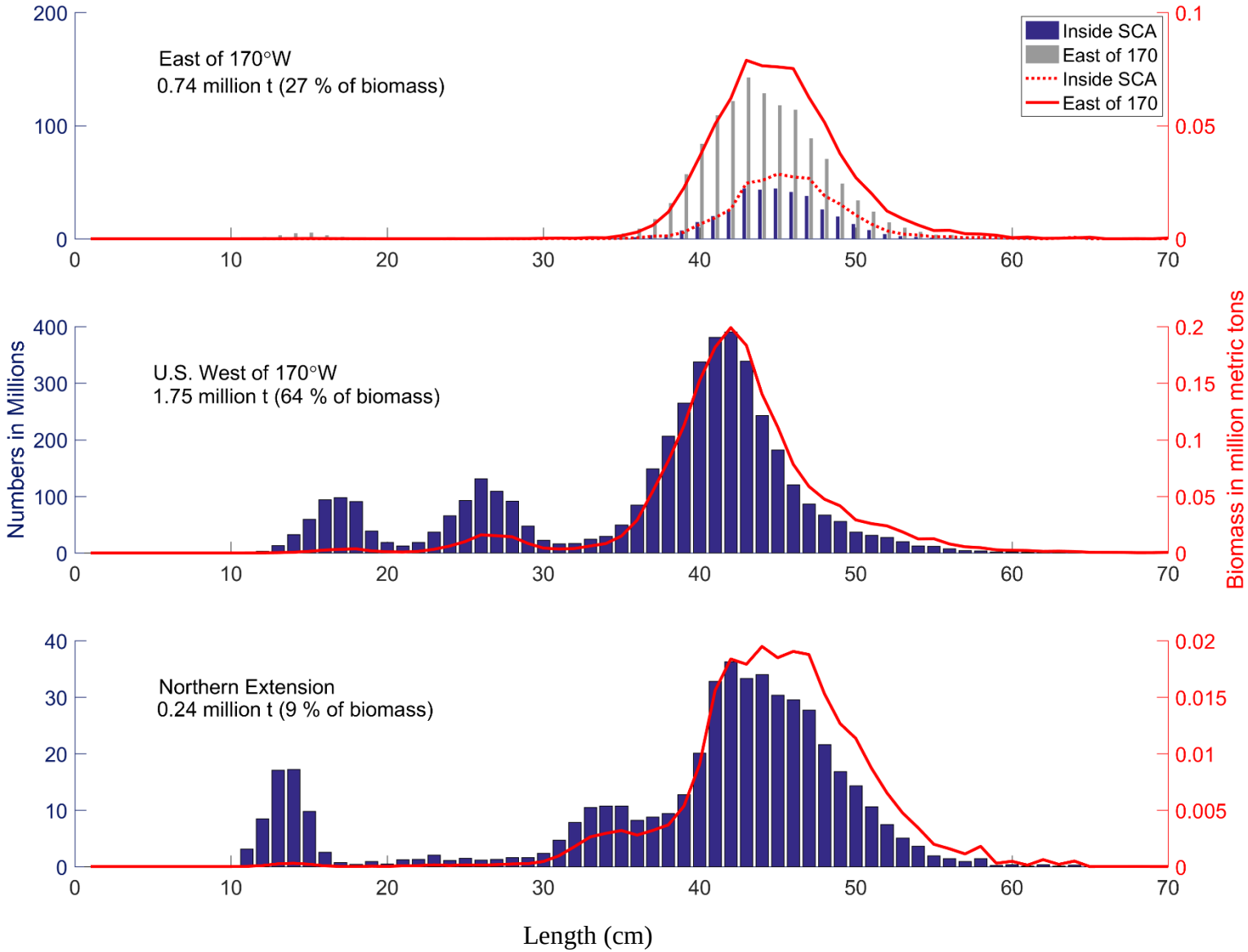

Figure 8. -- Population numbers (histogram bars) and biomass (lines) at length (cm) estimated for walleye pollock between 16 m from the surface and 0.5 m off the bottom from the summer 2018 eastern Bering Sea shelf acoustic-trawl survey in three geographic regions. The unsampled area estimates (west of 170° W) are included.

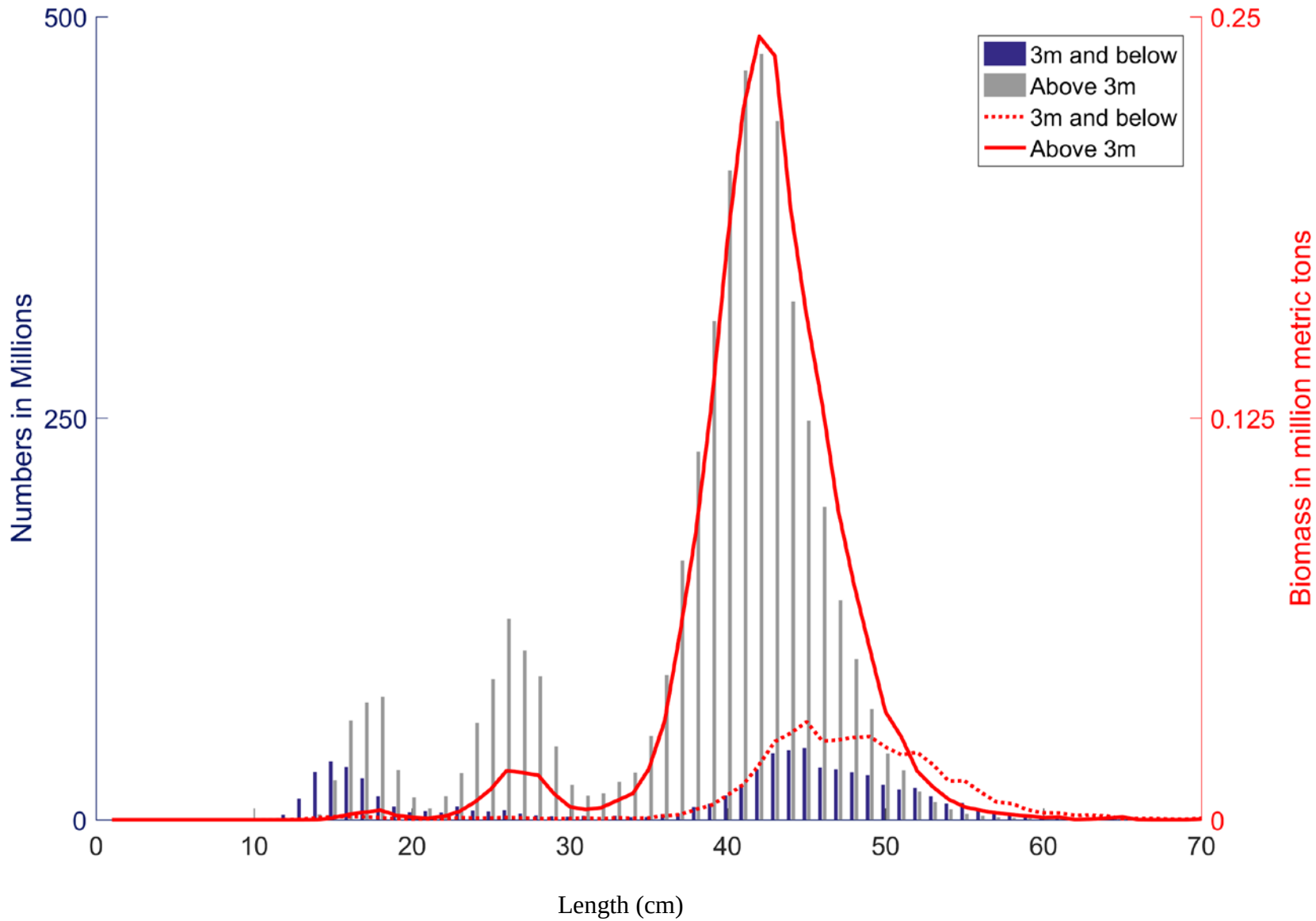

Figure 9. -- Population numbers (histogram bars) and biomass (lines) at length (cm) estimated for walleye pollock between 16 m from the surface and 3 m off bottom, and for 3 m to 0.5 m off the bottom from the summer 2018 eastern Bering Sea shelf acoustic-trawl survey. These estimates include the unsampled area but do not include the northern extension portion of the survey.

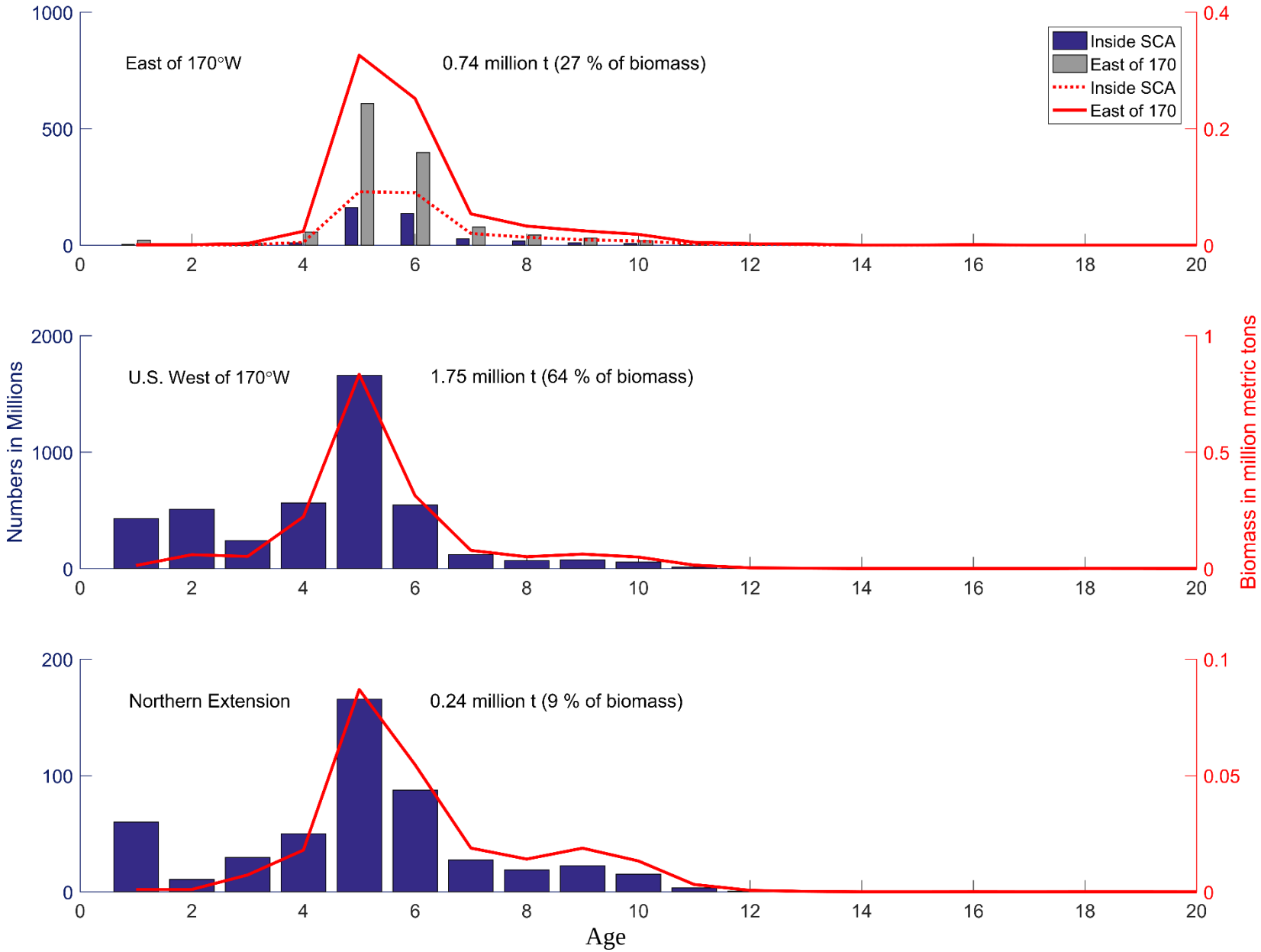

Figure 10. -- Population numbers (histogram bars) and biomass (lines) at age estimated for walleye pollock between 16 m from the surface and 0.5 m off the bottom from the summer 2018 eastern Bering Sea shelf acoustic-trawl survey in three geographic regions. These estimates include the unsampled area west of 170° W.

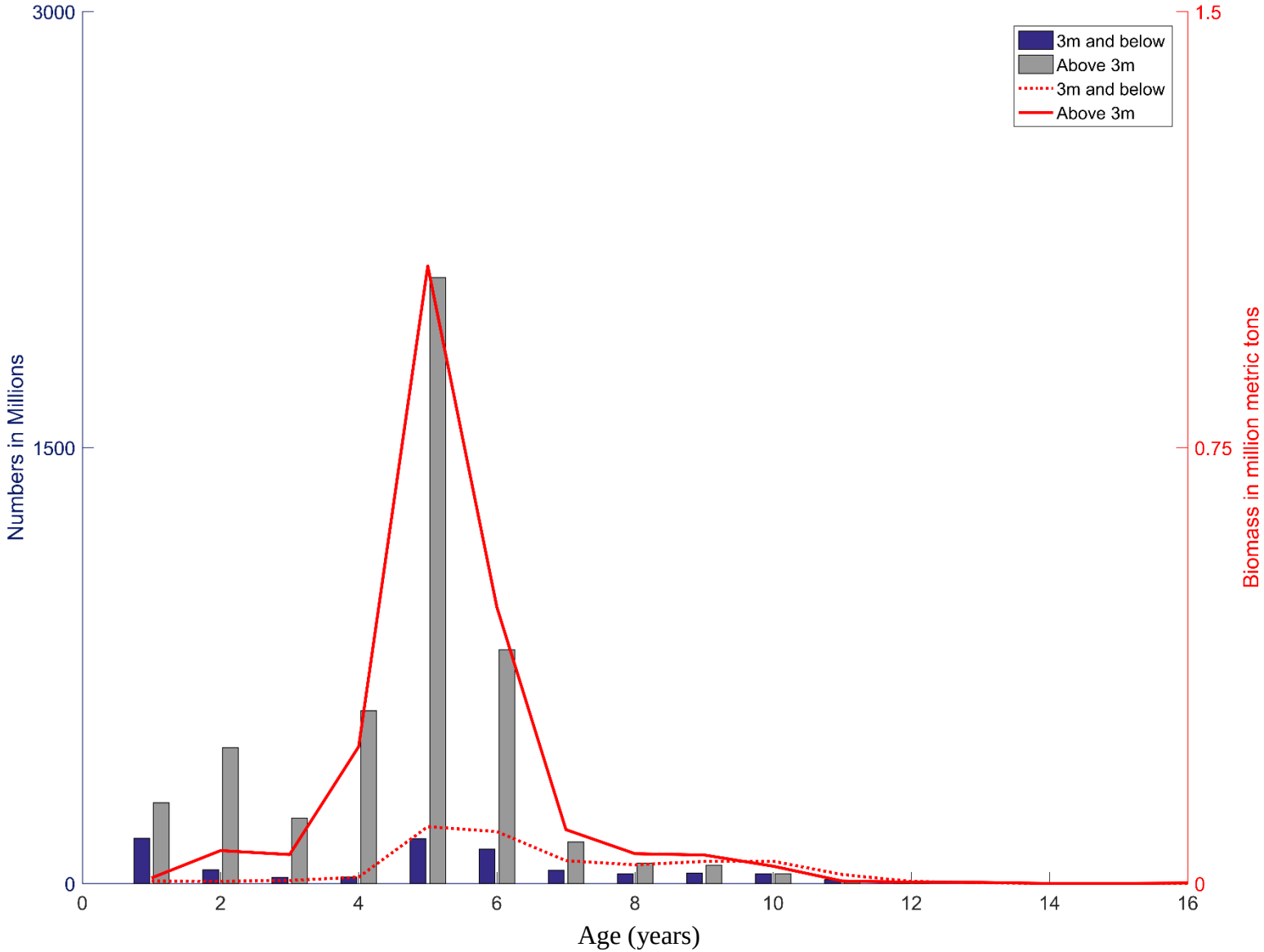

Figure 11. -- Population numbers (histogram bars) and biomass (lines) at age estimated for walleye pollock between 16 m from the surface and 3m off bottom, and for 3m to 0.5 m off the bottom from the summer 2018 eastern Bering Sea shelf acoustic-trawl survey. These estimates include the unsampled area west of 170° W, but do not include the northern extension area of the 2018 survey.

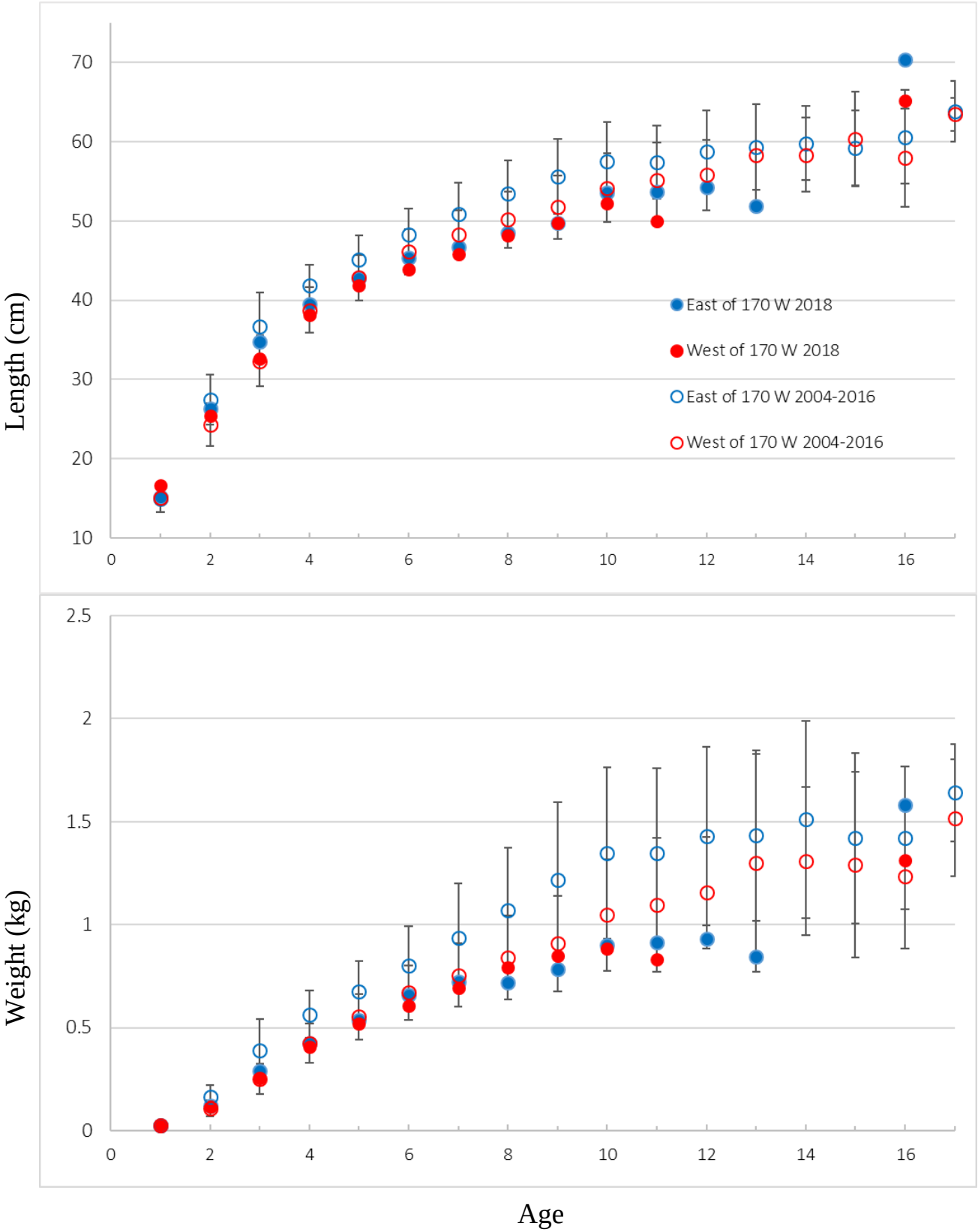

Figure 12. -- Mean length- (top) and weight- (bottom) at-age for walleye pollock in the U.S. EEZ east and west of 170°W for the summer 2018 eastern Bering Sea shelf acoustic-trawl survey, and mean estimates for 2004-2016 surveys combined. Error bars represent ± 1 standard deviation around the 2004-2016 means.

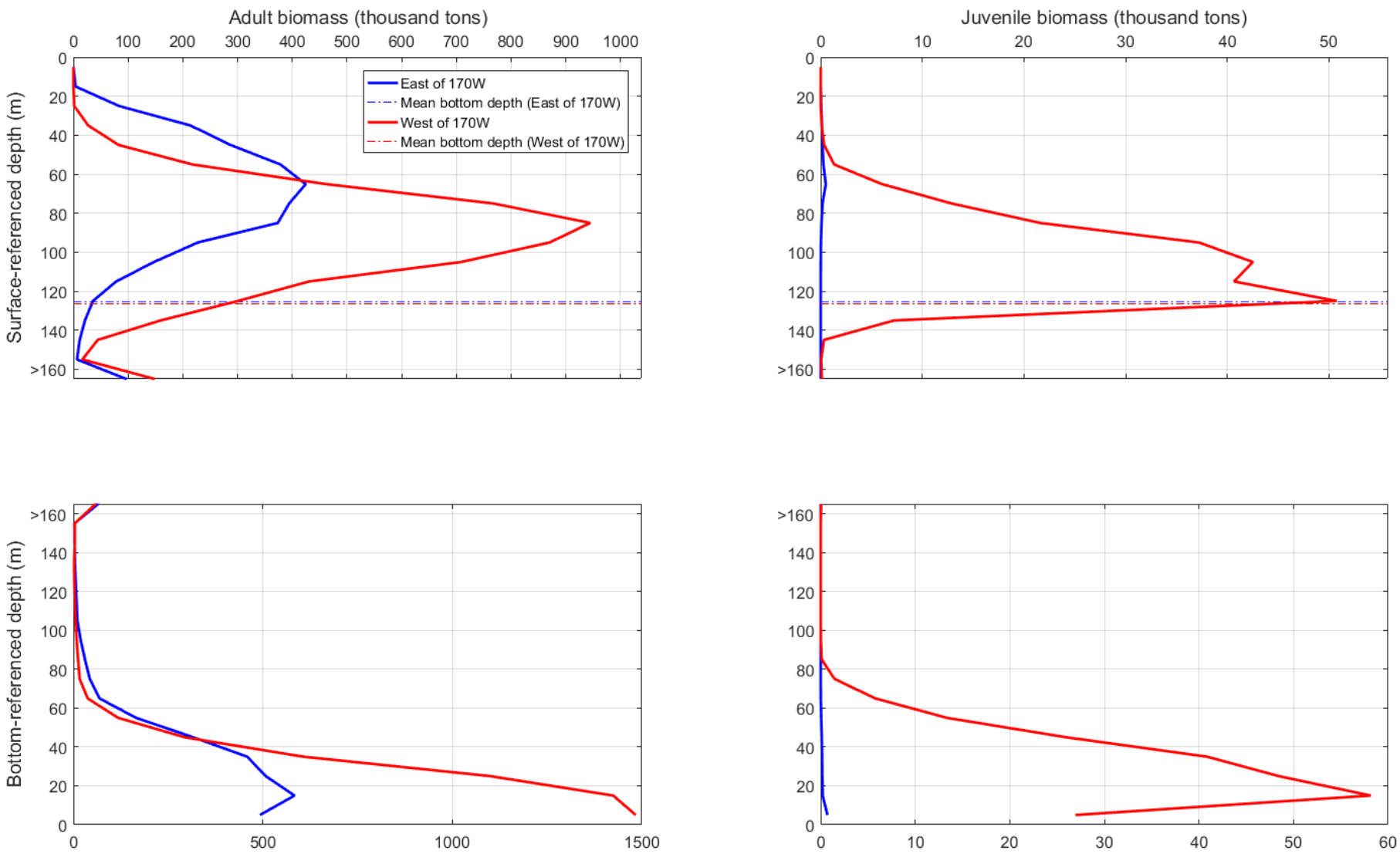

Figure 13.-- Depth distribution (m) of adult (≥ 30 cm FL) or juvenile (< 30 cm FL) walleye pollock biomass (thousand metric tons) east and west of 170°W longitude in the core survey area of the U.S. EEZ Bering Sea shelf during the summer 2018 acoustic-trawl survey. Depth is referenced to the surface (a, b) and to the bottom (c, d). Data were averaged in 10 m depth bins from near surface to within 0.5 m of the seafloor. Note that data from the unsampled area (3 western-most survey transects) are missing.

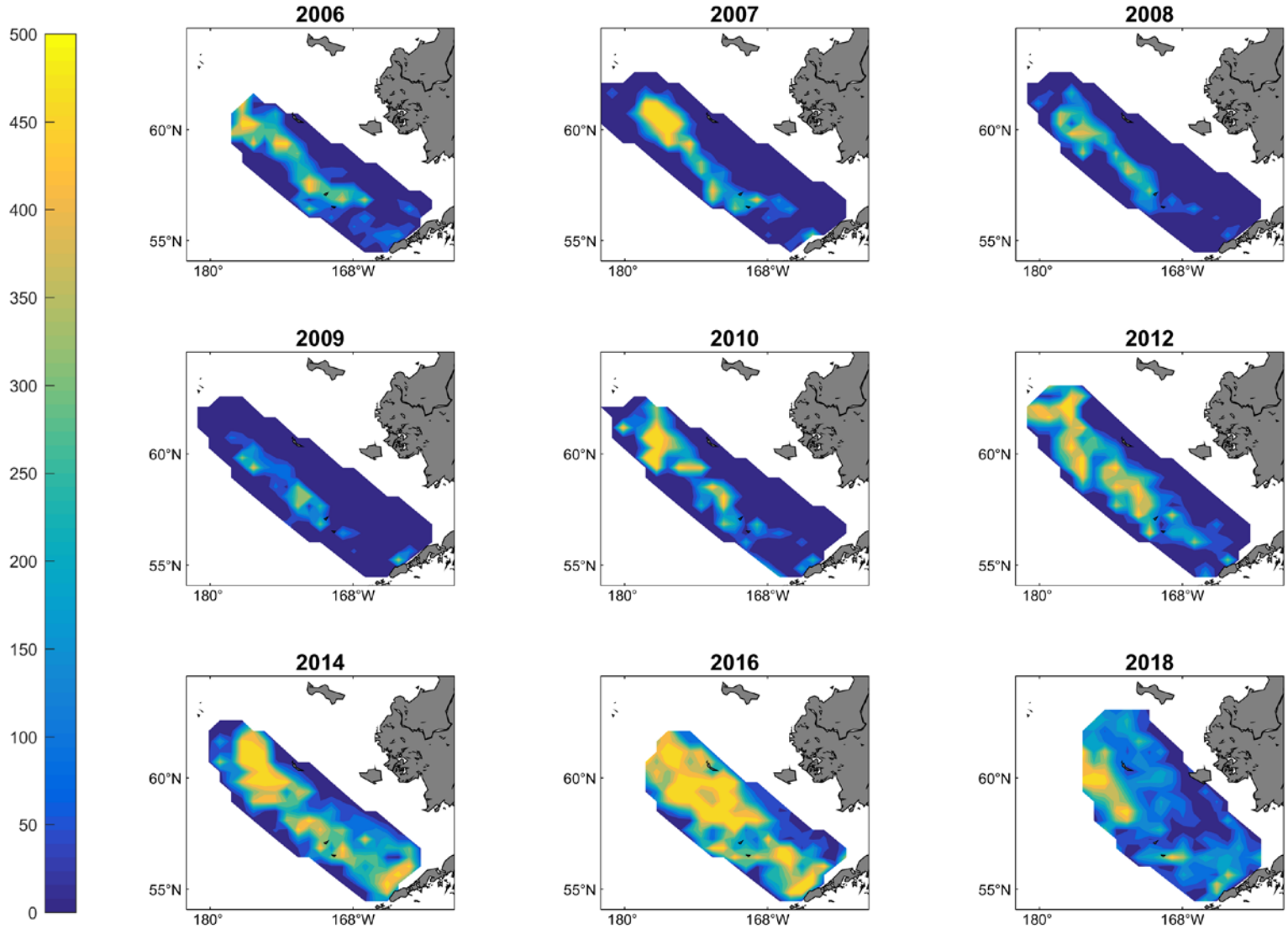

Figure 14 -- Walleye pollock backscatter (s_A, m^2 nmi^{-2}) between near surface and 0.5 m off bottom at 38 kHz observed along tracklines during summer eastern Bering Sea acoustic-trawl surveys conducted between 2006 and 2018. Backscatter data are shown in a "northern extension" and are missing from the westernmost 3 transects in 2018.

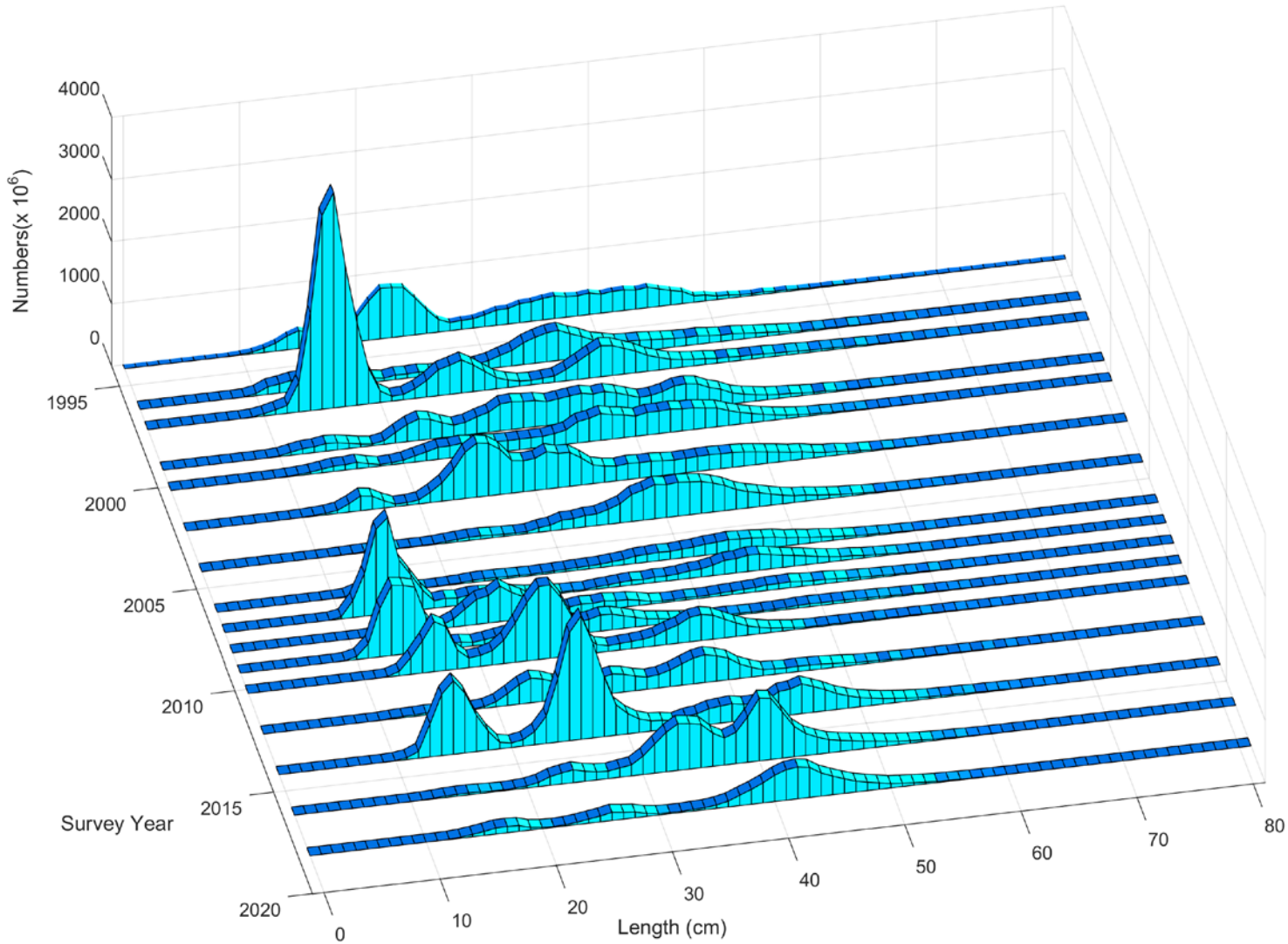

Figure 15. -- Historical numbers at length between near surface and 0.5 m off bottom in the core survey area of the U.S. EEZ for the summer eastern Bering Sea shelf acoustic-trawl surveys between 1994 and 2018.

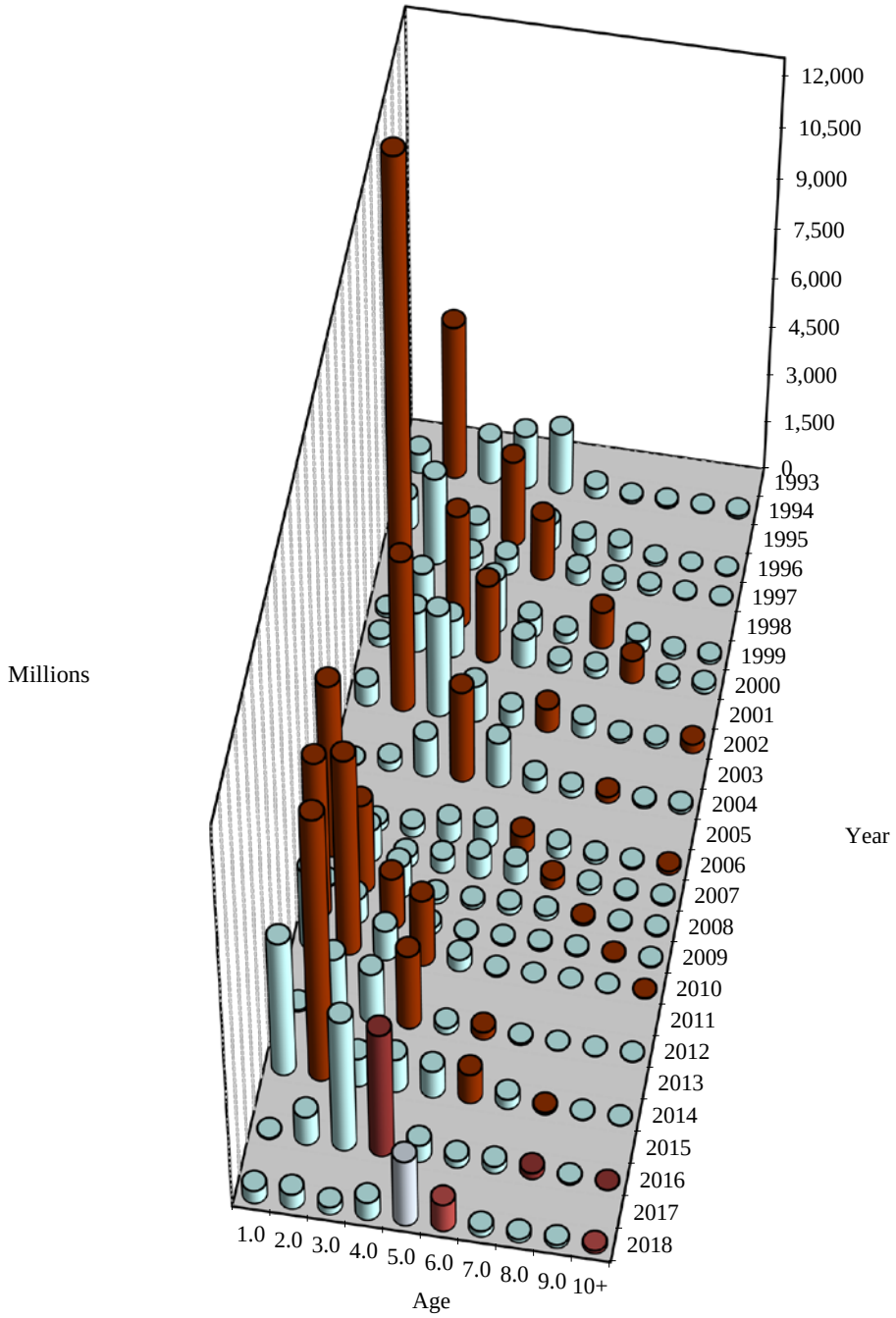

Figure 16. -- Historical numbers at age of walleye pollock between near surface and 0.5 m off bottom in the U.S. EEZ for summer eastern Bering Sea shelf acoustic-trawl surveys between 1994 and 2018. Strong year classes are indicated with dark columns.

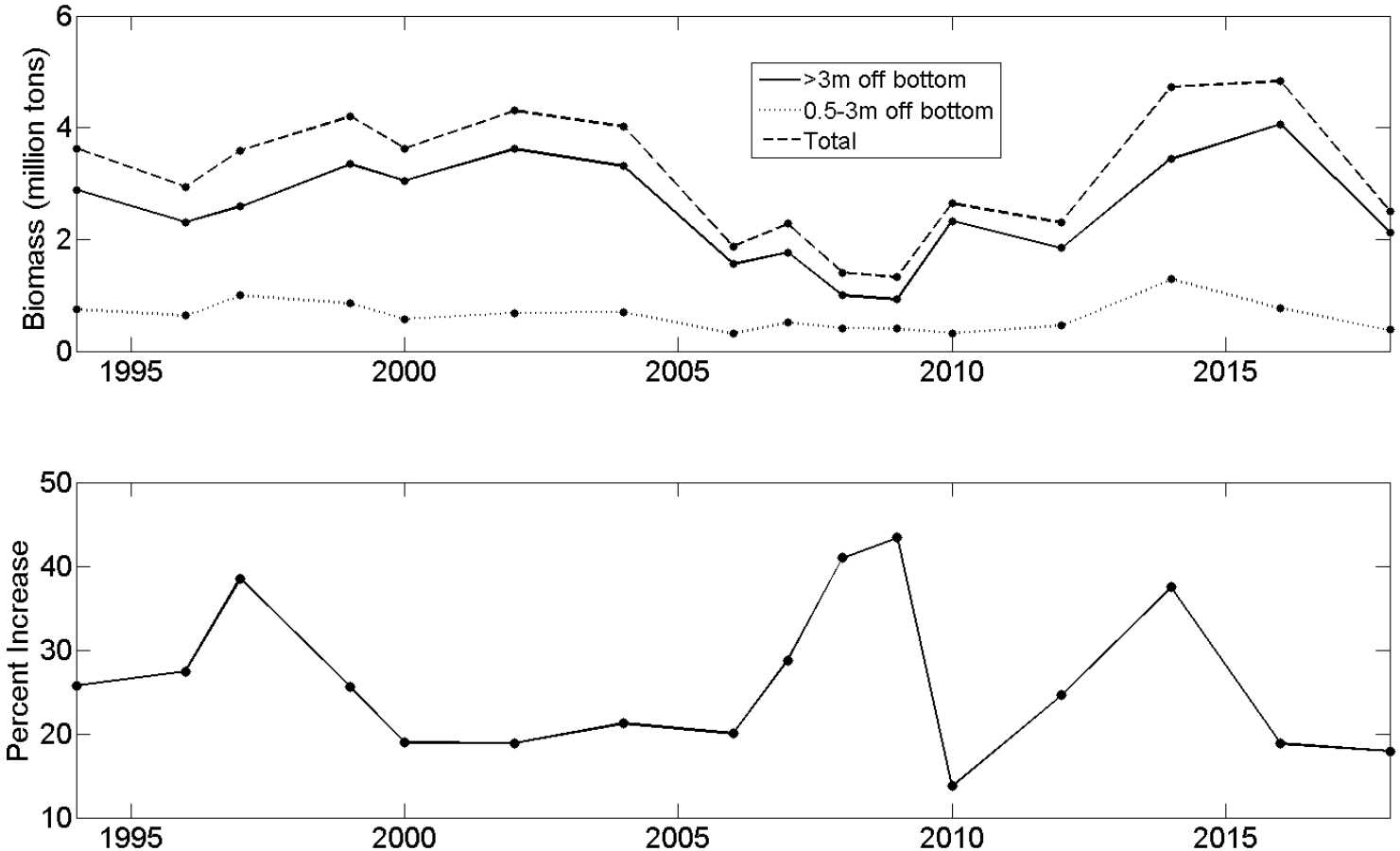

Figure 17. -- (Top panel) Pollock biomass by year in million metric tons for the region between the surface and 3 m above bottom (solid line), the region between 0.5 and 3 m above bottom (dotted line), and the sum of these two regions (dashed line). (Bottom panel) Percent increase from the region between the surface and 3 m above bottom to the total water column. Data are shown for the core survey area, and in 2018, include estimates from an "unsampled area" – the westernmost 3 transects -- estimated using bottom trawl survey backscatter information.

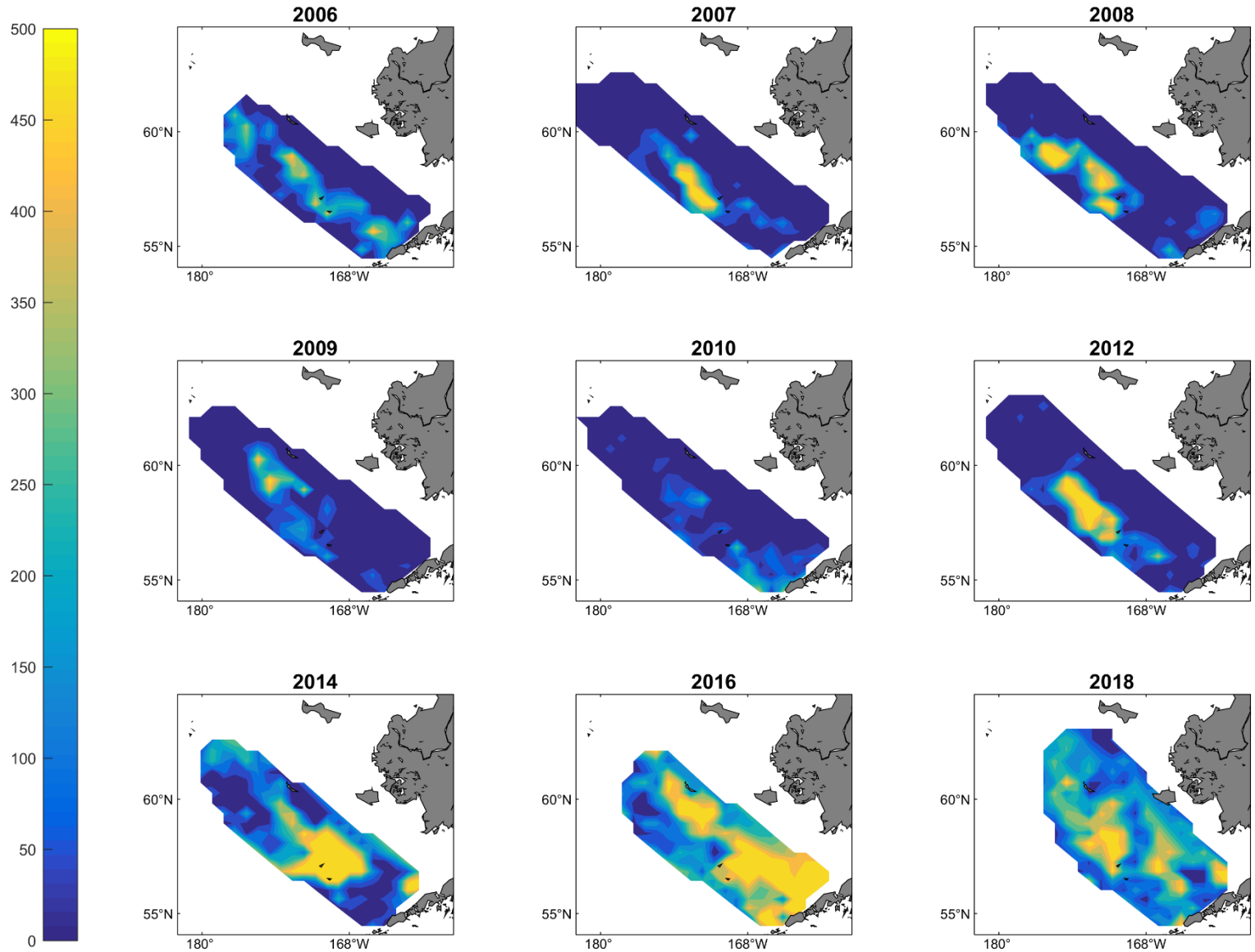

Figure 18.-- Non-pollock, non-fish backscatter (s_A, m^2 nmi^{-2}) from near surface to 0.5 m off bottom at 38 kHz frequency along tracklines during summer eastern Bering Sea acoustic-trawl surveys 2006-2018. Data are shown for a northern extension area and are missing from the westernmost 3 transects in 2018.

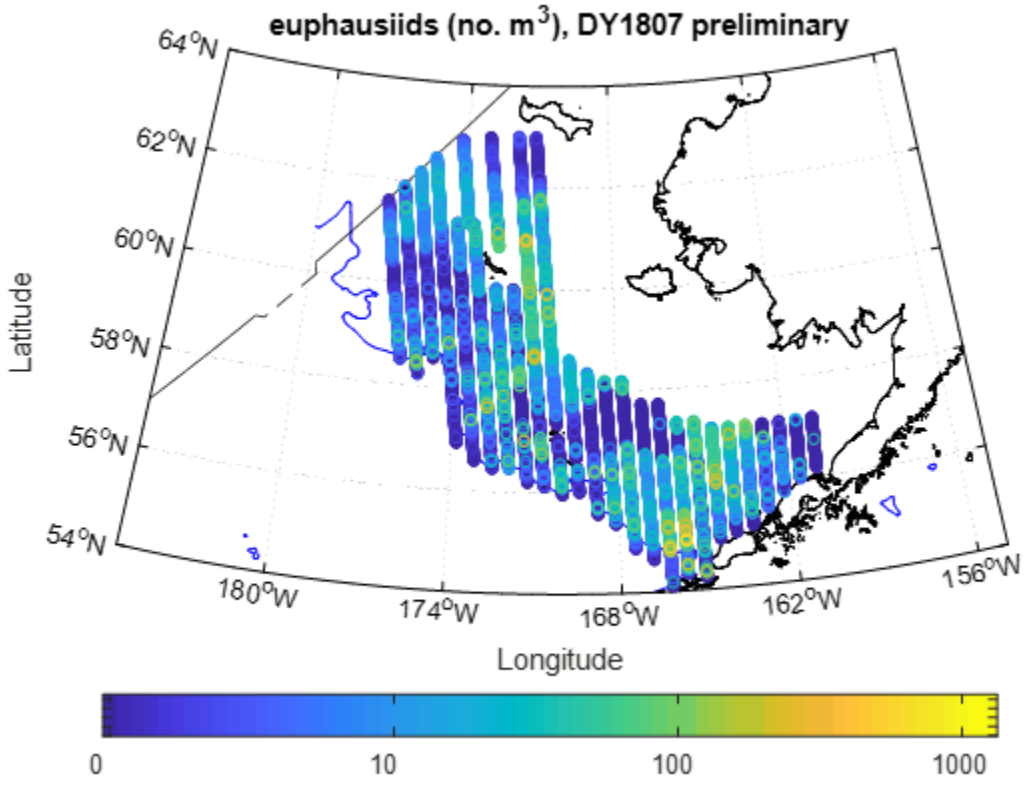

Figure 19. -- Preliminary map of the spatial distribution of euphausiid backscatter (s_A, m^2 nmi^{-2}) during the summer 2018 acoustic-trawl survey of the eastern Bering Sea shelf. Data are shown at 120 kHz.

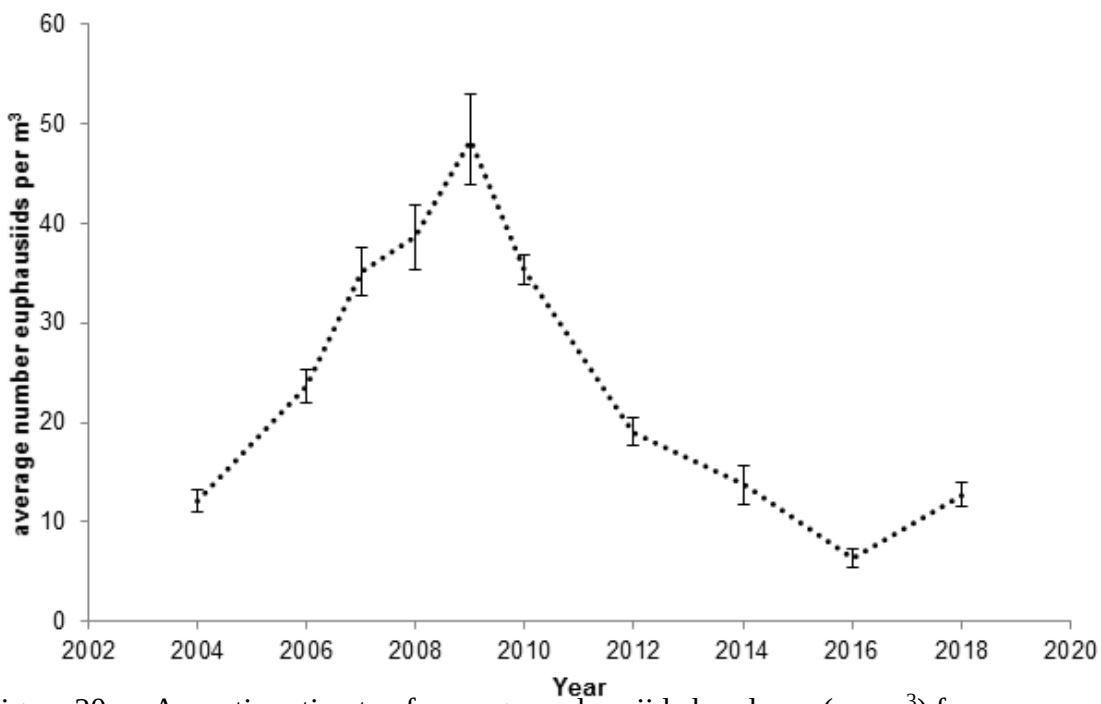

Figure 20. -- Acoustic estimate of average euphausiid abundance (no. m^3) from summer eastern Bering Sea acoustic-trawl surveys (2004-2018). Error bars are approximate 95% confidence intervals computed from geostatistical estimates of sampling error (Petitgas 1993).

Appendix I. -- Itinerary

Leg 1

6-7 June	Calibration in Captains Bay. Depart Dutch Harbor, AK. Transit to survey start area in Bristol Bay, eastern Bering Sea
8-27 June	Acoustic-trawl survey of the Bering Sea shelf (through transect 12).
	Transit to Unalaska Island, AK.
28 June	In port Dutch Harbor, AK.

Leg 2

1-2 July	Transit to survey resume point
3-7 July	Acoustic-trawl survey of the Bering Sea shelf
7 July	Propulsion motor failure
	Transit to Unalaska Island
8 July	In port Dutch Harbor for propulsion motor repair

Leg 3a

25 July	Transit to survey resume point
25 July-10 Aug.	Acoustic-trawl survey of the Bering Sea shelf
	Transit to Unalaska Island
11 Aug.	In port Dutch Harbor, AK.

Leg 3b

14 Aug.	Transit to survey resume point
15-20 Aug.	Acoustic-trawl survey of the Bering Sea shelf
20 Aug.	Propulsion motor failure
	Transit to Kodiak Island
25 Aug.	Acoustic sphere calibration in Kalsin Bay, Kodiak.
26 Aug.	End of cruise. Kodiak, AK.

Appendix II. -- Scientific Personnel

Leg 1 (6 June -28 June)

Name	Position	Organization	Nation
Denise McKelvey	Chief Scientist	AFSC	USA
Darin Jones	Fishery Biologist	AFSC	USA
Nate Lauffenburger	Fishery Biologist	AFSC	USA
Scott Furnish	Info. Tech. Specialist	AFSC	USA
Sarah Stienessen	Fishery Biologist	AFSC	USA
Mike Levine	Fishery Biologist	AFSC	USA
Matthew Phillips	Observer	AIS	USA
Lacee Sherman	TAS	NOAA TAS	USA

Leg 2 (1-8 July)

Patrick Ressler	Chief Scientist	AFSC	USA
Kresimir Williams	Fishery Biologist	AFSC	USA
Abigail McCarthy	Fishery Biologist	AFSC	USA
Chris Bassett	Info. Tech. Specialist	AFSC	USA
Sandi Neidetcher	Fishery Biologist	AFSC	USA
Jamie Giganti	Observer	AIS	USA
Matthew Phillips	Observer	AIS	USA
Joan Shea-Rogers	TAS	NOAA TAS	USA
Lee Teevan	TAS	NOAA TAS	USA

Leg 3a (25 July -11 August)

Taina Honkalehto	Chief Scientist	AFSC	USA
Rick Towler	Info. Tech. Specialist	AFSC	USA
Darin Jones	Fishery Biologist	AFSC	USA
Anatoli Smirnov	Fishery Biologist	TINRO	Russia
Mike Levine	Fishery Biologist	AFSC	USA
Abigail McCarthy	Fishery Biologist	AFSC	USA
Matthew Phillips	Observer	AIS	USA
Grace Workman	Intern	UW	USA
Liz Allyn	Intern	UW	USA

Leg 3b (14- 26 August)

Alex De Robertis	Chief Scientist	AFSC	USA
Abigail McCarthy	Fishery Biologist	AFSC	USA
Darin Jones	Fishery Biologist	AFSC	USA
Nate Lauffenburger	Fishery Biologist	AFSC	USA
Chris Bassett	Info. Tech. Specialist	AFSC	USA
Morgan Busby	Fishery Biologist	AFSC	USA
Colleen Harpold	Fishery Biologist	AFSC	USA
Matt Rogers	Fishery Biologist	ABL	USA

AFSC	Alaska Fisheries Science Center, Seattle WA
AIS	AIS, Inc., New Bedford, MA
TINRO	Pacific Research Institute of Fisheries and Oceanography Vladivostok, Russia
NOAA TAS	National Oceanic and Atmospheric Administration, Teacher at Sea Program
UW	University of Washington, WA

Appendix III- Age- 0 pollock backscatter impact on abundance

In the 2018 EBS survey age-0 pollock, which are poorly retained by the survey trawl, were observed in CamTrawl images where age-1^+ pollock were also present. An estimate of the potential bias this might introduce into survey estimates of age-1^+ pollock was undertaken by combining observed acoustic backscatter, trawl catches, and depth distributions of fishes observed in CamTrawl. The fundamental concept underlying this analysis was to account for the contribution of backscatter from age-0 pollock observed in the CamTrawl images by computing the fraction of backscatter in areas classified as age-1^+ pollock that could have been from age-0 pollock. The calculations assume that pollock are the primary sound scatters, which is a reasonable approximation given that pollock dominated fish abundance (> 95% of fish biomass in trawl hauls, see Table 3), and that jellyfish, the next most abundant organism in trawl catches, are very weak acoustic scatters compared to pollock (De Robertis and Taylor, 2014).

The numbers of age-0 and age-1+ pollock in each CamTrawl record were counted by analyzing every 50th image. Statistics were compiled on the relative abundance of age-0 and age-1^+ pollock in 10 m depth layers for each trawl haul. We combined estimates of scattering strength (Traynor, 1996), trawl catches, and assumptions about net selectivity to compute the potential proportion of the backscatter classified as being from age-1+ pollock during the survey that is in fact attributable to age-0 pollock.

Although both age-0 and age-1^+ pollock can be enumerated from the CamTrawl images, the relative proportion of age-0 and age-1^+ pollock observed by the camera is likely to be affected by the trawl capture process. That is, the AWT survey net is much more likely to retain large pollock than smaller pollock due to their stronger herding response during the trawl capture process. For this exercise, we assumed that all age-1^+ pollock entering the trawl mouth are retained, and that age-0 pollock act as passive particles exhibiting no herding behavior. The AWT's mouth opening has a cross-sectional area of 700 m^2, which is 175 times larger than the cross-sectional area of 4 m^2 where the CamTrawl is mounted. This leads to the assumption that all age-1^+ pollock, and only 1 of every 175 age-0 pollock entering the trawl mouth are retained and observed in the CamTrawl images. As a consequence of this selectivity assumption, these estimates should be considered an upper bound, as it is highly likely that age-0 pollock are herded to at least some degree, and that some larger pollock escape the trawl, both of which would lead to lower estimates of the impacts of age-0 pollock on the survey estimate.

For each interval (i.e., each 0.5 nmi EDSU along survey transects) and depth cell, the nearest haul used in the survey analysis was identified. Out of 97 AWT hauls conducted during the survey, 85 hauls yielded useable CamTrawl records. Some AWTs did not produce useful image data due to issues such as CamTrawl not working, incorrect mounting of the camera on the trawl,

and low visibility conditions. Backscatter in the areas where CamTrawl data were not available was excluded from further analysis.

The following calculations were performed for each analysis cell (i.e. interval *i* and depth *z*) attributed to pollock where CamTrawl was available in the nearest haul. The backscattering cross section (*HB*) for the closest catch of age-1$^+$ pollock in the interval *i* and depth layer *z* is defined as

$$HB_{i,z} = N_{TRAWL,i,z}{}^{PK} * \hat{\sigma}_{bs}{}^{PK},$$

where $N_{TRAWL,i,z}{}^{PK}$ corresponds to the number of adult pollock captured in the nearest trawl assigned to interval *i* and depth cell *z*. A single average length of 45 cm and the target-strength relationship of Traynor et al. (1996) was used to compute the backscattering cross section of adult pollock ($\hat{\sigma}_{bs}{}^{PK}$).

The number of age-0 pollock estimated to have entered the trawl mouth is defined as:

$$N_{TRAWL,i,z}{}^{AGE0} = \frac{N_{CAMTRAWL,i,z}{}^{AGE0}}{N_{CAMTRAWL,i,z}{}^{PK}} * N_{TRAWL,i,z}{}^{PK} * SR,$$

where *SR* is the selectivity ratio for age-0 relative to age-1$^+$ pollock, and $N_{CAMTRAWL,i,z}{}^{AGE0}$ is the total number of age 0 pollock observed in the CamTrawl images in interval *i* and depth layer *z* (similarly for age-1$^+$ pollock and PK). As described above, an *SR* of 175 was used based on ratio of the mouth opening of the net to the cross-sectional area of the location of the net where the CamTrawl was mounted. This amounts to assuming that age-1$^+$ pollock are completely retained, and that age-0 pollock are not herded at all and pass through the net when they encounter it.

The backscatter attributable to age-0 pollock (*A0B*) entering the trawl is

$$AOB_{i,z} = N_{TRAWL,i,z}{}^{AGE0} * \hat{\sigma}_{bs}{}^{AGE0}.$$

A single representative length of 4.5 cm for age-0 pollock and the target strength relationship of Traynor et al. (1996) was used to compute $\hat{\sigma}_{bs}{}^{AGE0}$, the backscattering cross section of age-0 pollock.

Then the proportion of haul backscatter for a given cell attributable to age-1$^+$ pollock relative to total backscatter is

$$P_{i,z} = \frac{HB_{i,z}}{HB_{i,z} + A0B_{i,z}}.$$

The observed backscatter with the acoustic contribution of age-0 pollock removed ($s_{A,\ corr,i,z}$) is:

$$s_{A,corr,i,z} = P_{i,z} * s_{A,i,z,obs},$$

where $s_{A,i,z,obs}$ is the observed backscatter attributed to age-1^+ pollock in each cell. The impact on the survey as a percent of the observed backscatter that was incorrectly attributed to age-1+ pollock rather than age-0 pollock was estimated as

$$I = \left(1 - \frac{\sum_{i,z} s_{A,i,z,corr}}{\sum_{i,z} s_{A,i,z,obs}}\right) \cdot 100.$$

The survey-wide impact, *I*, of accounting for the effect of age-0 pollock in areas attributed to age-1^+ pollock during the survey reduced the backscatter attributable to adult pollock by 3.4%. Review of CamTrawl image counts (Appendix II, Fig. 1) overlaid on echograms indicated that age-0 pollock did not contribute substantially to age-1^+ backscatter because age-0s were largely shallower than age-1^+ pollock. Given that this methodology represented an upper bound of *I* due to the selectivity assumptions, it was concluded that improperly accounting for the backscatter from age-0 pollock not retained in the AWT survey trawl was not a major concern during this survey, and no corrections to the survey abundance estimates were pursued.

Appendix III Table 1. -- Target strength (TS) to size relationships from the literature used to allocate 38 kHz acoustic backscatter to most species in this report. The symbols in the equations are as follows: *r* is the bell radius in cm and *L* is length in cm for all groups except pelagic crustaceans, in which case L is in m. The species for which the TS was derived is given.

Group	**TS** (dB re a m^2)	**Length type**	**TS derived for which species**	**Reference**
Pollock	$TS = 20 \log_{10} L - 66$	L = fork length	*Gadus chalcogrammus*	Traynor 1996
Fish with swim bladders	$TS = 20 \log_{10} L - 67.5$	L = total length	Physoclist fishes	Foote 1987
Fish without swim bladders	$TS = 20\log_{10} L - 83.2$	L = total length	*Pleurogrammus monopterygius*	Gauthier & Horne 2004
Jellyfish	$TS = 10\log_{10}(\pi r^2) - 86.8$	R = bell radius	*Chrysaora melanaster*	De Robertis & Taylor 2014
Squid	$TS = 20\log_{10} L - 75.4$	L = mantle length	*Todarodes pacificus*	Kang et al. 2005
Pelagic crustaceans	$^{*,+,\#}TS = A^*(\log10(BkL)/(BkL))^C + D((kL)^6) + E((kL)^5) + F((kL)^4) + G((kL)^3) + H((kL)^2) + I(kL) + J + 20\log_{10}(L/Lo)$;	L = total length	*Euphausia superba*	Demer & Conti 2005

*A = -930.429983; B = 3.21027896; C = 1.74003785; D = $1.36133896 \times 10^{-8}$;
E = $-2.26958555 \times 10^{-6}$; F=$1.50291244 \times 10^{-4}$; G = $-4.86306872 \times 10^{-3}$; H = 0.0738748423;
I = -0.408004891; J = -73.9078690; and Lo = 0.03835.
+If L < 15 mm, TS = -105 dB; and if L > 65 mm, TS = -73 dB.
#k = 2πfc, where f = 38,000 (frequency in Hz) and c = 1470 (sound speed in m/s).

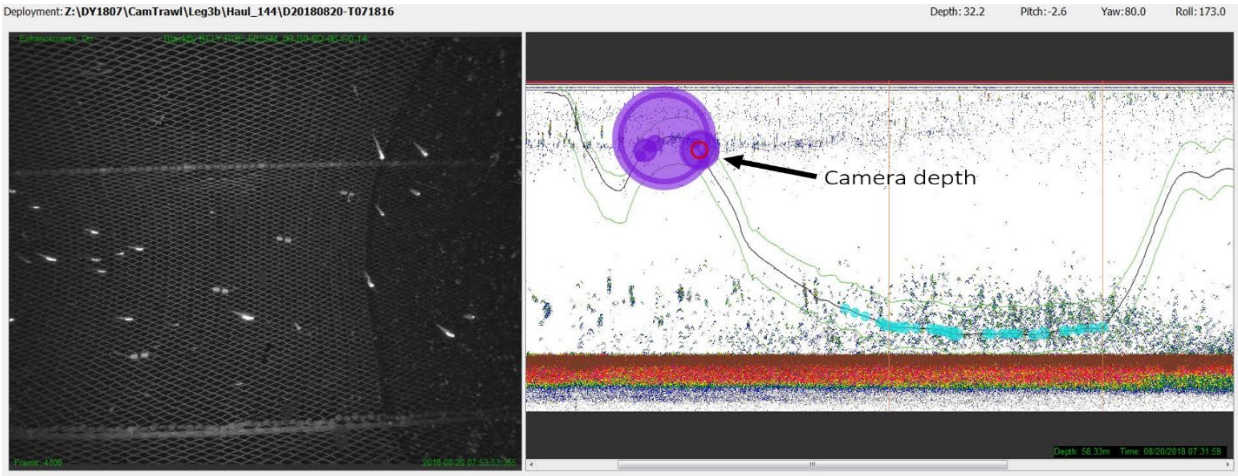

Appendix III Fig. 1. --Example of Camtrawl results from an AWT trawl haul. The left panel shows a Camtrawl image containing large numbers of age-0 pollock. The right panel shows the trawl path overlaid over a 38 kHz echogram. Age-0 pollock (purple circles) were observed when the trawl was in the shallow scattering layer, while older pollock (blue circles) were detected in a deeper scattering layer. The image at left was taken at the location indicated by the black arrow. Because age-0 pollock were primarily distributed near the surface during this survey, and little near-surface backscatter was attributed to age-1^+ pollock, accounting for the potential impact of age-0 pollock that were not retained in the trawl has only a relatively small impact on survey estimates of age-1+ pollock.

U.S. Secretary of Commerce
Wilbur L. Ross, Jr.

Acting Under Secretary of Commerce
for Oceans and Atmosphere
Dr. Neil Jacobs

Assistant Administrator for Fisheries
Chris Oliver

September 2020

www.fisheries.noaa.gov

OFFICIAL BUSINESS

National Marine
Fisheries Service
Alaska Fisheries Science Center
7600 Sand Point Way N.E.
Seattle, WA 98115-6349